A MICROFLUIDICS-BASED PARADIGM FOR CLINICAL LENTIVECTOR GENE TRANSFER

A Dissertation
Presented to
The Academic Faculty

by

Reginald Tran

In Partial Fulfillment
of the Requirements for the Degree
Doctor of Philosophy in the
Wallace H. Coulter Department of Biomedical Engineering

Georgia Institute of Technology
and Emory University
December 2016

A MICROFLUIDICS-BASED PARADIGM FOR CLINICAL LENTIVECTOR GENE TRANSFER

Approved by:

Dr. Wilbur A. Lam, Advisor
School of Engineering
Wallace H. Coulter Department of Biomedical Engineering
Georgia Institute of Technology

Dr. Joseph M. Le Doux
School of Engineering
Wallace H. Coulter Department of Biomedical Engineering
Georgia Institute of Technology

Dr. J. Brandon Dixon
School of Mechanical Engineering
Georgia Institute of Technology

Dr. Todd Sulchek
School of Mechanical Engineering
Georgia Institute of Technology

Dr. Christopher B. Doering
Department of Pediatrics
Emory University

Date Approved: October 26, 2016

ACKNOWLEDGEMENTS

I wish to acknowledge the following people for their continued support throughout my graduate work:

- My advisor, Dr. Wilbur A. Lam for his valuable guidance, support, and resources for my intellectual growth and independence. I am extremely appreciative of Wilbur's ability to be available through email or text message at all hours of the day, and his openness to suggestions. I owe much of my success to him for continually pushing me.
- My committee members:
    - Dr. J. Brandon Dixon for his helpful discussion and suggestions toward my interpretations of the data and the COMSOL model.
    - Dr. Christopher B. Doering for providing tremendous support, guidance, and resources to enable the development of this project. I appreciate all of the impromptu individual meetings we had to troubleshoot and plan next steps despite not being one of your own students.
    - Dr. Joseph M. Le Doux for paving the way for this project with his scientific contributions and ensuring that my analyses of the data were viewed with enough scientific rigor.
    - Dr. Todd Sulchek for his stimulating and discussions in device design and optimistic encouragement.
- Dr. Trent Spencer for also providing tremendous support, guidance, and resources to enable the development of this project.

- My lab members for all their support to help me develop both in the lab and outside. You have all been like family to me, and I am glad to have you in my life – even with all the minor squabbles, these have helped toughen up my skin throughout the years. In particular, I would like to individually acknowledge the lab members that have helped me grow since the beginning of graduate school:
    - I owe a great amount to Drs. Byungwook Ahn, Elaissa Hardy, and David Myers for teaching me how to be safe and efficient in the cleanroom to be successful in my microfabrication for this work.
    - I wish to thank Dr. Yongzhi Qiu and Dr. Myers for the impromptu discussions, support, and encouragement even during their coveted personal time. I can always rely on them to lift my spirits and motivate me to continue pushing forward when I feel stuck.
    - I consider myself extremely lucky to work with Yumiko Sakurai throughout all these years. I attribute much of the initial success in my project to her willingness to help out and her expertise in all biological matters. She is a great role model both inside and outside of the lab, and always encouraged me to pursue my interests and develop new ones.
    - I thank Robert Mannino for being a great companion inside of the lab, outside of the lab, and especially at the gym. Your support and acceptance as a friend has helped me make it through some particularly tough times.
    - I wish to further acknowledge Dr. Marcus Carden, Jordan Ciciliano, Meredith Fay, Dr. Hope Gole, Caroline Hansen, Jessica Lin, Dr. Sarah Mitchell, John Nicosia, Dr. Margo Rollins, and Erika Tyburski for giving

me many different perspectives in science and life. This environment would not feel like a real family without each and every one of you.

- Finally, I would like to acknowledge my undergraduate assistants, William Li and Emma Mihevc for helping me with various aspects of my project and enabling me to practice valuable skills as a mentor.

- My collaborators in the Spencer and Doering labs and at Expression Therapeutics, LLC for their assistance in gathering much of the data in this work. Particularly:
  - Jordan E. Shields for spearheading all of the animal studies so that I could test out my microfluidics with primary cells.
  - Allison M. Lytle for helping with the T cell flow cytometry and tissue harvesting.
  - Dr. Gabriella Denning for running the RT-PCR for vector copy number in the primary cell transductions.
- My friends have been one of the greatest sources of support and growth throughout my time in graduate school. In particular, I would like to acknowledge:
  - Dr. Marian Hettiaratchi for always being supportive and being the greatest science friend anyone could ever hope for.
  - Dr. Ariel Kniss-James and Peter James for being extremely kind and caring friends.
  - Dr. Torri Rinker for her insight and wise words.
  - Dr. Joshua Zimmerman for his silent, yet thoughtful support.
  - Dr. Michael Nguyen for always being there for me even though he had no idea what I was doing most of the time during my late night experiments.

    - Dr. Joel Christo and Josh Samuel for encouraging me to keep pushing forward.
    - Vi Nguyen for offering a kind and gentle hand and to support me in the final stretch.
- I am thankful for Sally Gerrish and Shannon Sullivan for being extremely helpful every step of the way to make sure that I was able to advance through the program and finish strong. I would also like to thank Marty Jacobson for his assistance in machining and helping me try out new ideas.

Last, but not least, I wish to acknowledge my family for supporting me through this journey. My parents have instilled hard-working values within me to help me accomplish my goals and conquer any obstacles that stand in my way. My sister has taught me to be strong and the importance of staying balanced. Although they did not fully understand everything I was doing along the way, they supported me to the best of their abilities and continually believed in me even when I didn't completely believe in myself. I am forever grateful for their love and care.

TABLE OF CONTENTS

LIST OF TABLES

Page

LIST OF FIGURES

Page

LIST OF SYMBOLS AND ABBREVIATIONS

AAV	Adeno Associated Virus
ADA	Adenosine Deaminase
BSA	Bovine Serum Albumin
CAD	Computer Aided Design
CAR	Chimeric Antigen Receptor
CGMP	Common Good Manufacturing Practices
CNC	Computer Numerical Controlled
DNA	Deoxyribonucleic Acid
ELISA	Enzyme-linked Immunosorbent Assay
FBS	Fetal Bovine Serum
fVIII	Coagulation Factor VIII
HEK	Human Embryonic Kidney
HIV	Human Immunodeficiency Virus
HPRT	Hypoxanthine Phosphoribosyltransferase
HSC	Hematopoietic Stem Cell
HSCT	Hematopoietic Stem Cell Transplantation
HUVEC	Human Umbilical Vein Endothelial Cell
IL-2	Interleukin-2
LDL-R	Low-Density Lipoprotein Receptor
LPL	Lipoprotein lipase
LV	Lentiviral Vector
MOI	Multiplicity of Infection

OTCD	Ornithine Transcarbamylase Deficiency
PDMS	Polydimethylsiloxane
PEG	Polyethylene Glycol
RAC	Recombinant DNA Advisory Committee
RT-PCR	Real-Time Polymerase Chain Reaction
SCID	Severe Combined Immunodeficiency Disease
TIL	Tumor Infiltrating Lymphocyte
TU	Transducing Units
UV	Ultraviolet
VCN	Vector Copy Number
VSV-G	Vesicular Stomatitis Virus Glycoprotein
$\dot{\gamma}$	Shear Rate (s^{-1})
η	Dynamic Viscosity ($kg \cdot m^{-1} \cdot s^{-1}$)
λ	Average number of events per interval for Poisson distribution
k_B	Boltzmann Constant ($kg \cdot m^2 \cdot s^{-2} \cdot K^{-1}$)
k	Number of events to be observed in a Poisson distribution
D	Diffusion Coefficient ($m^2 \cdot s^{-1}$)
T	Absolute Temperature (K)

SUMMARY

Clinical trials targeting hematopoietic stem cells and T cells for treatment of genetic disorders and cancers with chimeric antigen receptors, respectively, are finding increasing success using Human Immunodeficiency Virus (HIV)-derived lentiviral vectors (LVs)[1-4]. Improved safety and efficacy of current generation self-inactivating LVs, which can infect non-dividing cells that are often targets of clinical gene therapy, provide an attractive option for gene transfer of therapeutic transgenes[5, 6]. Despite these advances, LV manufacture remains inefficient, scale-limited, and expensive[7]. Lengthy *ex vivo* cell transduction protocols often require large quantities of LV to achieve the desired clinical outcomes[8, 9]. Ongoing clinical studies expose the limitations of the technology and highlight the need for improvements in clinical LV transduction efficiency as entire LV production runs may dose a single patient. Attempts to improve transduction through the use of polycations[10], spinoculation[11], recombinant fibronectin fragment coatings[12], or biological adjuvants[13] have been explored previously. High throughput screening has also been unsuccessful in identifying transduction-enhancing reagents[14]. Unfortunately, the sheer vector requirements for high levels of gene transfer remain problematic due partially to large minimum working volumes of standard transduction systems such as culture plates, flasks, and bags.

Moreover, the multiplicity of infection (MOI), a commonly used parameter representing the ratio of viral particles to target cells in a given transduction, has consistently proven to be unreliable to predict dosages of LV necessary for therapeutic benefit[15, 16]. As such, multiple rounds of transduction at MOI 100 is not uncommon in

clinical protocols. Instead, vector concentration is more recently emerging as a standardized parameter for transduction[17, 18]. The movement toward requisite LV (v/v)% for effective transduction suggests diffusion limitations inherent in standard transduction platforms, requiring increasingly larger amounts of LV as transduction systems are scaled toward clinical usage[19]. Therefore, significant amounts of LV are wasted in these systems.

The goal of this work was to investigate the use of microfluidics in clinical gene therapy to develop a novel platform for more efficient LV-mediated transduction. Several microfluidic devices have been developed in the Lam laboratory using different methods in order to achieve this goal (Chapter 3). By investigating factors such as MOI, (v/v)%, transduction height (diffusion distance), and transduction times in microfluidic devices compared to well plates requiring larger working volumes, we determined that microfluidic devices could be leveraged to create a more efficient transduction platform for gene therapy that significantly reduces the amount of virus required for efficient gene transfer (Chapter 4). Furthermore, we demonstrate that our system offers improvements in primary human T cell (Chapter 5) and murine *ex vivo* hematopoietic stem cell (Chapter 6) transduction with less LV requirements and shorter transduction times. With clinical gene therapy advancing rapidly into commercial application, associated advances in vector manufacturing and utilization will be essential to routine clinical implementation and globalization. Improvements in vector manufacture will not necessarily result in greater transduction efficiency. Extrapolating insight gained from this study to cost evaluations of ongoing clinical trials, we estimate that an order of magnitude reduction in vector costs per patient may be attainable by using microfluidics. Due to the large number of sources of variability in vector titration and inconsistent infectivity between various cell types, the

strategy for many clinical trials to achieve therapeutic transduction has essentially been to apply as much vector onto cells as possible without inducing detrimental toxicity. Continued development of the microfluidic transduction system may enable a more systematic approach to gene therapy that would also significantly reduce the wastes inherent in current clinical processes.

CHAPTER 1: INTRODUCTION

Through decades of research and innovation, viruses that once plagued humanity with sickness and disease have been transformed into tools with the potential to provide a permanent cure for various genetic disorders and cancers. In recent years, researchers and clinicians have achieved success in treating a variety of diseases using viruses that have been reprogrammed to transfer therapeutic genes rather than inducing pathogenesis[1, 2, 20, 21]. Though the technology has finally matured from proof of principle to true clinical efficacy, gene therapy is still restrained to phase I/II clinical trials due to complex and costly manufacturing that hamper progression to phase III/IV clinical trials and commercialization.

1.1 Motivation

Genetic hematologic disorders and malignancies such as sickle cell anemia, hemophilia, and acute lymphoblastic leukemia currently affect millions of people worldwide with several hundred thousand estimated new cases occurring annually. Disease management thus far has been limited to allogeneic bone marrow transplantation, injection of recombinant clotting factors, frequent blood transfusions, drugs, surgery, or radiation. However, such treatments severely limit the lifestyles of patients, and may not always prove to be effective. Many hematologic disorders are inherited, which makes them viable targets for clinical gene therapy since $CD34^+$ hematopoietic progenitor cells can be

harvested from the patient, genetically corrected *ex vivo*, and then transplanted back to minimize immunogenicity and provide a method for the patient to repopulate the body with healthy cells that produce functional proteins. Similarly, T cells genetically modified to express chimeric antigen receptors (CARs) have shown promise in the eradication of hematologic malignancies, which would normally avoid detection in the body[4, 22].

Lentiviral vectors (LVs) provide an attractive method for cell transduction, the process of inserting foreign deoxyribonucleic acid (DNA) into a cell with a viral vector, due to their ability to infect non-dividing cells with stable integration of DNA[6]. However, progress in the field has been severely hampered by low transduction efficiencies of current platforms despite various efforts to improve virus-cell interactions. The multiplicity of infection (MOI) is a commonly used parameter for viral transductions to determine the theoretical number of viral particles that will enter a target group of cells[15]. However, much higher MOIs, and therefore greater quantities of virus, are often used clinically to achieve any significant transduction efficiency depending on the cell type.

Previous studies have shown that viral transduction is a diffusion-limited process governed by Brownian motion[19]. With currently utilized methods, due to the short half-life of these self-inactivating viruses, many of the viral particles will never reach the target cells before decaying, resulting in the observed low rates of gene transfer. These barriers are mildly circumvented by using high concentrations of LV, which is both cost-prohibitive and potentially toxic to the target cells. *Thus, there is a clear need to develop a more efficient platform for lentiviral transduction to limit the amount of virus necessary to achieve therapeutic levels of transduction.*

Microfluidic devices can be designed to have a high surface area to volume ratio that allows for small sample volumes to be used[23]. Combined with the ability to perfuse fluids with tight control of flow conditions, microfluidics provide a novel technical capability in the gene therapy field that enables cells to be exposed to high vol./vol. concentrations of LV without increasing the amount of virus used, thereby overcoming the diffusion limitations and waste associated with current methods of viral transductions.

1.2 Research Objectives and Specific Aims

The *long term goal* of this work is to develop strategies to enhance the lentiviral transduction efficiency for clinical gene therapy. The ***overall objective*** of this project was to design microfluidic devices to promote more effective transport of viral particles to target cells. The ***central hypothesis*** of this project was that leveraging various microfluidic features could significantly reduce the amount of virus necessary to achieve therapeutic levels of gene transfer. This hypothesis was grounded upon the well-documented utilization of microfluidics for reagent miniaturization in biomedical research due to their high surface area to volume ratio, and was tested with these specific aims:

Specific Aim 1: Design and develop various microfluidic devices for lentiviral transduction of non-adherent cells. The *working hypothesis* of this aim was that the high surface area to volume ratio of μFluidics would enhance lentiviral transduction efficiency compared to current transduction protocols conducted in well plates. Microfluidic devices of varying sizes and materials were designed in the Lam laboratory to develop a

microfluidic platform for lentiviral transduction, and are described in detail in Chapter 3. A GFP-encoding lentiviral vector was used to transduce non-adherent K562 and Jurkat cells serving as a surrogate of the hematopoietic target cells of clinical gene therapy. Efficiency of immobilization of cells in the devices and their removal were also characterized. From the work conducted toward this aim, we were able to demonstrate the feasibility of a microfluidic transduction platform with a small-scale device.

Specific Aim 2: Determine and optimize key parameters for achieving therapeutic levels of gene transfer using microfluidics. The *working hypothesis* of this aim was that determining parameters that directly impact transduction in the microfluidic could lead to better design and utilization to further improve transduction efficiency. A systematic approach was used to determine how mass transfer principles interact with existing biological and biochemical adjuvants to affect transduction efficiency and kinetics. GFP expression was assessed via flow cytometry to evaluate transduction efficiency. A computational model of the transport of viral particles to cells in the microfluidic versus a cell culture well allowed for parameters such as virus concentration, cell density, and fluid height to be assessed *in silico*. Chapter 4 discusses the findings of these studies, in which we narrowed down the parameter space to achieve efficient transduction using microfluidics. Together, these parameters were optimized to develop a scaled up microfluidic device and transduction protocol capable of transducing upward of 10^6 cells, a relevant goal for preclinical trials.

Specific Aim 3: Translate the microfluidic lentiviral transduction technology to clinically relevant LV products and systems. The *working hypothesis* of this aim was that existing protocols for clinical transductions could be adapted for use with microfluidics. Primary human T cells were transduced in the microfluidics using clinical grade LV encoding for GFP or a high titer coagulation factor VIII (fVIII) LV. Transduction efficiency and cell viability were assessed by measuring GFP expression and 7AAD dead cell staining via flow cytometry. Vector copy number (VCN) was measured by the real time polymerase chain reaction (RT-PCR) to determine true virus integration and efficiency of transduction. The findings and results of our work with primary human T cells can be found in Chapter 5. Microfluidic transduction efficacy was also assessed *in vivo* using primary murine Sca-1^+ hematopoietic stem and progenitor cells from C57BL/6J hemophilia A mice. The isolated cells were transduced in a standard 6-well and in the microfluidic transduction system with the fVIII-LV for direct comparison. Transduced cells were then transplanted into lethally irradiated hemophilia A donor mice. Transduction efficiency and engraftment were assessed by measuring fVIII plasma levels via chromogenic assay and flow cytometric analysis of recipient versus donor cells, respectively. Vector copy number was measured from cells of the blood, spleen, and bone marrow after at least 8 weeks when fVIII levels typically stabilized. These results are discussed in Chapter 6.

1.3 Significance of Results

This work presents significant contributions to the fields of gene therapy, hematology, cancer immunotherapy, and cell manufacturing. It is clear that transduction

efficiency is the limiting factor to clinical translation of gene therapy applications. Hematopoietic stem cells (HSCs) are one of the most promising and frequently utilized cellular targets for *ex vivo* lentiviral vector-based gene therapy applications, which include the correction of several inherited diseases[8]. The reason for their attractiveness is now well defined. HSCs have the ability to self-renew, as well as differentiate into all lineages of the hematopoietic system. Engineered T cells are also proving to be remarkably efficacious anti-cancer agents[24]. However, despite some early phase 1/2 clinical trial successes, the field remains severely hampered by inefficient LV manufacturing and target cell transduction. The microfluidic transduction platform and the concepts developed from this work address these limitations by offering greater utilization efficiency of this severely limited resource simply by adapting existing protocols to a different system. While the implications for the potential of this work to impact clinical gene therapy are tremendous, microfluidics also have the potential for use as a more accurate tool to assess viral titer. The high transduction rates yielded from the microfluidics were often higher than expected from the amount of LV added to the system, indicating that the titer may be lower than reported. This was not surprising, considering that the current process to calculate viral titer is also diffusion limited, as discussed elsewhere previously[16]. The scalability of this platform also provides a powerful clinical tool that can allow for optimization of viral dosages through small-scale transductions. Overall, this investigation of using microfluidic devices designed specifically for lentiviral transduction clearly demonstrates the versatility of this platform, which offers virus and time savings, and has various modes of use depending on constraints.

CHAPTER 2: BACKGROUND AND LITERATURE REVIEW

2.1 Gene Therapy

2.1.1 Basic Principles of Gene Therapy

Gene therapy is the process of modifying a patient's genetics for therapeutic benefit. This effect can be achieved in a variety of methods including transduction using viral vectors, introduction of exogenous nucleic acids through non-viral vectors, and genome editing techniques that can remove or insert gene segments at desired locations. Genetic modification is a broad term that can be achieved by, but is not limited to the addition or replacement of a gene, knockdown of a pathogenic gene, or complete correction of a mutated gene. Vectors can be delivered directly to specific targets *in vivo* or utilized *ex vivo* whereby cells are collected, modified outside of the body, and transplanted back into the patient. The scope of this work focuses specifically on lentiviral vectors and their applications in *ex vivo* hematopoietic stem cell transplantation and cancer immunotherapy.

2.1.2 Key Events in Gene Therapy History

The concept of gene therapy was originally conceived even before Watson and Crick had discovered the double helix structure of DNA[25]. Several decades of research drawing from the fields of genetics, molecular biology, and virology have resulted in a

maturing sub-field of clinical medicine that aims to provide solutions to "incurable" diseases. In this section, we will describe some major milestones in gene therapy history that propelled the field forward or resulted in major setbacks. Extensive gene therapy history reviews including the basis and discovery of genetics and the transfer thereof can be found elsewhere, but are beyond the scope of this work[26-28]. The viral vectors discussed in this section will primarily focus on the impact these vectors made on the field. Section 2.1.3 will instead summarize more details and tradeoffs of different viral vectors.

As early as 1980, researchers were introducing cloned genes into mammalian cells. Notably, Martin Cline piloted a controversial human gene therapy trial in β-Thalassemia patients without permission from the UCLA institutional review board[29]. Although no clinical benefit was achieved, the patients also did not experience any negative effects. This trial was conducted following two other animal studies by Cline where murine bone marrow cells were transfected with genes to produce dihydrofolate reductase and another where murine bone marrow cells had again been transfected with a herpes simplex thymidine kinase gene to confer methotrexate resistance[30, 31]. All studies utilized a calcium phosphate transfection method where a calcium phosphate-DNA precipitate is formed to facilitate binding of DNA to the cell surface, which then induces endocytosis for DNA delivery[32]. However, severe criticism of these animal studies imply that advancing to human subjects may have even been unwarranted[29]. While the backlash of this incident was severe and left a negative mark on Martin Cline's career, it made some positive contributions to the progression of gene therapy by quelling fears at the time of safety concerns and sending a clear message to investigators to adhere to the established rules and

regulations in addition. All future human gene therapy trials would henceforth be required to receive approval by the NIH Recombinant DNA Advisory Committee (RAC).

Around that same time, retrovirus research had advanced well enough that many groups began developing retroviral vectors for *in vitro* correction of human cells. Three different research groups are credited for independently developing retroviral vectors nearly concurrently: Shimotohno and Temin as well as Wei *et al*. in 1981 and Tabin *et al*. in 1982[33-35]. The growth of retroviral vector usage created a notable shift from chemical transfection techniques to viral vectors for gene therapy. Not only were the retroviral vectors more efficient than chemical transfection, but they demonstrated efficacy in human and other mammalian cells. *In vitro* treatment of human disease was demonstrated in 1983 by Miller et al., in which they corrected cells obtained from humans deficient in hypoxanthine phosphoribosyltransferase (HPRT) with a retrovirus expressing human HPRT[36]. By 1986, Kantoff et al. showed that retroviral vectors could be used to correct adenosine deaminase (ADA) deficiency severe combined immunodeficiency disease (SCID)[37].

In 1988, the RAC approved the first clinical protocol for gene transfer into humans. The goal of the study was not for gene therapy, but instead for human gene marking in an attempt to track tumor-infiltrating lymphocytes (TILs) in patients with metastatic melanoma for treatment optimization[38]. By modifying the TILs to confer resistance to neomycin, the *in vivo* distribution and survival of the cells could be determined. This study successfully demonstrated that genetically modified cells derived from retroviral vectors could be safely administered to humans with implications for the use of lymphocytes in future gene therapy applications. Following the first RAC approval for human gene

transfer, the FDA approved the first human gene therapy clinical trial in 1990. Michael Blaese directed the effort to use retroviral vectors to treat ADA-SCID in two children by transducing their T cells to produce the ADA enzyme that was deficient in their condition[20]. The patients were still given polyethylene glycol (PEG)-ADA, so the extent of the therapy's effectiveness was unclear. However, the dosage of PEG-ADA was able to be reduced, indicating that the therapy was viable. Overall, the study further supported the claim that retroviral vectors could offer safe gene therapy treatments for patients with ADA-SCID.

Several clinical trials followed into the next decade. However, the first gene therapy-related death caused major setbacks to the field. On September 17, 1999, Jesse Gelsinger experienced lethal complications directly related to the adenoviral vector administered for the treatment of a partial ornithine transcarbamylase deficiency (OTCD)[39, 40]. This occurred a mere 98 hours after receiving the vector, resulting in systemic inflammation and multi-organ failure. Investigations of possible mechanisms of action point to innate immune responses from certain components of the vector capsid. Adenoviral vectors are typically administered *in vivo*, bearing greater risk to immune responses. Soon after that tragic incident, another major setback for the gene therapy field occurred. A SCID-X1 gene therapy trial led by a group of researchers in Paris initially reported the first "cure" for a disease using a retroviral vector in April 2000[41]. X-linked SCID-X1 syndrome is a fatal disease that is caused by a deficiency in the γ-c chain receptor, which prevents developing lymphocytes from maturing into functional T cells and natural-killer cells. By delivering a functional γ-c chain receptor gene to hematopoietic stem cells, the treated patients were able to develop functional immune systems. However, two of the

three patients eventually developed disorders that bared similarities to leukemia. The complications are believed to have developed from insertional mutagenesis caused by vector integration close to or in the LMO2 oncogene, leading to uncontrollable replication that likely resulted from single transduced cells in which the oncogene was activated. These two events triggered researchers and clinicians worldwide to re-evaluate the risks of gene therapy, stalling its progression for several years.

Lentiviral vectors soon found increased usage and emerged as the safer alternative to many of the other viral vectors[42]. They also offered key advantages that were unavailable with other vectors such as the ability to stably integrate into both dividing and non-dividing cells[6]. Due to its derivation from the human immunodeficiency virus Type 1 (HIV-1), there was a major focus on biosafety. By the third generation, LVs were stripped of six of the nine genes that encode for virulent components, leaving them as self-inactivating and replication incompetent without altering their ability to transfer genetic material[5, 43].

In 2012, the European Union recommended Glybera (alipogene tiparvovec), the first commercial gene therapy product in the Western world, for approval. Glybera is an adeno-associated viral (AAV) vector used to treat lipoprotein lipase (LPL) deficiency, which is an orphan disease that causes inflammation of the pancreas due to the buildup of abnormally large particles of fat in the blood[44]. However, estimates of the cost for this therapy are as high as $1,000,000 for the average adult, which would require several rounds of intramuscular injections of the vector. As such, the model for payment of such an expensive drug is still undetermined due to the novelty of pricing a curative therapy[45]. Thus, there is a clear need to push for commercialization of other gene therapy products that remain in Phase I/II testing.

2.1.3 Viral Vectors Used in Clinical Gene Therapy

As discussed in the previous section, LVs are not the only option for gene transfer in a clinical setting. However, among the various vectors, LVs are the best option for targeting hematopoietic stem cells and T cells, the major targets of *ex vivo* gene therapy. They are the only vector that can integrate into both dividing and non-dividing quiescent cells, have a relatively large packaging capacity, and can integrate their genome into target cells for a potential lifelong cure.

Table 2.1: Table of commonly utilized viral vectors and their properties

Vector	Host Genome Interaction	Infection Targets	Packaging Capacity	Virion Diameter	Genome Size
Adenovirus	Non-Integrating	Dividing and Non-dividing cells	7.5 kb	18 – 26 nm	38 – 39 kb
Adeno-Associated Virus	Non-Integrating	Dividing and Non-dividing cells	4.5 kb	70 – 90 nm	5 kb
Lentivirus	Integrating	Dividing and Non-dividing cells	8 kb	80 – 130 nm	3 – 9 kb
Retrovirus	Integrating	Dividing Cells Only	8 kb	80 – 130 nm	3 – 9 kb

2.2 Production of Lentiviral Vectors

Lentiviral vector stocks are generated from transient transfection of producer cell lines using the calcium phosphate method[32, 46]. Typically, human embryonic kidney (HEK) 293T cells are used due to their high rates of transfection and protein production. The third generation design of lentiviral vectors utilizes four plasmids to encode for fully active lentiviral particles that lack virulent elements and the ability to form functional recombinants[43]. One plasmid contains the therapeutic transgene of interest while the

remaining three plasmids are required for the packaging of LVs. In particular, these are often pMDL, pRev, and pVSVG for vesicular stomatitis virus glycoprotein (VSV-G)-pseudotyped LVs. The pMDL plasmid encodes for Gag-Pol precursor proteins that form structural proteins, integrase, and reverse transcriptase that are common to all retro- and lentiviruses. The pRev plasmid provides the Rev gene, which is necessary for the production of LV particles from the producer cell lines. Finally, the fourth plasmid encodes the envelope protein. pVSVG is a popular choice due to the broad tropism of the VSV-G envelope, enabling transduction of a variety of cell types[47]. Other envelope proteins may be used in favor of VSV-G for specific targeting of different cell types[48].

After transient transfection, the media is exchanged to allow for transiently transfected cells to produce lentiviral particles. The supernatant, which should contain viral particles within 24 hours, is then collected and stored, and fresh media is added back to the cells. This process may be repeated, but is limited due to the cytotoxicity related to VSV-G, *gag,* and *pol* expression in producer cell lines[47, 49-51]. When all viral supernatant has been collected from a given production run, it is then filtered to remove cell debris, though the titer will still be low. To obtain higher titer LV stocks, the filtered viral supernatant is concentrated by ultracentrifugation at speeds as high as 70,000*g* for 2 hours at 20°C. Further ultracentrifugation through a sucrose cushion or chromatography-based purification can be performed to remove residual contaminants from LV production that may contribute to vector toxicity[46]. However, this step can also lead to a reduction in titer.

Large scale production conforming to current good manufacturing practices (CGMP) has been characterized[7]. All materials and reagents must also conform to CGMP conditions, including the lentiviral plasmids. The process must be able to produce

consistent batches of LV, and the resulting product must meet an expensive panel of specifications including sterility and pH requirements, as well as testing negative for mycoplasma and replication competent lentivirus. Additional processing is also required to remove residual additives such as benzonase and DNase, which are used to degrade contaminating DNA from the transient transfections. Despite the large scale production, final volumes ranging from 56-574 μL were achieved, with titers ranging from 5.2-3.0 x 10^8 TU/mL after 7-12 weeks of virus production per production run. A pediatric clinical trial utilized 180mL batches ranging from 2.1-7.6 x 10^8 TU/mL titers for each patient, highlighting the severe bottleneck to commercialization due to the limitations in vector production combined with high vector requirements from low transduction efficiency[1].

2.3 Existing Additives Used to Enhance Transduction Efficiency

Many commercially available products have been developed to enhance transduction efficiency. These compounds are typically added during transduction to facilitate binding of virus to cells, though their mechanisms of action differ.

2.3.1 Polycations

Hexadimethrine bromide, more commonly known as polybrene, is a commonly used reagent in gene therapy to enhance transduction efficiency by reducing charge shielding between the negatively charged surfaces of cells and viral envelope by providing a positive charge as a bridge (**Figure 2.1**)[10, 52] . Protamine sulfate is another popular cationic polymer that is considered to work similarly to polybrene, but with reduced toxicity[53]. However, both of these additives are shown to induce mild toxicity and anti-

proliferative effects at high concentrations[54]. Therefore, a balance between transduction enhancement and toxicity should be considered before use. A dosage of 8 μg/mL is normally the upper limit for polybrene usage.

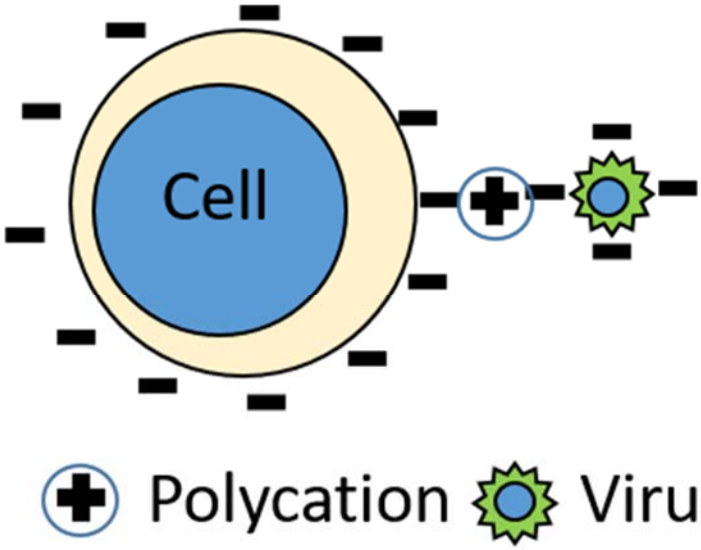

Figure 2.1: Proposed mechanism of polycation gene transfer enhancement. Polycations provide a positive charge to reduce the charge shielding between the negatively charged surfaces of cells and viral particles.

2.3.2 Recombinant Fibronectin Fragments

RetroNectin is a recombinant fibronectin fragment that is believed to enhance transduction efficiency using retroviral and lentiviral vectors by bringing cells and viral particles in closer contact for binding (**Figure 2.2**)[12]. The RGDS peptide sequence of fibronectin binds to the variable lymphocyte antigen (VLA)-5 integrin ($\alpha_5\beta_1$) while the CS-1 peptide sequence binds the VLA-4 integrin ($\alpha_4\beta_1$). RetroNectin also contains a heparin-binding domain, which contains positively charged amino sidechains for binding of the

negatively charged surfaces of the viral particles. Thus, RetroNectin can also be used to immobilize cells when adsorbed to surfaces. In an optimized protocol for retroviral transduction in RetroNectin-coated bags, Dodo *et al*. suggest that RetroNectin is better adsorbed onto materials such as polystyrene, cyclo-olefin, polyethylene, and Teflon compared to other materials such as ethylene vinyl acetate and polyolefin[55]. A major limitation of RetroNectin usage is its steep cost at $1,442 per 2.5mg of CGMP-grade product. The suggested surface concentration is 4-20μg/cm^2, which would be enough to coat one cell culture bag for a clinical trial.

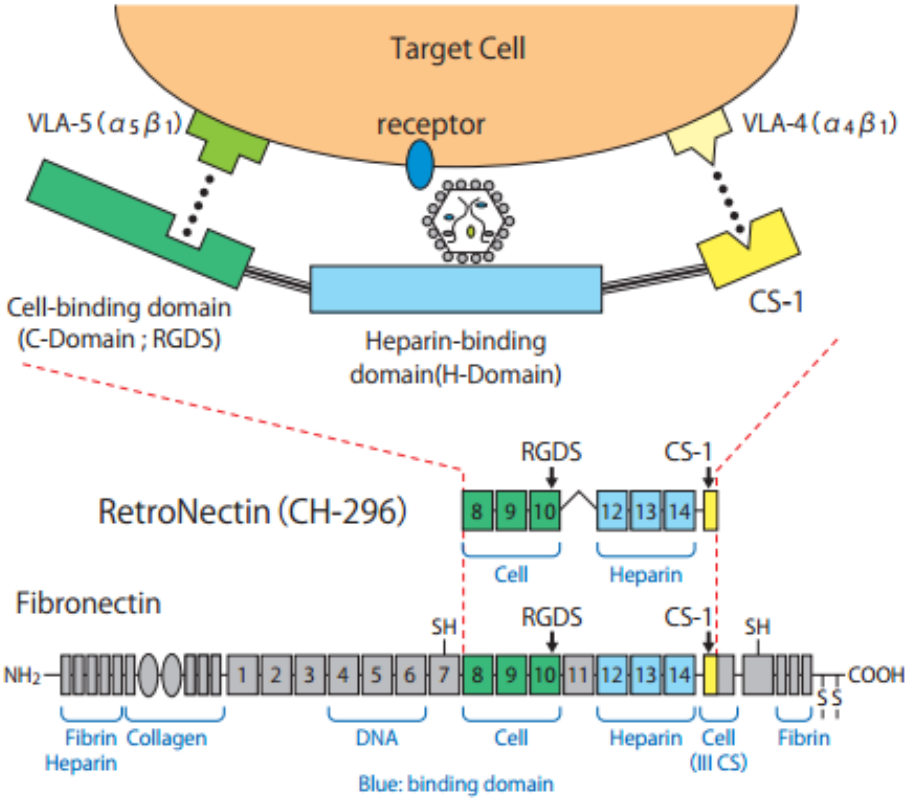

Figure 2.2: Hypothesized mechanism for RetroNectin enhancement of gene transfer. Cells can bind to the fibronectin RGDS cell-binding domain and the CS-1 site via VLA-5 and VLA-4 surface integrins, respectively. Retrovirus and lentivirus binds to the heparin-binding domain. Binding of cells and virus bring them in close proximity to enhance transduction efficiency. Image taken from Takara RetroNectin product manual.

2.3.3 Biological Adjuvants

Rapamycin is an immunosuppressive compound that is normally used to prevent organ transplant rejection. Recent studies have investigated the use of rapamycin for enhancing transduction efficiency of lentiviral vectors in hematopoietic stem cells. It was found to increase LV cytoplasmic entry through enhancement of endocytic events following LV binding (Figure 2.3)[56]. As such, rapamycin is the only transduction enhancing compound that acts by modulating cellular functions rather than enhancing nonspecific binding to the cell surface. More characterization of the effects of rapamycin are required, but FDA approval is still required since use in clinical transduction protocols would be off-label.

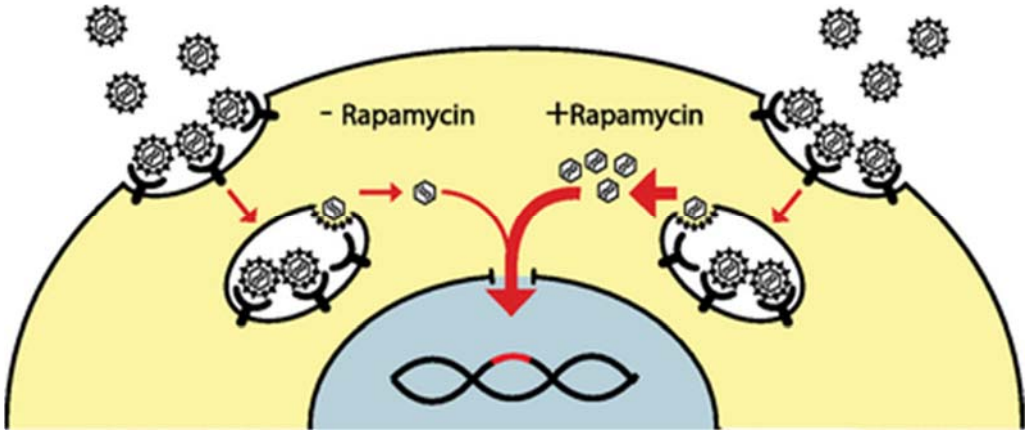

Figure 2.3: Rapamycin enhances post-binding viral entry into cells, which has the downstream effect of enhancing vector integration. Image taken from [56].

2.4 State of the Art Transduction Methods and Their Limitations

In addition to using additives for enhancement of transduction efficiency, alternative methods in the way transductions are actually performed have been developed in an effort to further enhance transduction efficiency. These include spinoculation, magnetofection, and flow-through transductions.

2.4.1 Spinoculation/Spinfection

Named for its mechanism of action, spinoculation or spinfection works by centrifuging virus and cells together so that the virus is deposited onto cells (**Figure 2.4**). Spin speeds on the order of 10^3 x g are typical to achieve enhancement[11]. However, ultracentrifugation is typically used to concentrate LV stocks, which requires centrifugation speeds as high as 25,000 RPM (10^4-10^5 x g)[57]. At such relatively low spin speeds, it is surprising that spinoculation works as proposed. Guo *et al*. showed that centrifugation at the elevated speeds enhance viral binding, entry, postentry DNA synthesis, and nuclear migration by modulating actin and cofilin activity rather than purely by virus sedimentation[58]. In addition to requiring cells to be exposed to high centrifugal forces, spinoculation protocols also require cells to be kept at room temperature for several hours outside of a CO_2 environment while spinoculation occurred. As such, it may not be suitable to cells that are sensitive to high gravitational forces or temperature and pH changes.

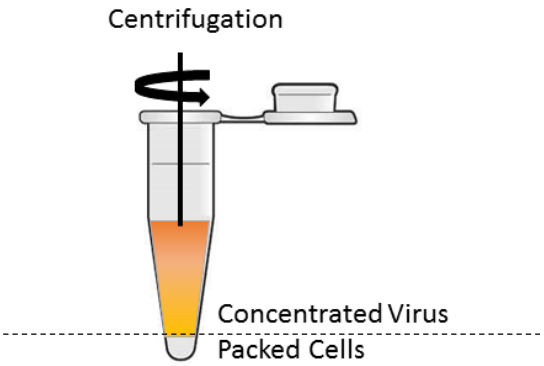

Figure 2.4: Spinoculation utilizes centrifugation to deposit viral particles onto cells.

In a related method, Le Doux *et al*. described a process in which cationic and anionic polymers were added at an equal-weight ratio were added to retroviral stocks to form high molecular weight precipitates consisting of retrovirus and polymer complexes, which could then be simply centrifuged at low speeds to deposit virus onto cells[59]. This method was shown to enhance gene transfer by 10-20 fold compared to the original retroviral stock formulation without the charged polymers.

2.4.2 Magnetofection – Magnetic Nanoparticle-based Transduction

Coupling LVs with magnetic nanoparticles have demonstrated some efficacy in enhancing transduction efficiency. Similar to spinoculation, this method relies on physically manipulating virus for deposition onto cells (**Figure 2.5**). Magnetofection was originally demonstrated for use with nucleic acids or adenoviral vectors, but ViroMag and LentiMag are both commercially available products that are marketed toward forming magnetic nanoparticle complexes with lentivirus or retrovirus to surpass diffusion limitations and enhance transduction efficiency[60]. Shamir *et al*. have demonstrated the use of the ViroMag system to transduce mammary epithelial organoids with LVs[61].

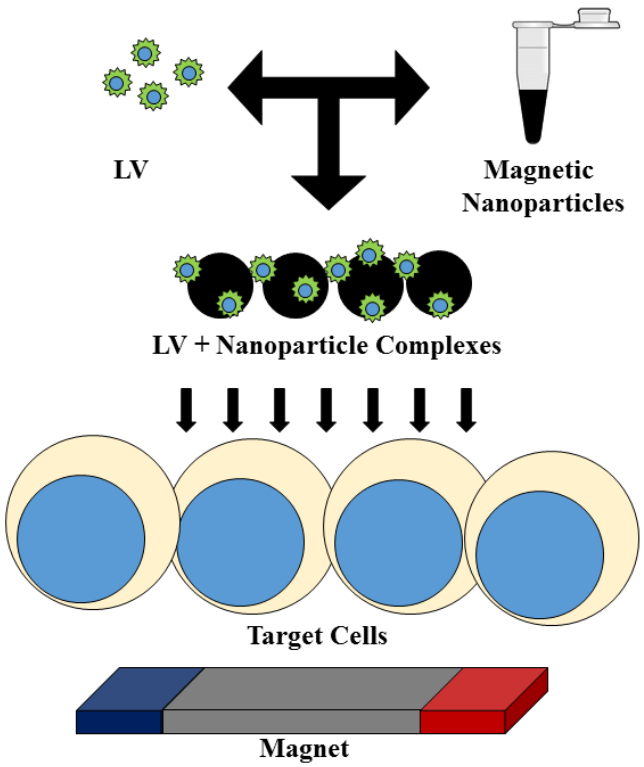

Figure 2.5: Schematic of magnetofection mechanism. Magnetic nanoparticles form complexes with virus, which are then brought into closer proximity with target cells using magnetic force to increase virus-cell binding.

2.4.3 Flow-through Transductions

Instead of relying on centrifugation or magnetic forces to bring virus to cells, Chuck and Palsson described a method that relied on fluid flow to direct retroviral particles to cells (**Figure 2.6**)[19, 62, 63]. The cells were immobilized on a porous mesh so that virus could come into contact with the cells while virus-containing media was passed through. Despite being conceptualized in the mid-1990s, this method has not gained widespread use in clinical gene therapy as initially proposed.

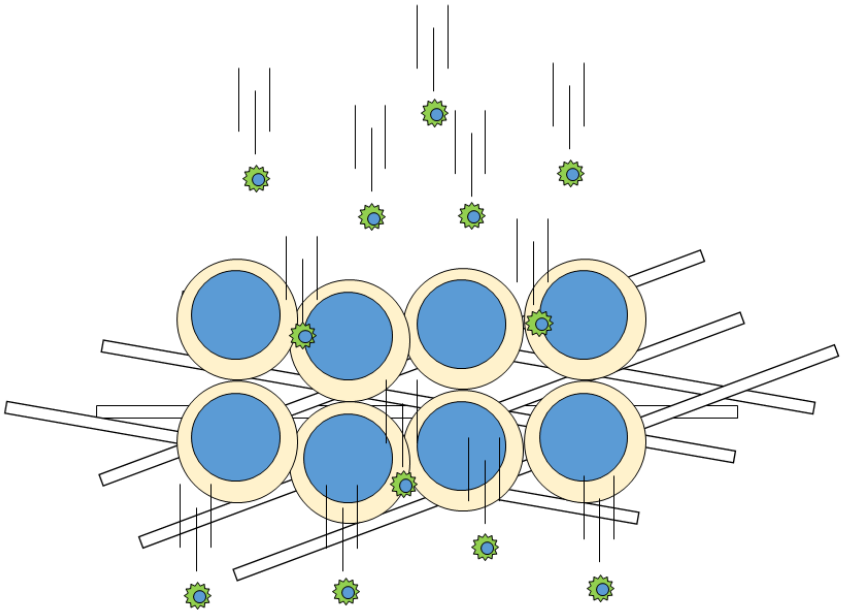

Figure 2.6: Schematic of flow-through transductions. Flow-through transductions require cells to be immobilized on a porous mesh while virus-containing media is flowed directly through the mesh so that viral particles are targeted directly at cells.

2.5 Problems with Standard Systems

2.5.1 Standard Systems Have Large Working Volumes

One of the major issues with standard systems is the large working volume, which drastically increases the LV requirements when LV v/v% is used as the standardized metric to determine vector dosage[16]. As such, the difference between a microfluidic and a comparable well plate could be as much as an order of magnitude greater LV usage (**Figure 2.7**). For a given surface area, fluid height/diffusion length also increases proportionally with total volume, further contributing to diffusion limitations.

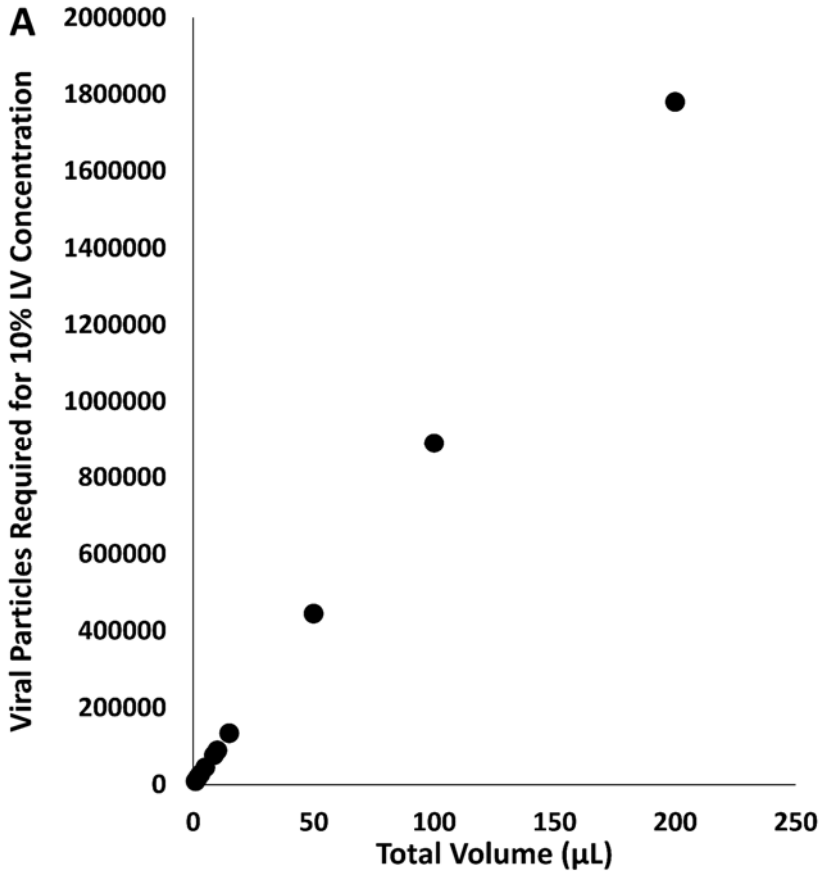

Figure 2.7: Microfluidics enable minimization of LV usage to maintain specific LV v/v% concentrations. Comparable systems requiring larger working volumes would significantly increase LV requirements to maintain the same concentration.

2.5.2 Diffusion Limitations

Related to the issue of large working volumes are diffusion limitations. Static transductions rely on Brownian motion for the transport of viral particles to cells[19]. However, retroviral and lentiviral vectors have been shown to have short half-lives of 6-10 hours[64]. From an estimation of mean square displacement of a retroviral particle with an 8-hour half-life, Chuck *et al*. estimated that the viral particle would only be able to be displaced 480-610µm by Brownian motion within one half-life[19]. Therefore, most of the virus is wasted in standard diffusion limited systems, making microfluidics a suitable

platform to natively enhance transduction efficiency while maintaining compatibility with the additive compounds and state of the art technologies aimed at increasing transduction (**Figure 2.8**).

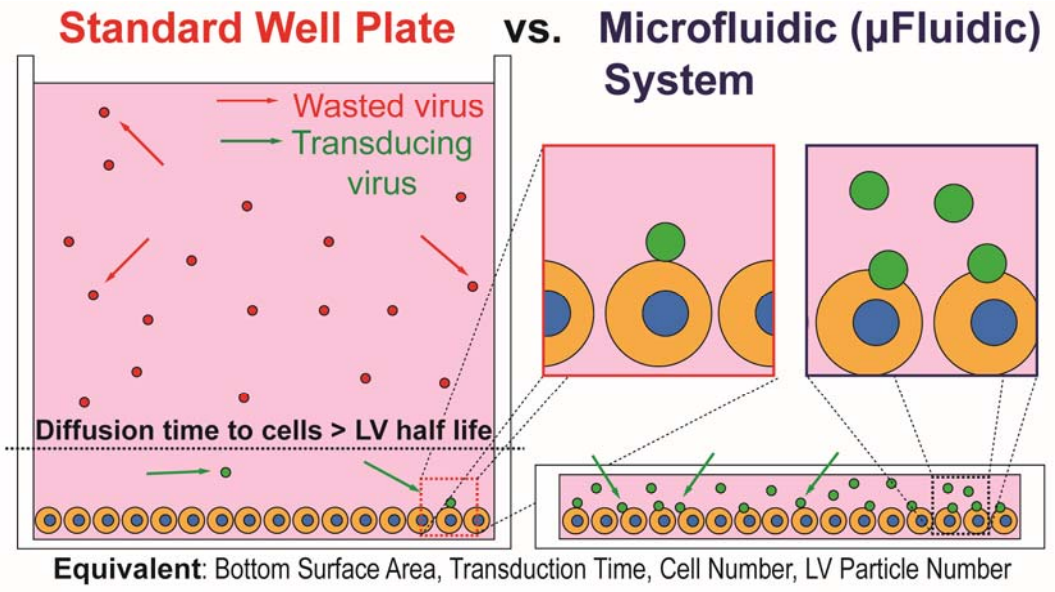

Figure 2.8: Schematic of issues with diffusion-limited systems. Microfluidics are a potential solution to overcoming these diffusion limitations for enhanced transduction.

2.6 Titration of Lentiviral Vectors

One of the major issues leading to wasteful usage of vector arises from the fact that determination of the number of infectious particles are in a given LV preparation stock solution is non-trivial and subject to extreme variability with differences on the scale of orders of magnitude[65]. Here we discuss some of the different methods currently used to calculate titer, and describe some issues associated with these methods.

2.6.1 Physical Titer

Enzyme-linked immunosorbent assays (ELISAs) can be used to measure the p24 antigen, which is a component of the envelope protein for VSV-G pesudotyped LVs[46].

Quantification of titer using this method gives the amount of vector particles in nanograms, though it does not necessarily correlate with functional vector particles[66]. As such, the physical titer may often be an overestimate of the actual amount of infectious particles due to the detection of unincorporated p24[67]. Using this method, serial dilutions of vector are tested using ELISA kits for the p24 antigen, and an average titer can be calculated.

2.6.2 Biological Titer

By including a reporter gene such as GFP in the transfer plasmid, a biological titer can be calculated by transducing cells with serial dilutions of the vector stock and assessing transduction using flow cytometry. From this method, the number of transducing units (TU) can be calculated per microliter (TU/μL) can be backwards-calculated from the percentage of transduced cells, the number of cells plated at the time of transduction, and the volume of vector added to each condition[46, 68]. However, vector integration does not perfectly correlate with protein expression due to position-effect variegation[69]. Since the transgene integrates at semi-random locations, the gene may sometimes remain inactive despite integrating into the genome due to abnormal positioning with the heterochromatin. This method may also be combined with RT-PCR to quantify how many copies of the vector transgene have integrated into the target cells, though the issues of diffusion limitation may still cause the titers to be underestimated using this method[15, 16]. Together, these various methods are used to correlate the amount of input vector with gene expression of transduced cells (**Figure 2.9**)[66]. The serial dilutions must cover a wide enough range such that the upper limit results in a saturation of vector, leading to a plateau in transduction. By calculating the slope of the linear portion of the curve, the titer of infectious transducing units can be estimated for future experiments.

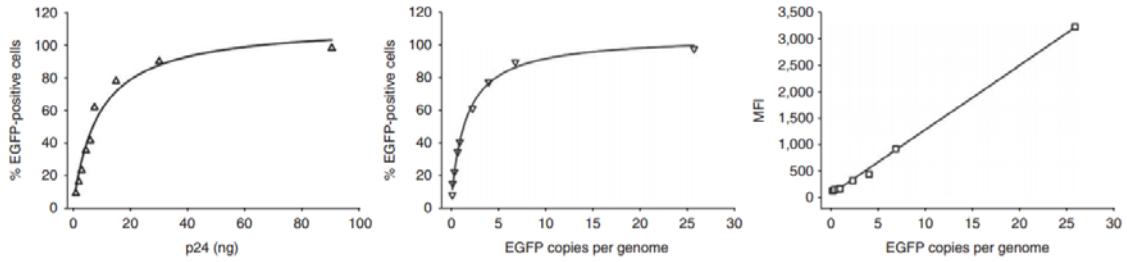

Figure 2.9: Examples of titration curves for lentivirus titer determination. Calculations are made by calculating the slopes of the linear portions of the curves. Image taken from [66].

2.7 Multiplicity of Infection is Unsuitable to Predict Transduction

In the fields of gene therapy and virology, the multiplicity of infection (MOI) is a parameter that is commonly used to define a particular dosage of viral vector. It is given by the ratio of viral particles to the number of target cells exposed to virus. Having a 1:1 virus to cell ratio, with the MOI being equal to 1, does not guarantee that every cell will be infected by a single virus. Viral entry is a statistical process in which some cells will remain uninfected while others will be infected by multiple viruses. The population of infected cells is therefore best described by a Poisson distribution.

The Poisson distribution is a discrete probability distribution that gives the probability of an event occurring over time or space given a known average instance of occurrence (Equation 1).

$$P(k\ events\ in\ interval) = \frac{\lambda^k e^{-\lambda}}{k!} \qquad (1)$$

Where k is the number of events to be observed and λ is the average number of events per interval.

In the context of viral infections, if there is a single viral particle and a single cell within a confined space, the cell should theoretically be infected once given sufficient time. This corresponds to a MOI of 1. Therefore, λ is equivalent to the MOI, which represents 1 viral infection per cell. In practical terms, transductions usually target anywhere from thousands to millions of cells rather than just a single cell. As the number of cells increase over a given area, the number of viral particles added to the system must also increase to maintain the 1:1 virus:cell ratio for MOI 1. Due to the increased number of targets for the viral particles, there is now a heterogeneous population of cells that have varying numbers of viral infections. The Poisson distribution can therefore approximate the distribution of probabilities for a given cell being infected by k viral particles with a specified MOI, λ. With this information, the percentages of cells containing at least 1 vector copy can be approximated by calculating the probability that a cell remains uninfected and subtracting from unity (Equation 2).

$$P(\geq 1) = 1 - P(0) = 1 - \frac{\lambda^0 e^{-\lambda}}{0!} = 1 - e^{-\lambda} \qquad (2)$$

Defining the multiplicity of infection with these assumptions provides a theoretical framework for determining how many cells can ideally be transduced for a given MOI. This defines the upper limit of transduction. In practical usage, there are definite limitations. The viral particles are not stable, and have a half-life on the order of hours when incubated with cells at 37°C[64, 70]. Furthermore, diffusion limitations prolong the time taken for viral particles to reach cells, making it so that many viral particles will never have a chance to reach cells before decaying. Biological differences such as expression levels of

the receptors to the virus envelope will also determine binding of cells to virus for infection[71]. This can drastically create discrepancies in observed transduction versus theoretical achievable transduction based on MOI. For this reason, MOI has been criticized as an unreliable parameter[16, 72]. Since determination of viral titer is also diffusion limited, different theories regarding viral infectivity and titer have been generated. Some groups have posited that there are mixtures of infectious and non-productive viral particles while others have argued that it may not actually be an issue, and diffusion limitations play a larger role[19, 73].

CHAPTER 3: DEVELOPMENT OF A MICROFLUIDIC PLATFORM FOR LENTIVIRAL TRANSDUCTION

3.1 Introduction

The creation of an entirely new interdisciplinary field began with the realization that semiconductor technology, traditionally used for the production of microchips, could be used for analysis and manipulation of fluids at the microscale. Early usage of microfluidic technology began with chemical analysis, providing benefits such as miniaturization and low reagent consumption with high sensitivity. Since then, microfluidic utility has expanded to a multitude of applications including molecular analysis, diagnostics, cell assays, physiologically recapitulated *in vitro* systems, cell sorting, and various other fields of biomedical research.

3.2 Fabrication Techniques Used for Lentiviral Transduction Microfluidics

Microfluidic devices can be produced using a variety of methods depending on material choice or the tolerances required, which are determined largely by the constraints of the application. Devices that rely heavily on precise fluid physics often rely on advanced fabrication techniques that require cleanroom facilities and expensive equipment. Alternative relatively inexpensive fabrication techniques exist, which can greatly reduce the complexity of production while retaining key advantages conferred by microfluidics. However, reproducibility and resolution are lost using these techniques compared to more traditional techniques. The following sections will cover different fabrication methods used to produce microfluidic devices for lentiviral transduction.

3.2.1 Photolithography

Of all methods used to produce the microfluidic lentiviral transduction devices for this study, photolithographic methods enable the highest resolution and reproducibility, but require the most time and specialized equipment to generate. A master mold, usually consisting of a silicon or glass wafer patterned with a photosensitive epoxy called photoresist, must be made in a cleanroom. SU-8 is a popular choice of photoresist for soft lithography due to its ease of use and durability. Typically, a computer aided design (CAD) drawing of the microfluidic devices is submitted to a photomask company for production. The photomask is a soda-lime glass or quartz substrate coated with a layer of chrome, in which laser etching or electron-beam lithography is used to produce the desired patterns. These methods of patterning can be used to produce extremely high resolution photomasks, down to the sub-micron scale depending on the method used and the limitations of the tools. The master molds that are used to produce the actual microfluidic devices are made by patterning photoresist onto a glass or silicon wafer by exposing ultraviolet (UV) light through the photomask, which either crosslinks the photoresist or makes it soluble to special chemicals known as developer solution depending on the type of photoresist used.

The microfluidic devices themselves are typically made from an optically transparent silicone elastomer known as polydimethylsiloxane (PDMS). A crosslinking agent is typically mixed with the PDMS at a 1:10 ratio (crosslinker:PDMS), which hardens the PDMS as the crosslinker evaporates. Increasing the temperature accelerates the reaction. Curing PDMS on the silicon master molds results in the transfer of patterns to the PDMS. In the case of microfluidic channels, the master mold consists of raised features of the channel patterns, which become trenches in the PDMS when peeled from the mold.

After punching inlet and outlets and covalently bonding to another PDMS or glass surface using a plasma bonder, the trenches are sealed, resulting in a fully enclosed microchannel. This method can be repeated hundreds of times to consistently produce microfluidic devices as long as the integrity of the master mold is maintained. A schematic of the process is shown below in **Figure 3.1**[74] and an example of the SU-8 mold used for microfluidic lentiviral transduction is shown in **Figure 3.2**.

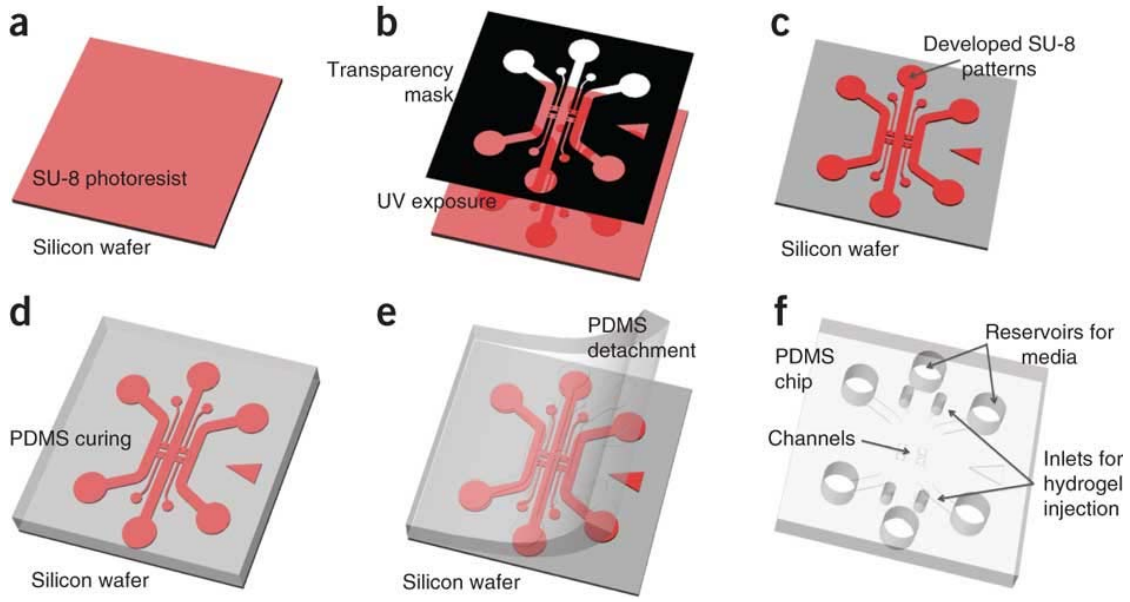

Figure 3.1: Schematic of fabrication process for microfluidic devices using photolithography and soft lithography. (a) SU-8 photoresist is spun onto a silicon wafer. (b) UV light is exposed to the photoresist through a photomask or transparency to transfer the pattern. (c) Uncrosslinked photoresist is removed using photoresist developer. (d) PDMS is poured and cured on the mold. (e) The PDMS is cut and detached from the mold. (f) Inlet and outlet holes are punched, and the channel is covalently bonded to a flat sheet of PDMS or glass using oxygen plasma. Image is taken from [74].

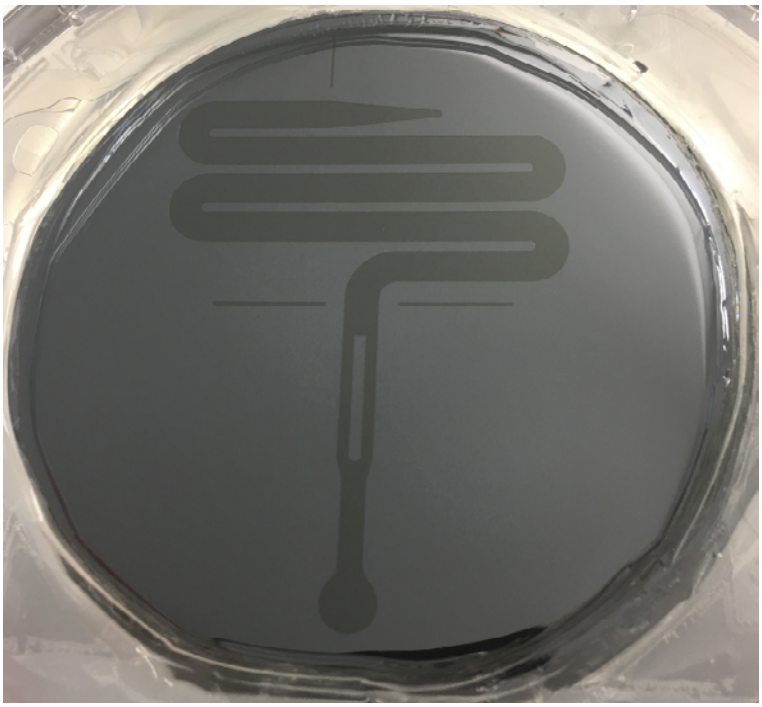

Figure 3.2: Silicon mold of scaled up transduction device made using photolithography. Scale bar = 10 mm.

3.2.2 Computer Numerical Controlled Micro-milling of Master Molds

For larger devices that do not require high resolution features, computer numerical controlled (CNC) micro-milling can be used to produce metal master molds[75]. Depending on the channel design, producing a master mold with this method may actually be preferable since producing a thick uniform layer of photoresist is not always feasible. The turnaround time to produce a master mold from a CAD drawing is also much faster than possible with photolithography using this method. However, this technique is limited to a minimum height of approximately 200µm and minimum feature gaps of 381µm (0.015”). In this study, a CNC mill (HAAS OM 1) (**Figure 3.3a**) was used to remove material from the top surface of an aluminum block using a 1/16” end-mill to a depth of ~200µm. The spindle speed used was between 20,000 and 25,000 RPM at a feed rate of 5”/min. The

scaled up transduction device was large enough that there were no issues achieving the desired channel widths. After a few de-burring steps and smoothing, the aluminum master mold can be used similarly to a silicon master mold (**Figure 3.3b**). However, the channel walls will not be as smooth, though this was not critical for the transduction devices.

Figure 3.3: Examples of CNC mill and resulting microfluidic mold. **A)** HAAS OM 1 CNC mill used to produce aluminum molds for microfluidics. **B)** Resulting aluminm mold of scaled up transduction microfluidic. Scale bar = 10mm.

3.2.3 Microfluidic Xurography

For rapid prototyping of microfluidic designs, microfluidic xurography can be used to produce devices without requiring master molds entirely[76]. Xurography refers to the process of creating patterns with the use of a razor blade. This can easily be achieved with an inexpensive craft cutter, which is normally used for cutting patterns into paper, vinyl, or other similar sheets. Instead, microfluidic devices can be made by cutting patterns into thin films or double-sided adhesives. The lentiviral transduction microfluidics used in this study were produced by cutting patterns into a silicone double-sided adhesive (3M, St.

Paul, MN, USA) with a Silhouette craft cutter (Silhouette America, Inc., Lindon, UT, USA). The patterned adhesive was then applied to either a polystyrene petri dish or a flat sheet of PDMS, which served as the base. A thicker block of PDMS with pre-punched inlet and outlet ports was then adhered to the top surface of the silicone adhesive to fully seal the channel. The thickness of the adhesive layer determines the channel height. The entire process is summarized in **Figure 3.4**. Due to minor perturbations as the razor blade is dragged across the surface, the cut silicone adhesive becomes frayed, resulting in a microfluidic channel with smooth top and bottom surfaces from the PDMS/polystyrene, but rough sidewalls. Decreasing the cutting speed helps to reduce the roughness, but the sidewalls will never be as smooth and well-defined compared to microfluidics made from a silicon master mold. However, this method was sufficient to produce rapid prototypes for the microfluidic lentiviral transduction device. Previous studies have determined that the resolution for this technique are dependent on the cutter, but also by factors such as blade angle, cutting speed, and the type of cutter used[77]. The resolution is in the range of 200μm.

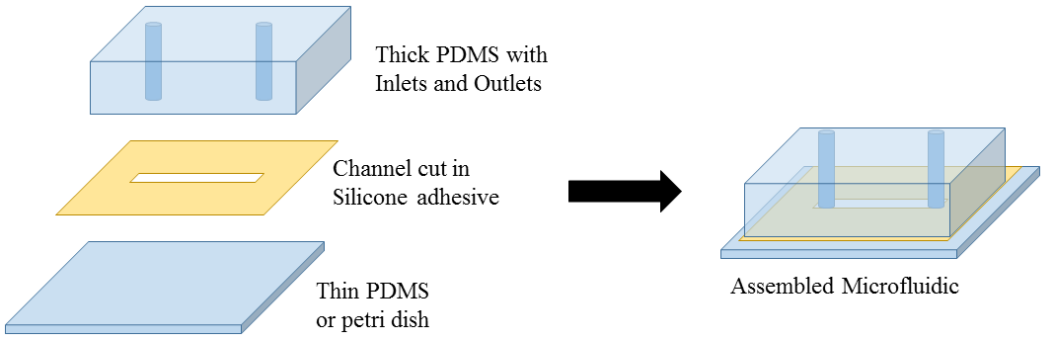

Figure 3.4: Schematic of simplified microfluidic fabrication using xurography. A craft cutter is used to cut channel patterns in a double-sided silicone adhesive. The adhesive is transferred to a thin piece of PDMS or petri dish and then sealed off with a thicker piece of PDMS with inlet and outlet ports punched in.

3.2.4 Hot Embossing of Thermoplastics

Though most microfluidic devices are made from PDMS, some applications require the microfluidics to be made from different materials. Thermoplastics are a popular alternative for mass production of disposable microfluidics, though up front tooling costs make it undesirable for prototyping of different devices designs. To that end, we developed a simplified prototyping method to produce polystyrene microfluidics from PDMS molds (**Figure 3.5**)[78]. Using PDMS molds enables micro-scale patterns beyond the resolution of other fabrication techniques to be transferred directly to the polystyrene[79]. Other embossing methods have higher production throughput, but require specialized tools such as a heated hydraulic press, and are more limited in feature resolution[80].

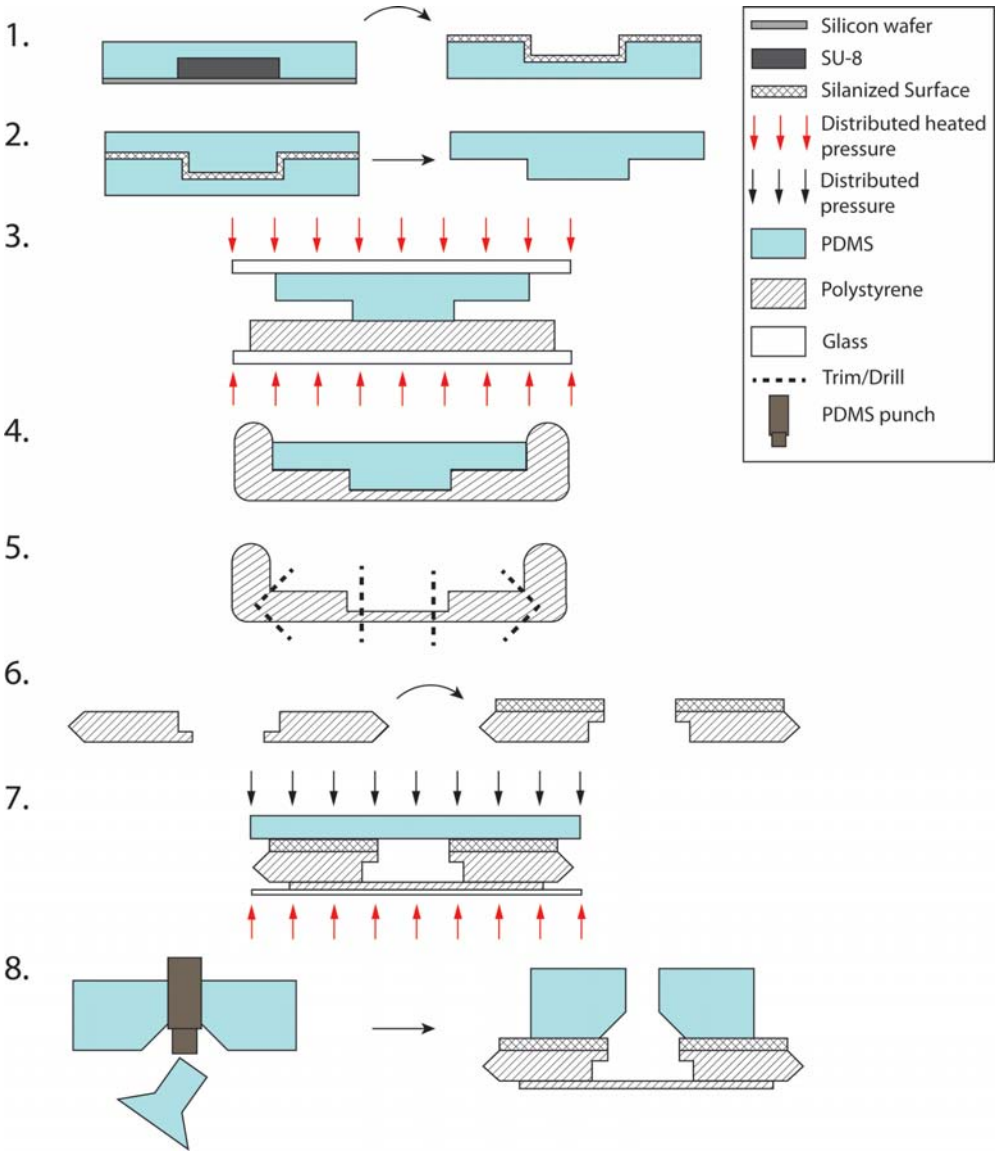

Figure 3.5: Schematic of perfusable PS device fabrication for cell culture. (1) Cut out a PDMS mold from patterned photoresist of the desired channel geometries and treat with HMDS. (2) Pour PDMS (5:1 ratio PDMS:crosslinker) onto the HMDS treated mold and cure to produce a PDMS die with raised features of the channel. (3) Emboss the channel into a PS slide using the PDMS die in a convection oven. (4) Allow the PS to cool before removing pressure. Edge beads will form around the perimeter. (5) Trim the edge beads off and drill inlet and outlet ports. (6) Silanize the top surface. (7) Thermally bond a thin sheet of PS to the embossed PS using approximately 10 kPa pressure for 5 min. (8) Create a PDMS port with tapered holes and plasma treat the device and PDMS to covalently bond.

From an SU-8 master mold, the peeled PDMS can be treated with hexamethyldisilizane (HMDS) for use as a PDMS master mold, which can then be used to

cast additional PDMS to obtain a negative of the original pattern. The negative pattern serves as a PDMS die, which can be used to transfer the pattern directly to a thermoplastic such as polystyrene when distributed heat and pressure are applied. The embossed polystyrene channel can then be coupled with a thin sheet of bare polystyrene to thermally bond the two pieces together, sealing the channel. Following silanization treatment of the embossed polystyrene using (3-Aminopropyl)triethoxysilane (Sigma-Aldrich, St. Louis, MO, USA), a bare block of PDMS with pre-punched inlet and outlet ports can be plasma bonded for use as an adapter for inlet and outlet ports. Using a PDMS die for pattern transfer results in smooth surfaces, though deformation of the PDMS can occur if the embossing pressure is too high, resulting in altered channel dimensions.

However, under optimized conditions, uniform channel dimensions can be reproduced without distorting the cross-sectional area as shown by 3D material confocal scanning (**Figure 3.6a**) and confocal microscopy z-stack of a polystyrene channel filled with fluorescently tagged bovine serum albumin (BSA) (**Figure 3.6b**). The devices were also robust enough to withstand high enough shear stress for HUVEC flow culture. No device leakage was observed for shear stress below 300 dyn/cm^2, with critical failure consistently occurring at shear stress of 700 dyn/cm^2 or higher (**Figure 3.6c**).

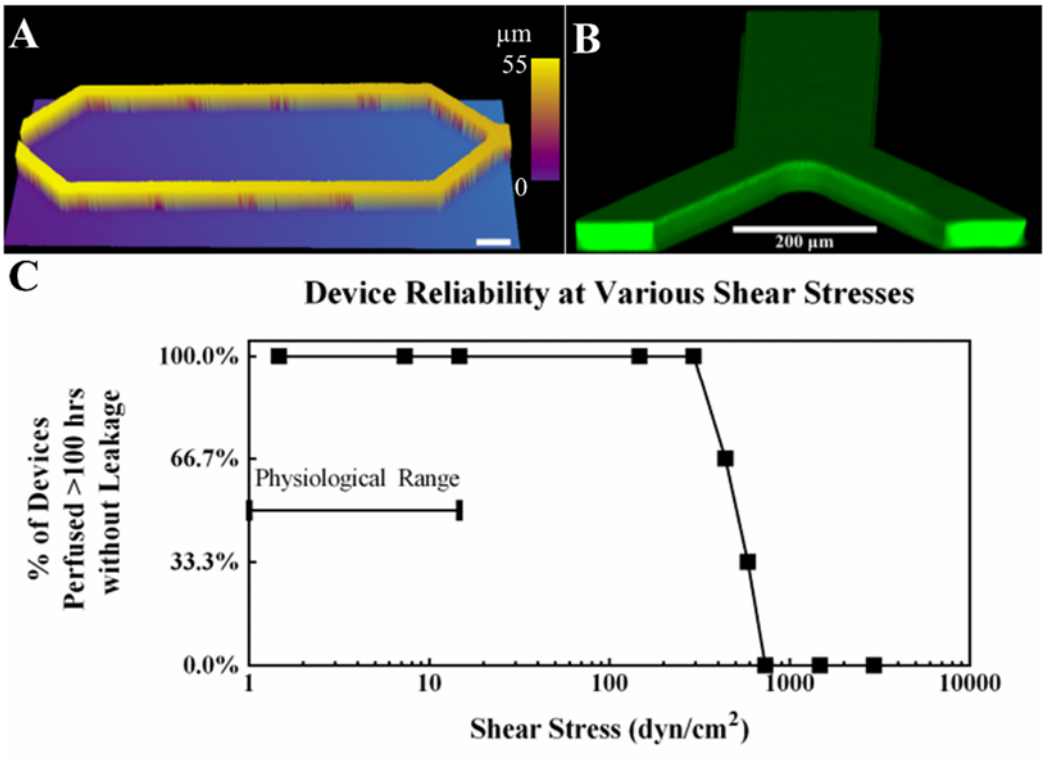

Figure 3.6: PS device characterization. **(a)** 3D laser material confocal scan of embossed channel profile. **(b)** Reconstructed z-stack of bonded channel filled with fluorescent BSA. **(c)** Plot of the percentage of devices that were able to be perfused continuously for at least 100 hours without leakage for various shear stresses. n = 3. Scale bars = 200 µm.

Finally, we determined that polystyrene microfluidics could be used to culture human umbilical vein endothelial cells (HUVECs) under flow to achieve a confluent monolayer encompassing all surfaces and adopting a phenotype that aligned with the flow, which was the first demonstration of perfusion-based HUVEC culture in a polystyrene microfluidic of size scale less than 100µm (**Figure 3.7a and b**).

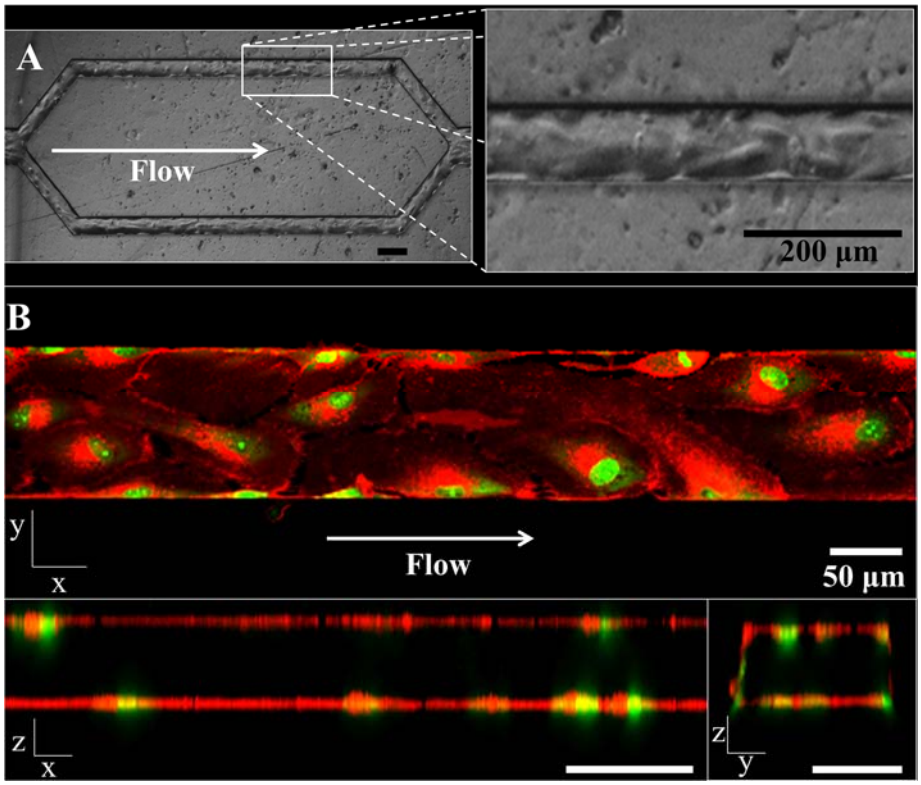

Figure 3.7: Endothelialization of PS device. **(a)** Phase contrast images of zoomed out branch region. **(b)** Confocal fluorescence image of endothelial cells in the smallest branch (width < 100 µm) with orthographic views showing flow alignment and confluency along all channel walls. Red = cell membrane and green = cell nuclei. Black scale bars = 200 µm and white scale bars = 50 µm.

Although a cleanroom is still required to produce the initial master mold, all additional steps can be completed using common equipment found in most laboratories. This method serves as a simple way to prototype thermoplastic microfluidic designs. Once a suitable design is selected, more advanced methods such as injection molding can be used to produce higher quality microfluidics with greater throughput.

3.3 Material Selection

Microfluidic devices can be made from a variety of materials with the earliest types being made from silicon and glass[81]. With the development of soft lithography, PDMS

offered a robust alternative that simplified production and became a mainstay for microfluidic device material selection[82]. As the applications of microfluidics expanded, different material properties were required, prompting the exploration of alternative material choices. Thermoplastics such as polystyrene and polymethylmethacrylate were thus used due to their higher stiffness and decreased permeability[83]. Finally, demand for more physiologically compatible long-term culture of cells in microfluidics called for hydrogel microfluidics[84, 85]. For the lentiviral transduction microfluidics, ease of fabrication and protein adsorption were determined to be the most important properties affecting material selection. As such, all microfluidic devices designed for lentiviral transduction were made from either PDMS or polystyrene.

3.3.1 Polydimethylsiloxane (PDMS)

From the conception of soft lithography, polydimethylsiloxane (PDMS) has been greatly favored by bioengineers due to its prototyping cost-effectiveness, ease of use, and high level of reproducibility from master molds, enabling a large range of microfluidic applications for biological research including cell analysis and cell culture[86]. In determining different design considerations for a microfluidic lentiviral transduction platform, devices made entirely from PDMS were the path to greatest consistency and production throughput. Furthermore, the elasticity of PDMS allows for loading of cells and connection of tubing to a syringe pump for media exchange since the PDMS can deform to produce an interference fit. Gas permeability is another important characteristic of PDMS, since it allows for crucial gas exchange to occur within the microchannels and provides a means of removing any air bubbles that form within the device.

Most importantly, PDMS is generally accepted to be biocompatible[87]. PDMS-based microfluidics have been used for *in vitro* recapitulation of the microvasculature due to the small size scale and flow-based cell culture made possible by microfluidics. These studies have shown that cells can be cultured within microfluidics for several days with no negative effects on cell viability or alterations to cell physiology (**Figure 3.8**)[88].

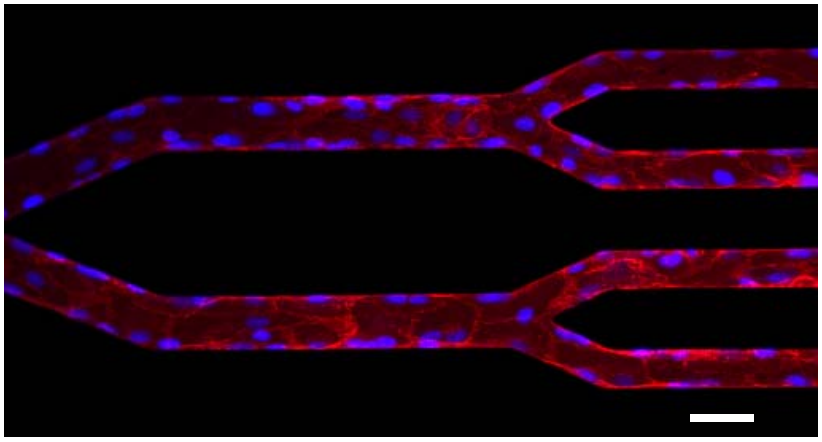

Figure 3.8: Example of HUVEC culture in PDMS microfluidics. Red stain is a membrane dye. Blue stain is a nuclear dye. Scale bar = 50μm.

Moreover, PDMS typically has poor cell adhesion properties, requiring functionalization with adhesive proteins[89]. Taken together, these properties demonstrated potential for PDMS to be used in a microfluidic lentiviral transduction platform since cells have been shown to remain viable in microfluidic culture for the duration of typical transduction protocols and PDMS exhibits tunable adhesion for efficient cell removal or immobilization for flow-based transductions.

3.3.2 Polystyrene

Polystyrene was another suitable material choice for the lentiviral transduction microfluidic. As the most characterized and commonly used substrate material for cell

culture, it was conceivably beneficial for microfluidic cell culture to be conducted in polystyrene-based microsystems[23]. In addition, there have been a few reports of potential drawbacks of PDMS-based devices, including uptake of small hydrophobic molecules from the media, leaching of uncrosslinked oligomers into the culture media, and hydrophobic recovery of the channel surfaces, which were of concern since cells would have to be transduced within the microfluidic for at least several hours to as much as several days[90]. Finally, RetroNectin, a recombinant fibronectin fragment that contains binding domains for both non-adherent cells and lentivirus for increased virus-cell contact, has been suggested to be optimally adsorbed onto polystyrene, cyclo-olefin, polyethylene, or Teflon[55].

From our experience with endothelialized polystyrene-based microfluidics, we initially explored hot embossed hybrid PDMS-polystyrene microfluidic devices for our microfluidic lentiviral transduction platform. In addition to a RetroNectin coating, our device contained embossed micro-divots to provide greater surface area for increased cell adhesion during flow-based transductions. By applying the same silanization technique directly to the embossed polystyrene channel[91], we were able to produce a hybrid PDMS-polystyrene microfluidic that could efficiently immobilize cells on the bottom polystyrene surface while retaining gas permeability for long term cell culture. The modified fabrication process is shown below in **Figure 3.9**.

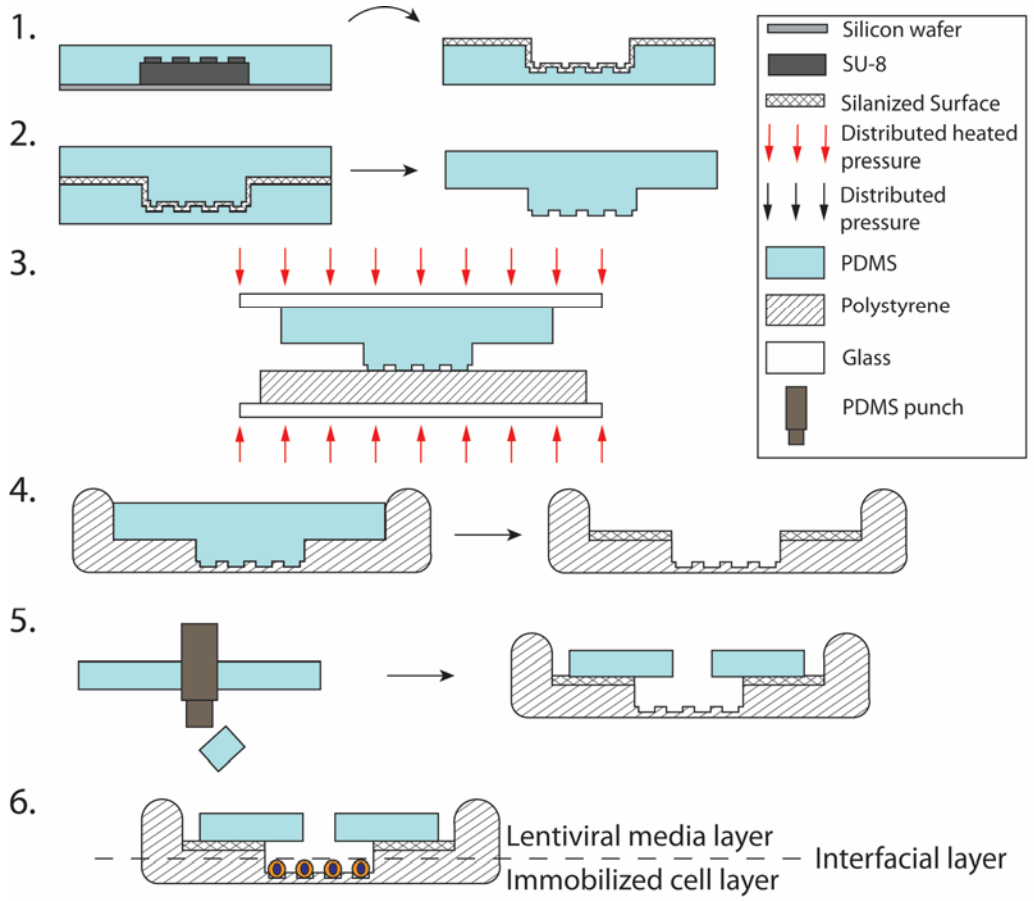

Figure 3.9: Schematic of hybrid polystyrene-PDMS device, which can be used for lentiviral cell transduction. Steps 1-4 are similar to those shown in **Figure 3.5**. Briefly: (1) Cut PDMS from silicon mold and HMDS treat. (2) Pour PDMS (5:1 PDMS:crosslinker) in HMDS-treated PDMS mold to produce a PDMS die. (3) Emboss. (4) Allow to cool and remove die. Additional trimming is not necessary. Silanize the top surface. (5) Punch inlet and outlet ports in a flat slab of PDMS and align with the embossed channels (6) The completed device will enable non-adherent cells to be immobilized in the embossed divots within the emboss channels, allowing for an immobilized cell layer to come into homogeneous contact with a lentiviral media layer.

Although we were able to achieve enhanced transduction based on estimates from image analysis (**Figure 3.10a and b**), we determined that the hot embossing method was unsuitable for the production throughput required in order to properly characterize the system as a lentiviral transduction platform. Furthermore, scaling up toward clinically relevant cell numbers would not be trivial. We investigated if traditional PDMS-based

microfluidics could be sufficient by assessing three key parameters: 1) Long-term culture of cells for 28-48 hours, 2) Efficient cell removal from the devices, and 3) RetroNectin immobilization efficiency.

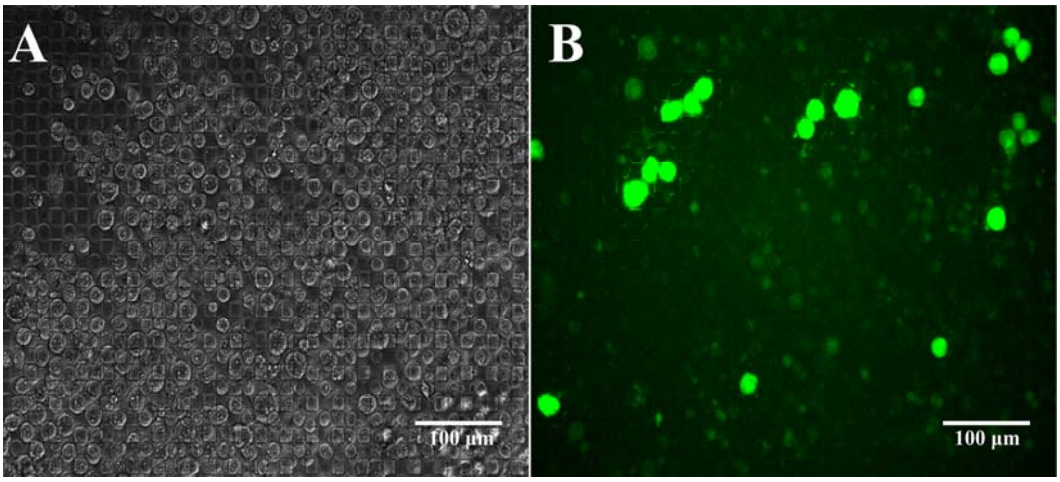

Figure 3.10: K562 cells transduced in the hybrid polystyrene-PDMS device. **(a)** Phase contrast image of K562 cells immobilized in the divots. **(b)** Fluorescence image of cells expressing GFP after 24 hours of perfusion of lentiviral media followed by a 96 hour incubation period. Cells can be seen expressing GFP at various levels. Scale bar = 100 µm.

3.4 PDMS-based Device Characterization

3.4.1 RetroNectin Immobilization Efficiency

Although RetroNectin is optimally adsorbed onto plastic surfaces such as polystyrene and cyclo-olefin[55], we sought to determine if RetroNectin adsorption to PDMS would also be sufficient since many other adhesive proteins such as fibronectin, collagen, and fibrinogen have been shown to be effectively adsorbed onto PDMS surfaces for cell culture[88, 89]. Using a surface concentration of 1.05 µg/cm^2, we were able to conclude that having RetroNectin did indeed have an impact on cell immobilization, as demonstrated by

cell retention after mild perfusion at 1 μL/min ($\dot{\gamma}$ = 2.4 s^{-1}) (**Figure 3.11a and b**). This surface concentration is nearly fourfold less than the recommended minimum surface concentration from the Takara product specifications. To avoid having to use trypsin or high flow rates to remove cells from the device, we used the minimum empirical surface concentration that would immobilize most of the cells for the lower range of flow rates examined for flow-based transductions.

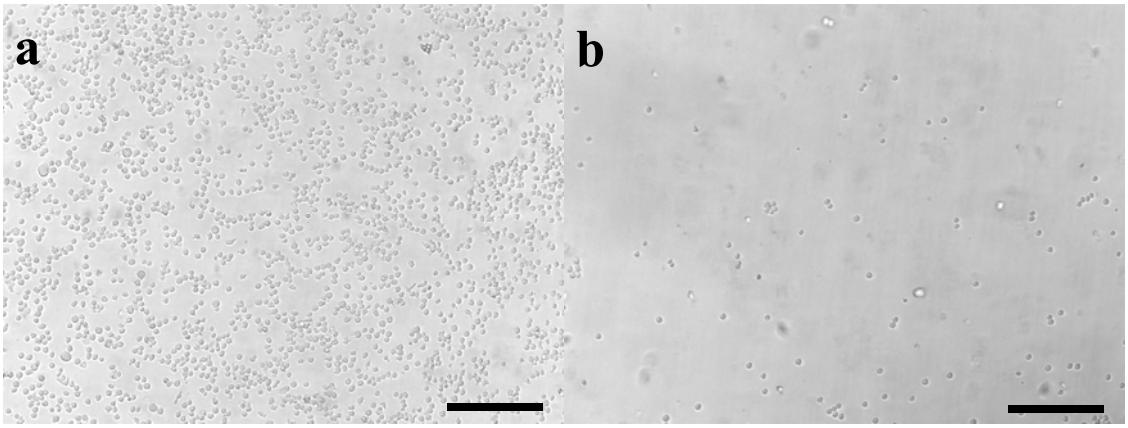

Figure 3.11: Assessment of RetroNectin coating on PDMS. a) RetroNectin-coated microfluidics or b) negative control bare microfluidic following mild perfusion. Scale bars = 100μm.

Quantitation of the RetroNectin immobilization efficiency was characterized by loading cells inside PDMS microfluidics compared to polystyrene 6-wells, with and without RetroNectin coatings. Cells were incubated for 2 hours to allow cells to settle and adhere to the bottom surfaces. The microfluidics were perfused with PBS for one hour at a flow rate of 1mL/hr. Effluent containing non-immobilized cells were collected and counted following perfusion. The 6-well plates were similarly flushed with PBS, and aspirated to collect non-immobilized cells. The number of cells recovered from flushing were compared to the initial cell count loaded into the microfluidics and 6-wells to obtain a

percentage of cells recovered from flushing (**Figure 3.12**). No significant differences were detected between cell recovery from 6-wells and microfluidics, though RetroNectin coatings significantly decreased cell recovery after flushing (2-way ANOVA, $p<0.001$).

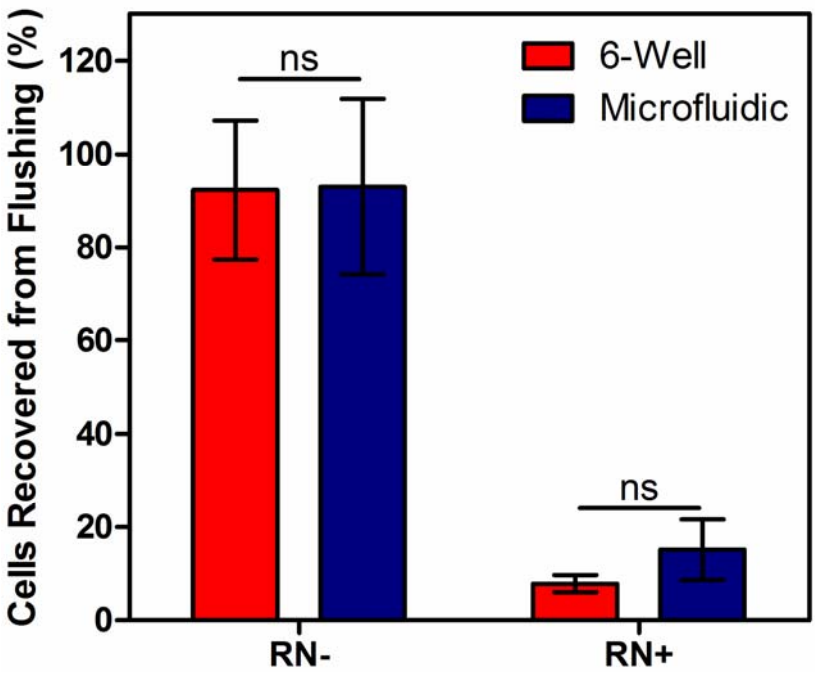

Figure 3.12: Cell immobilization quantification with and without RetroNectin in polystyrene microfluidics compared to PDMS microfluidics.

3.4.2 Cell Recovery Efficiency

For shorter transduction times, the RetroNectin coating may not be necessary since transductions can be performed under static conditions without the need for media exchange by perfusion. Under these conditions, it is preferable to minimize cell adhesion to the microfluidic surfaces. To determine if there was any significant non-specific adhesion that reduced cell recovery from the devices, we incubated bare microfluidics and

6-wells with 1, 2, and 4 million cells for 5 hours and compared them to cell count controls to obtain a recovery percentage (**Figure 3.13**).

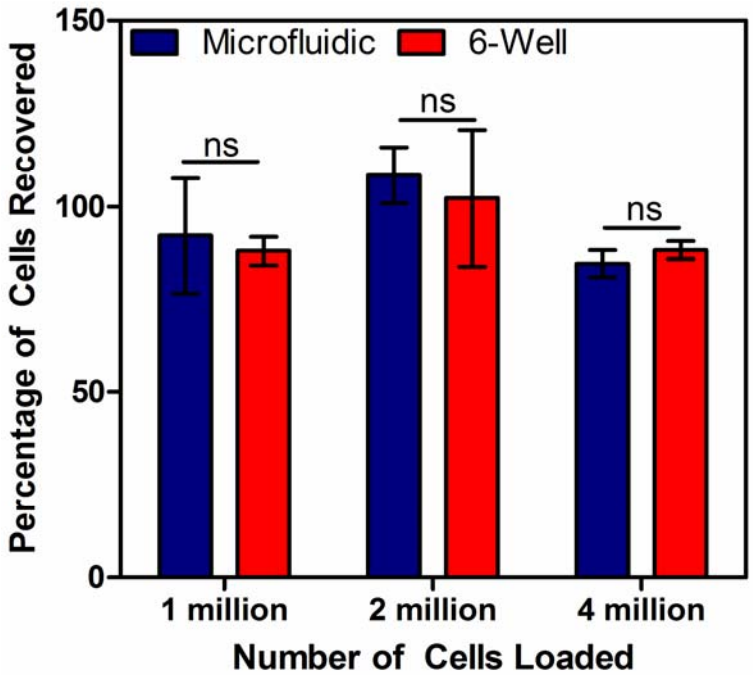

Figure 3.13: Cell recovery efficiency of microfluidics versus 6-wells for various cell numbers.

No significant differences in cell recovery were observed between the microfluidic and 6-well, indicating that use of PDMS-based microfluidics for lentiviral transduction does not result in decreased yield compared to standard systems.

3.4.3 Long-term Microfluidic Cell Culture

Typical transduction protocols call for exposing cells to virus overnight, and often require multiple rounds of transduction, which could result in up to 48 hours of exposure to vector[92]. To ensure that a PDMS-based microfluidic lentiviral transduction system

would be suitable for long term immobilization and cell culture without adverse effects, we transduced and cultured cells under flow in RetroNectin-coated devices. A mixture of virus and cells were loaded into devices. Cells were incubated for 2 hours to allow most of the cells to settle to the bottom surface of the channel and adhere to the RetroNectin. A syringe pump loaded with LV-containing media was then connected to the microfluidic and flowed at 0.577 μL/min for 6 hours. Afterward, LV-free growth media was perfused through the microfluidics for 72 hours and epifluorescence imaging was used to assess transduction. This proof-of-concept test demonstrated that cells could be transduced uniformly throughout the channel (**Figure 3.14a and b**) and continued to expand in culture, indicating that cell viability and proliferation were unaffected. Furthermore, issues of sterility did not arise, as all cell loading and manipulation was performed in a sterile cell culture hood. The channels provided a sealed environment that isolated cells from non-sterile environments. Devices made from silicone adhesive xurography were sterilized and assembled under sterile conditions. The microfluidics were also placed inside sterile petri dishes for an added barrier against contamination. Potential issues in sterility could be stymied by sterilizing devices with ethanol or UV treatment.

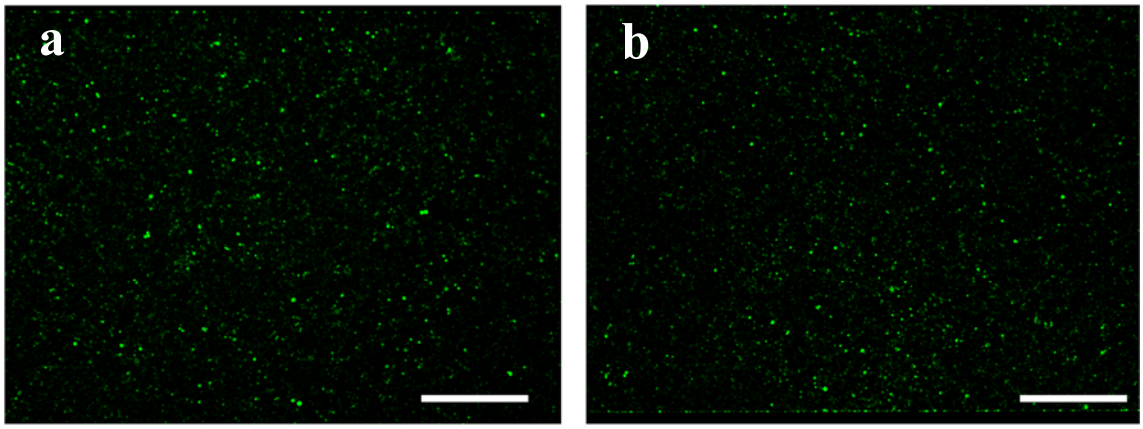

Figure 3.14: Epifluorescence images of cells transduced and cultured in microfluidics for at least 3 days. **a)** Upstream region of the device and **b)** downstream region of the device, demonstrating heterogeneity. Scale bars = 100μm.

3.4.4 Characterization of Static Microfluidic Cell Culture Viability

Under static cell culture conditions in the microfluidic, nutrient depletion over time is a major concern due to the reduced volumes. To that end, we utilized ethidium homodimer-1 viability staining to assess cell viability from recovered cells cultured in the microfluidic for 5 hours. Since dead cells are not easily distinguishable from cell debris and other particulates that are normally gated out, quantification from flow cytometry may have been underestimated, but was otherwise low. Normalized percentages of ethidium homodimer-1 staining are shown below, with actual percentages ranging from 0.2-0.5% (**Figure 3.15a**). Cell counts were also taken immediately after removal from the microfluidics and 6-wells. After 72 hours of continued cell culture, cells were counted again to determine if cell proliferation had been affected (**Figure 3.15b**). Both microfluidic and 6-wells resulted in a nearly 6-fold increase in cell counts after 72 hours.

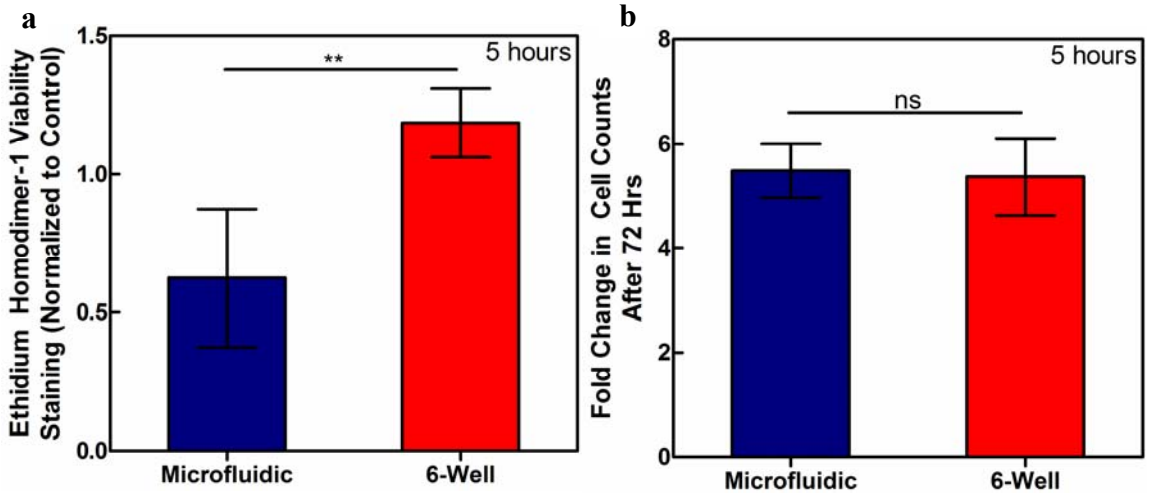

Figure 3.15: Cell viability characterization in static culture. (**a**) Ethidium Homodimer-1 viability staining quantified by flow cytometry. **p<0.01 two-tailed t-test. n=4. (**b**) Fold change in cell counts after 72-hour expansion.

3.5 Device Scale-up Toward Clinically Relevant Cell Numbers

The original test device consisted of a series of four parallel channels, each with surface area equivalent to a 96-well (0.32 cm^2), shown below next to the scaled up device used in all experiments where diffusion height was not an independent variable (**Figure 3.16**).

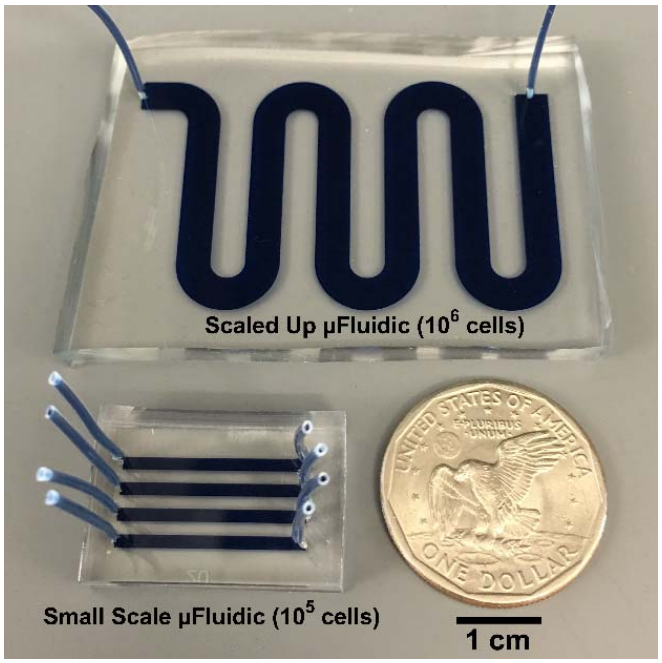

Figure 3.16: Dye-loaded small and large scale microfluidic devices. The large scale device has the same surface area as a 6-well (9.5 cm^2) while the small scale microfluidic has the same surface area as a 96-well (0.32 cm^2). Scale bar = 1cm.

While the small scale devices had the advantage of high production throughput and ease of height variation, the cell throughput for transduction analysis was limiting due to the low cell capacity. Transductions in small scale devices were limited to approximately 70,000 cells. Thus, we scaled up our device size to accommodate cell numbers on the order of 10^6 cells. Since it was important to compare transduction to standard cell culture systems, we designed the microfluidic to have the same surface area as a 6-well plate (9.5 cm^2) so that the only difference between the two systems was the diffusion height. The channel widths were constrained by between an upper and lower limit. Narrow channels would need to be longer in length, significantly increasing fluidic resistance, which would have impeded cell loading. Conversely, shorter wide channels would have been prone to collapsing due to extremely high aspect ratio, which would have required supports that would reduce cell recovery. Furthermore, air pockets can easily form in large channels that

would make uniform loading difficult. As such, we designed channels with a ~1:50 height:width aspect ratio and used thick pieces of PDMS to prevent channel collapse. Different channel designs tested are shown below in **Figure 3.17**.

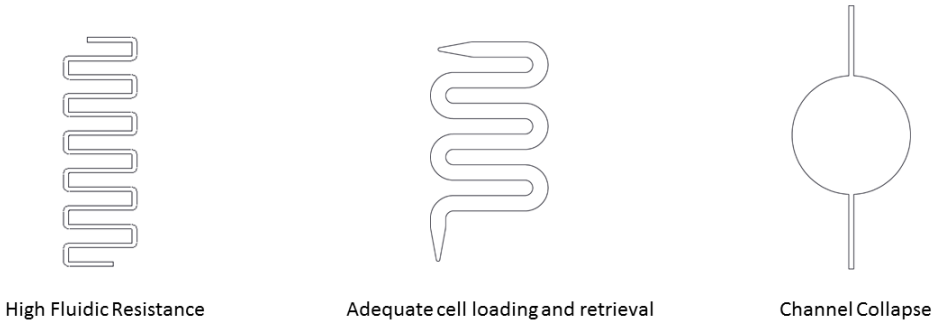

Figure 3.17: Examples of different channel designs tested. All designs utilize the same surface area (9.5 cm^2) to match a 6-well. Narrow channels require longer lengths that increase fluidic resistance. Wide channels are prone to collapse and heterogeneous cell loading and removal. A 1:50 aspect ratio was sufficient to achieve efficient and homogeneous cell loading.

However, this marginally decreased production throughput as a single channel encompassed nearly the entirety of a 4-inch silicon wafer. A wide range of heights at the larger scale was also infeasible due to issues with uniformity over large surface areas for thick layers of SU-8.

Finally, we assessed the scalability of transduction in a PDMS-based microfluidic. For constant MOI, transduction time, LV v/v% concentration, height, and cell surface density, we performed simultaneous transductions in small scale and large scale devices. All other factors such as LV volume, surface area, and number of cells transduced were scaled up by a factor of 4.8. We determined that as long as the diffusion height remained

constant, all other factors could be directly scaled up to achieve the same amount of transduction (**Figure 3.18**).

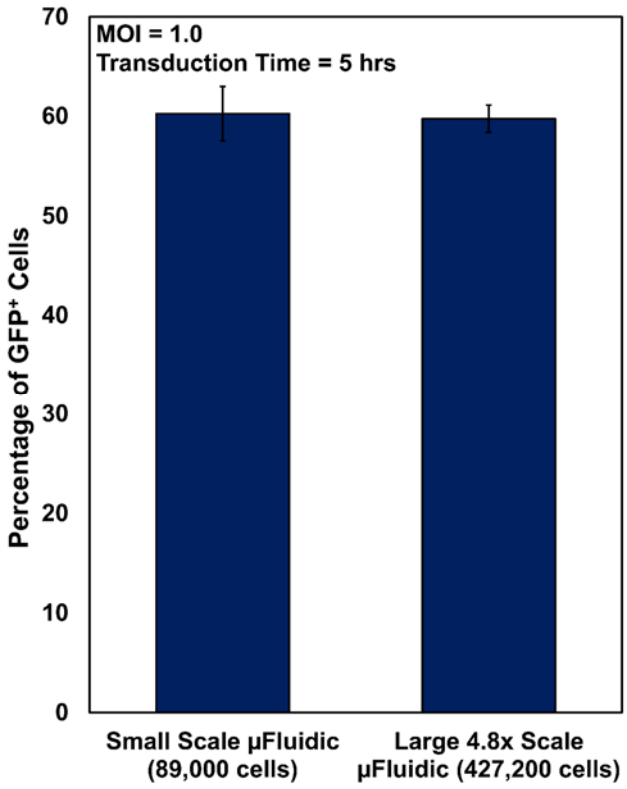

Figure 3.18: Scaling up microfluidics by a factor of 4.8 (number of cells, total volume, surface area, and LV particles) while maintaining constant LV (v/v)%, MOI, channel height, and transduction time results in nearly identical percentages of transduced cells *(n = 4)*. Data represent mean ± s.d. of technical replicates from one experiment.

Continued scale up toward clinically relevant numbers will require alternative fabrication methods since photolithography is typically limited to 4-5 inch silicon wafers. Larger wafer sizes are available, but would be extremely cost-prohibitive. CNC micro-milling could produce a 200µm high mold with surface area of approximately 250 cm^2 (**Figure 3.19**). Such a device would be able to transduce 10^8 cells under static conditions.

Microfluidic xurography could be another option to produce a clinical scale device, though the shorter channel heights would require flow-based transductions or extremely high titer LV. The device could readily be fabricated using existing 245mm bioassay dishes.

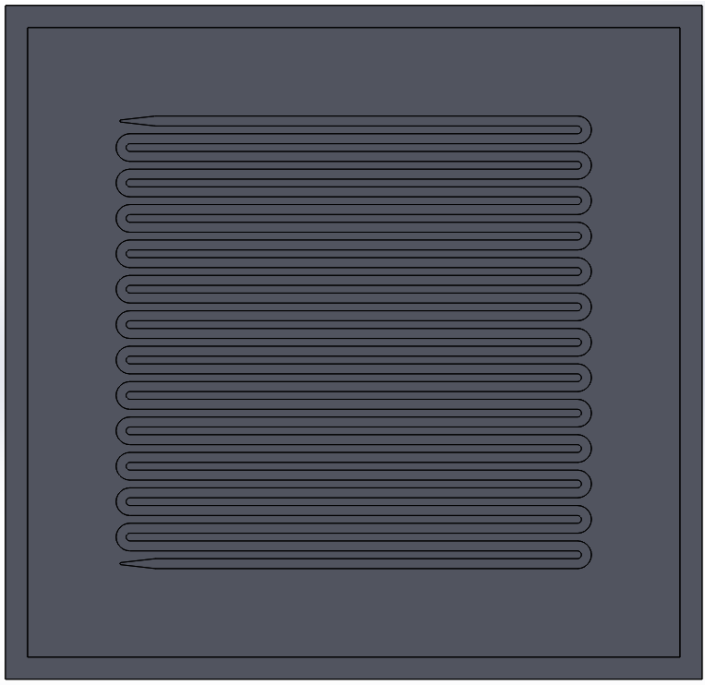

Figure 3.19: Example mock-up of a clinical scale device mold capable of transducing 10^8 cells. Each side would be 31.45cm long.

CHAPTER 4: DETERMINING CRITICAL PARAMETERS AFFECTING TRANSDUCTION EFFICIENCY

4.1 Introduction

In Chapter 3, we discussed different microfluidic fabrication methods and design considerations for developing our microfluidic lentiviral transduction platform. We decided to pursue PDMS-based devices due to their reliable fabrication, low batch-to-batch variability, and comparatively high throughput relative to polystyrene-based hot embossed microfluidics. Our preliminary data showed that cells could be easily removed from PDMS-based devices with high efficiency, but that PDMS is also able to be sufficiently coated with RetroNectin for immobilization of non-adherent cell types in perfusion-based transductions.

In this chapter, we sought to narrow down the parameter space of microfluidic transduction to determine which factors were most critical to enhancing transduction efficiency. From preliminary experiments, we showed that simply using the same amount of LV in a microfluidic versus a comparable well plate could improve transduction. By virtue of shifting from a diffusion-limited system to a microfluidic, there are inherently major differences presented. Although parameters such as surface area, cell number, transduction time, and amount of LV used are identical, other parameters such as fluid/diffusion height and total volume are significantly reduced by 1-2 orders of magnitude, which increases the LV v/v% as a direct result. As such, diffusion limitations are overcome, and transduction is enhanced.

4.2 Materials and Methods

4.2.1 Microfluidic Device Fabrication

All devices were designed to have equivalent surface area to a comparable polystyrene well plate. Small scale devices had matching surface area with individual wells of a 96-well plate (0.32 cm^2) while all large scale devices had matching surface area with individual wells of a 6-well plate (9.5 cm^2).

Small scale devices with volumes ranging from 1-15µL and 92µL large scale devices were made using traditional soft lithography as described in Section 3.2.1. The small scale devices were used for all experiments requiring microfluidic devices of varying heights and volumes. Of all small scale devices, only the 3µL device was used for the half-life assessment experiments. The 92µL devices were used for all other cell line experiments except for the transduction kinetics experiments. Briefly, a thick layer of SU-8 2025, 2050, 2100, or 2150 photoresist (MicroChem, Westborough, MA, USA) was spincoated onto a silicon wafer to achieve a uniform layer. For a 30 second spin at 3000RPM, the thickness of the photoresist should be equal to the last 3 digits of the specific formulation of SU-8. The spin speeds were adjusted to achieve the desired heights of the channel. The photoresist was baked at 95°C according to manufacturer guidelines to drive out the solvent. The device pattern was then crosslinked into the photoresist by exposing the coated wafer to 365nm wavelength UV light through a photomask containing the desired patterns. Uncrosslinked photoresist was removed by treatment with SU-8 developer. The completed molds were treated with hexamethyldisilizane (Sigma-Aldrich, St. Louis, MO, USA) overnight by evaporation onto the surface before casting PDMS (Sylgard 184) (Dow Corning, Midland, MI, USA).

Microfluidic devices for assessment of transduction kinetics were made using double-sided silicone adhesive transfer tape (3M, St. Paul, MN, USA). Channel patterns were drawn using AutoCAD software (Autodesk, San Rafael, CA, USA). The channels were then cut from the double-sided silicone adhesive using a Silhouette craft cutter (Silhouette America, Inc., Lindon, UT, USA). The double-sided silicone adhesive containing the channel pattern was then applied to a 150mm polystyrene petri dish, followed by a flat slab of PDMS with inlet and outlet ports pre-punched to seal the channel. The resulting device was 48μL in volume with a height of approximately 50μm.

4.2.2 RetroNectin Coating of PDMS Microfluidics

Devices were coated with 10 μg RetroNectin (Takara Bio Inc., Kusatsu, Shiga, Japan) (1.05 $\mu g/cm^2$) the day before transduction. 6-well plates were also coated with the same amount for static controls. 2% BSA in PBS was incubated in the devices and 6-wells for 30 minutes at room temperature to block non-specific binding immediately before transduction. The blocking solution was then flushed out with PBS and aspirated from the devices and 6-wells prior to use.

4.2.3 Jurkat and K562 Culture and Transduction

K562 and Jurkat cells (ATCC) were cultured in RPMI 1640 media supplemented with 10% fetal bovine serum (FBS), L-Glutamine, 25 mM HEPES, and 1% Pen/Strep. GFP-LV was supplied by Expression Therapeutics, LLC (Tucker, GA, USA) and was prepared by commercial manufacturing organizations for clinical development of a $CD34^+$ fVIII-LV gene therapy product candidate. The GFP-LV utilized the EF-1 Alpha promoter, which provides constitutive expression of the target transgene for a broad range of cell

types. For all transductions, the amount of LV used between microfluidics and comparable well plates were identical unless otherwise noted. All cell line transductions used 8µg/mL polybrene. To maintain equal amounts of LV and cells, stock mixtures of cells and LV for specified MOIs were prepared. Microfluidic devices were then loaded with the appropriate volume to fill the channels. Well plate comparisons were loaded with the same volume and diluted to the indicated volumes in the 96-wells and to 1mL total volume in the 6-wells. After the specified transduction times, cells were washed with PBS, collected into 15mL conical tubes, and centrifuged at 200 x g. The supernatant was then aspirated to remove unbound residual vector, and cells were re-suspended in fresh growth media for continued culture.

4.2.4 Spinoculation Comparison

Using a similar spinoculation protocol to O'Doherty *et al*., we adjusted the incubation times so that 2,000,000 cells could all be exposed to the same amount of LV for the same total amount of time across all conditions. Cells were centrifuged at 1200 x g at room temperature in a 6-well plate for 2 hours followed by a 3-hour incubation at 37°C. Total volume had to be increased to 2mL so that the entire well plate surface would remain wetted. Cells were then processed as normal to stop the transduction as described in Section 4.2.3.

4.2.5 Secondary Transductions for Residual LV Qualification

Residual LV from transduction kinetics was assessed for MOI 0.43 conditions at 0.5, 1, 2, 6, 12, and 24 hours. At each time point, cells were removed from the microfluidics and 6-wells. Instead of discarding the supernatant after centrifugation, the supernatant was

collected and added to 1,000,000 naïve Jurkats and re-suspended with fresh media with 8µg/mL polybrene to a total volume of 2mL. All secondary transductions were conducted in a 6-well for 6 hours. In doing so, all conditions would have equal cell numbers, total volume, fluid height, and transduction time. The only difference was the amount of LV in each well, which should be proportional to the amount of residual LV from the primary transductions.

4.2.6 Consecutive Transductions for LV Replenishment in Microfluidics

PDMS 92µL microfluidics were coated with RetroNectin as described in Section 4.2.2 to immobilize cells. A single dose of vector mixed with cells at MOI 1.2, equating to 30% LV v/v% concentration, was initially pipetted into the devices for 4 hours for the consecutive transductions. After four hours, a second dose of cell-free LV at the same MOI was loaded into the devices to replace the spent vector. A 1.5mL tube with a hole drilled in the cap was placed at the device outlet to collect any non-adherent or weakly adherent cells. Static control transductions were carried out as described in Section 4.2.3 and also utilized the same surface concentration of RetroNectin.

4.2.7 Lentivirus Half-life Temperature Sensitivity Assessment

In order to assess LV half-life in the microfluidic, aliquots of LV were stored at 4°C, a temperature at which LV half-life has been shown to be on the order of several days[70, 93]. As temperature increases, the LV half-life rapidly decreases to the order of several hours at 37°C. LV samples were removed and incubated at room temperature and 37°C for 0, 5, 12, or 24 hours prior to transduction. After the indicated pre-incubation period, 70,000 cells were transduced in 3µL small scale microfluidics and 96-wells for 5

hours. Cells were then processed as described in Section 4.2.3 and assessed for GFP expression as in Section 4.2.7

4.2.8 Transduction Efficiency Assessment

Cells were maintained in culture following removal from the devices and wells for at least 72 hours before assessing GFP expression to allow time for stable gene expression. Transduction was quantified with a BD C6 Accuri flow cytometer. Cells were gated based on non-transduced controls. An example of flow cytometry histograms of non-transduced, well-transduced, and microfluidic-transduced cells are shown below in **Figure 4.1**.

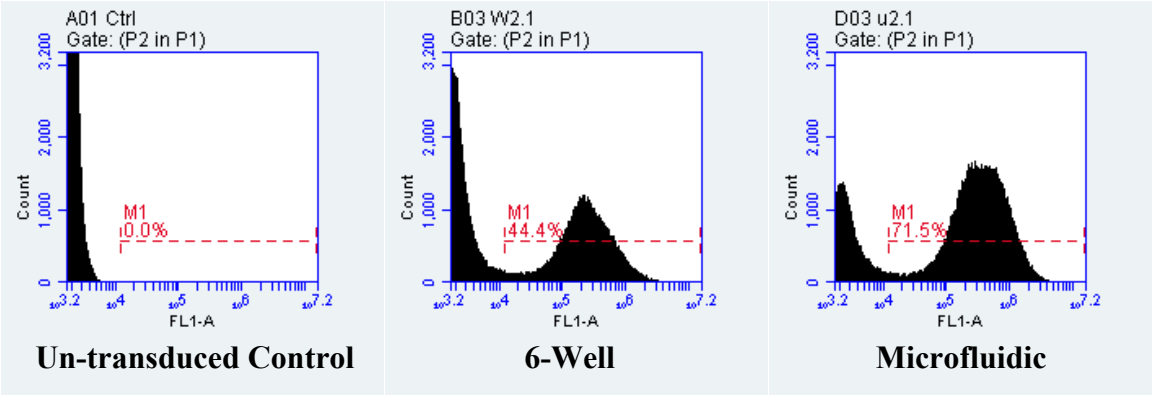

Figure 4.1: Example flow cytometry histograms of control, 6-wells, and microfluidics.

4.2.9 COMSOL Modeling

We adapted the built-in biosensor model in COMSOL as a simplified framework for transduction in our microfluidic system compared to a 6-well. The model utilized the governing diffusion equation for the transport of a dilute species (LV) and a surface reaction (LV binding to cells). The diffusion coefficient for LV transport in media was estimated from the Stokes-Einstein equation (Equation 3).

$$D = \frac{k_B T}{6\pi\eta r} \qquad (3)$$

Where k_B is the Boltzmann constant, T is the absolute temperature, η is the dynamic viscosity, and r is the radius of the particles in motion. The values for the input variables are given below in **Table 4.1**. Due to the similar size of retroviruses and lentiviruses, the diffusion coefficient used was within the range of other reported values for retroviral vectors[16, 19, 94].

Table 4.1: Values used to estimate diffusion coefficient of LV

Variable	Definition	Value
k_B	Boltzmann Constant	$1.380648527 \times 10^{-23}$ kg·m^2·s^{-2}·K^{-1}
T	Absolute Temperature in Incubator	310 K
η	Dynamic Viscosity	6.913 kg·m^{-1}·s^{-1}
r	Particle Radius	5.0×10^{-10} m
Together: D = 6.57×10^{-8} cm^2·s^{-1}		

The following differential equation (Equation 4) is solved by the COMSOL model to describe the transport of the LV particles, *P*:

$$\frac{\partial c_P}{\partial t} + \nabla \cdot (-D\nabla c_P) = 0 \qquad (4)$$

Where *D* is the coefficient calculated from Equation 3 and c_P is the LV concentration for static transductions. The adsorption and desorption of LV particles at the bottom surface of the microfluidic and 6-wells where the cells settle to results in a net flux that is described by the Equation 5, where the net flux at the boundary, N_P is:

$$N_P = -r_{ads} + r_{des} \qquad (5)$$

Where r_{ads} is the rate of adsorption defined by an adsorption rate, k_{ads}, and r_{des} is a rate of desorption defined by the desorption rate, k_{des}.

The microfluidic was simulated as a 2D axisymmetric model of the 6-well with 50µm height. Due to rotational symmetry of the geometry and conditions about an axis, running the simulation this way significantly simplified the model and reduced computation times. 3D modeling of the microfluidic produced identical results given the same inputs since all parameters were matched except for the geometry (**Figure 4.2**). Essentially, the 2D axisymmetric simulation performed calculations on a 2D rectangle and used symmetry to treat the microfluidic as an extremely flat disk that was 50µm in height. This was contrary to the 3D model, which modeled the microfluidic as a long rectangular channel with the same surface area and height. The model was then divided into millions of individual 3D elements in which the governing differential equations were applied to each element to simulate the input conditions. The difference between the last two points was less than 2%, but computational time was reduced by several orders of magnitude.

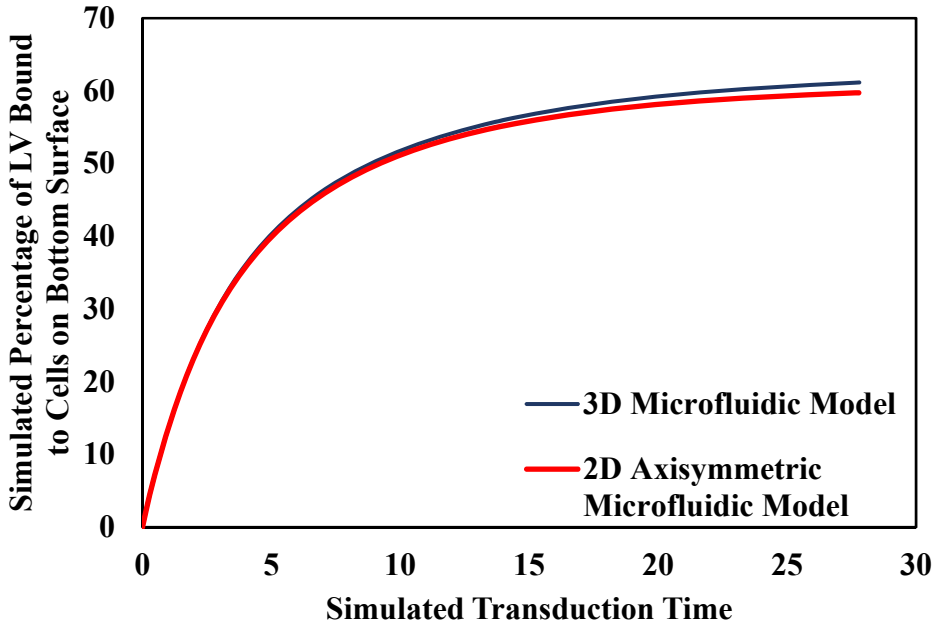

Figure 4.2: Comparison of 2D axisymmetric vs. 3D models of the microfluidic. For identical input parameters, the largest difference between the two simulations was less than 2%.

Sensitivity analysis of k_{ads}, k_{des}, and D for the microfluidics and 6-well demonstrated that adsorption rate was the determining factor for the percentage of viral particles bound to the cell-laden surface **(Figure 4.3).** The desorption constant, which is independent of the initial vector concentration, was not sensitive to order of magnitude changes. These results support other reports of virus binding as the rate-limiting step to transduction[94]. Finally, increasing the diffusion coefficient, D, did not serve to improve transduction in the microfluidic, but increased transduction in the 6-well, highlighting the existing diffusion limitations.

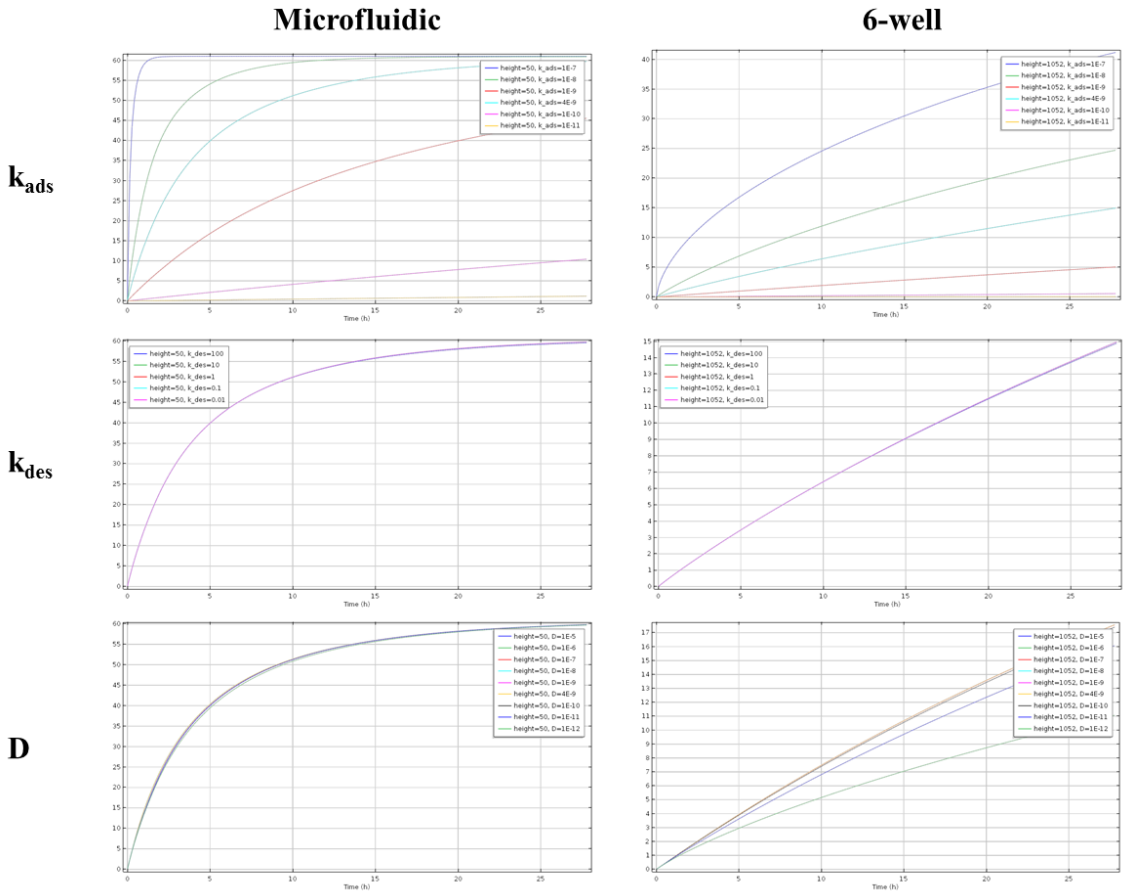

Figure 4.3: Sensitivity analysis of COMSOL model parameters. The sensitivity of viral particles bound to cells with respect to order of magnitude changes in k_{ads}, k_{des}, and D were plotted.

A parametric study was conducted to determine the best k_{ads} and k_{des} values to fit the data from the transduction kinetics experiment. We adjusted the values of k_{ads} and k_{des} to match previously reported values of the dissociation constant for VSV-G-LV with its receptor, the low-density lipoprotein receptor (LDL-R)[71]. The error between simulated and experimental results is plotted for each condition in **Figure 4.4**. Error was initially extremely high for the microfluidics, but decreased exponentially for increasing time while the 6-well error remained relatively steady. This highlights the need for an

additional parameter to model the rate-limiting steps of viral entry, which is not taken into account for this model. Final values of the simulation parameters are displayed

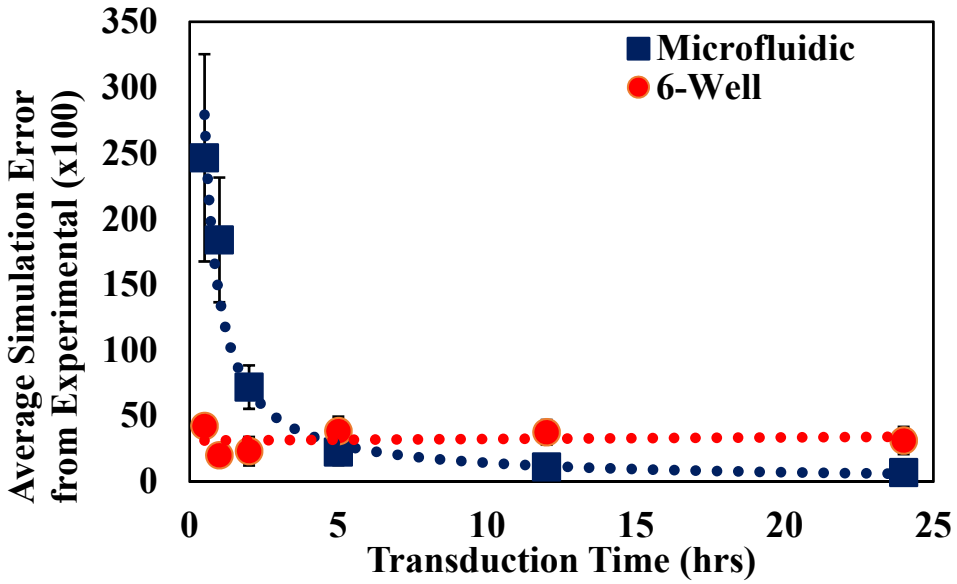

Figure 4.4: Error between simulated and experimental results for each time point, averaged between different LV amounts used.

Table 4.2: COMSOL parameters used in model

Variable	Definition	Value
k_{ads}	Adsorption rate constant	6×10^{-9} m/s
k_{des}	Desorption rate constant	6×10^{-1} mol·m^{-2}·s^{-1}
D	Diffusion Coefficient	6.57×10^{-12} m^2·s^{-1}
d_sites	Density of biding sites (n_cells/surface area)	1.0514×10^{9} mol·m^{-2}
radius	6-well/Effective Microfluidic Radius	0.0174 m
n_cells	Number of cells	1×10^{6}
height	Fluid height	1.052×10^{-3} m (6-well) 5.0×10^{-5} m (Microfluidic)

4.3 Results and Discussion

4.3.1 The Influence of Diffusion Height on Transduction Efficiency

One of the first parameters investigated was the fluid height in which transduction occurred. Using microfluidic devices of varying heights and comparable 96-wells with increasing total volumes to achieve the specified fluid heights, all transductions were conducted with 1µL of GFP-LV for 4 hours and 70,000 cells, resulting in a MOI of 1.27. As a result of varying fluid heights with constant surface area, the total volumes increased proportionally with fluid height. Therefore, for constant LV amount, the LV v/v% concentration is inversely proportional to fluid height and total volume. For every 1µL volume increase, the fluid height increases by 31.1µm. As expected from basic particle diffusion calculations, transduction is shown to be inversely proportional to fluid height/total volume (**Figure 4.5**). However, a plateau was observed for transductions in which the fluid heights were between 30-90µm, indicating that LV transport was no longer diffusion-limited as associated increases in LV concentration did not further increase transduction. This highlights that microfluidics enabled transductions to operate in a range where MOI was relevant and unencumbered by diffusion limitations. In the absence of diffusion limitations, estimations for vector integration based on MOI may be derived from a Poisson distribution. Noting that some cells will be infected multiple times while others remain uninfected, the Poisson distribution describes the MOI-dependent probability of interaction between the vector and cells. Thus, decreasing the height below 90µm did not serve to enhance transduction any further.

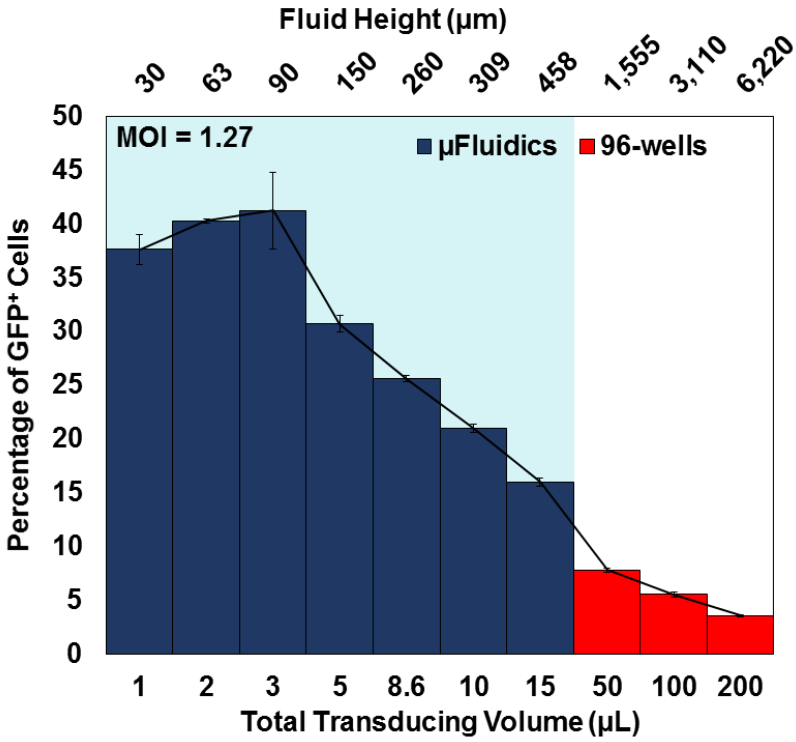

Figure 4.5: Decreasing diffusion height increases transduction until saturation or toxicity occurs. Transductions using the same amount of LV and cells (constant MOI) for various volumes/fluid heights made possible only in a microfluidic system. A plateau is observed at heights <100µm, indicating a shift away from diffusion limitations *(n = 2 8.6µL µFluidics, n = 3 15µL µFluidics, n = 4 for all other conditions*) Data represent mean ± s.d. of technical replicates from one experiment. Transduction time = 4 hours.

4.3.2 Concentration-dependence of Transduction Efficiency

Since the LV v/v% concentration is another factor that can change transduction efficiency, we investigated the effect of keeping LV v/v% concentration while varying the fluid height. The transduction time was kept constant at 4 hours, and 70,000 cells were transduced per condition. To maintain constant LV v/v% concentration with increasing fluid height, the amount of LV in each condition had to increase proportionally. MOI ranged from 0.127 to 25.4. Due to the 200-fold increase in amounts of LV between the lowest and highest fluid heights, the amount of transduced cells generally increased with

increasing LV as expected. In the case of the 96-well transductions where LV was in excess, a plateau was reached, demonstrating the diffusion limitations of standard systems (**Figure 4.6**). Increasing the amount of vector only marginally increased the percentage of transduced cells in the 96-well conditions because the added vector was still unable to reach the cells due to diffusion limitations for the given transduction time.

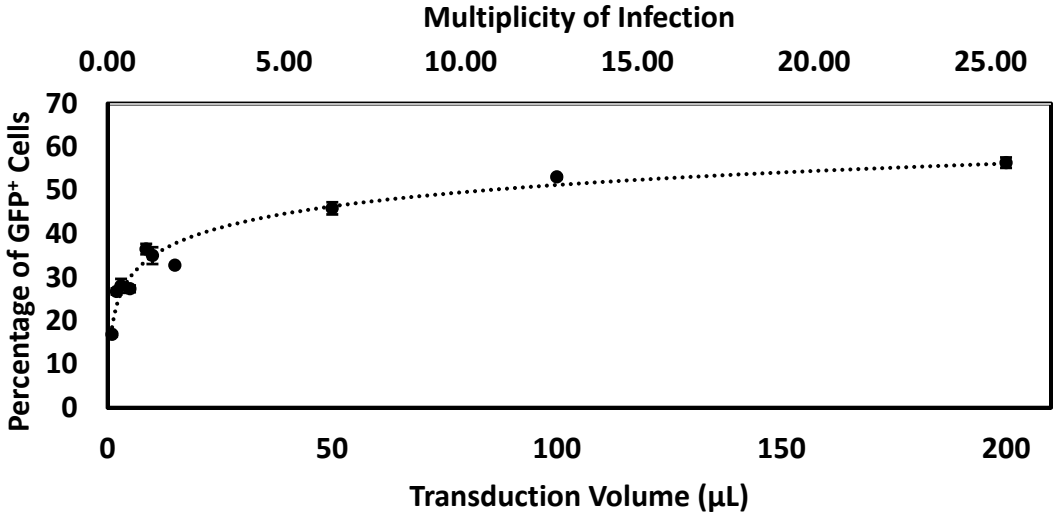

Figure 4.6: Transduction of microfluidics and 96-wells of varying volumes at constant 10% LV v/v% concentration demonstrates that large increases in MOI does not proportionally increase transduction due to diffusion limitations. Transduction time = 4 hours.

Assuming a Poisson distribution for the probability of a cell being infected with one or more LV particles, we defined a utilization efficiency to compare the theoretical LV usage required to obtain the percentage of transduced cells observed versus the amount of LV actually used. Equation 6 provides the average percentage of cells that will probabilistically be infected by at least one viral particle for a given MOI, *m*. This percentage is calculated by determining the probability that a cell will not be infected and subtracting from unity.

$$Theoretical\ Transduction = (1 - e^{-m})\ x\ 100\% \qquad (6)$$

Thus, the percentage of cells infected with at least 1 viral particle, or the total percentage of positive transgene-expressing cells, can be plotted against the MOI to estimate transduction for a given MOI (**Figure 4.7**). However, this does not factor in transduction time and only accounts for the amount of vector that is able to reach the cells for the given transduction time. As such, the results shown in **Figure 4.6** highlight the discrepancy between MOI and actual transduction achieved. Despite using MOI 25.4, only 56.4% of cells were transduced, which indicates that only ~3% of the total LV reached the cells.

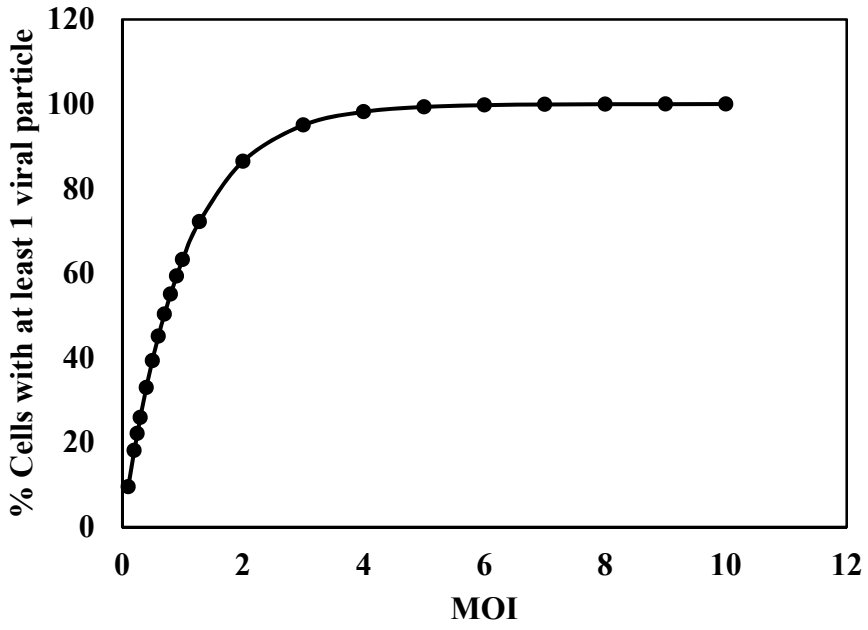

Figure 4.7: Theoretical percentage of transduction for given MOI from Poisson distribution of infectivity.

The utilization efficiency can therefore be calculated by taking the ratio of the theoretical number of viral particles estimated to obtain the observed transduction based on a Poisson

distribution of virus integration with the number of viral particles actually loaded into the system (Equation 7).

$$Utilization\ Efficiency = \frac{-Cell\# * \ln(1 - \frac{\%Transduced\ Cells}{100})}{Number\ of\ Input\ Viral\ Particles}\ x\ 100\% \qquad (7)$$

Alternatively, calculating the utilization efficiency in which the numerator is directly calculated from the percentage of transduced cells assuming one single virus integration for each transduced cell provides a slight underestimate, but still reveals high utilization efficiency for the shortest microfluidic heights.

Comparing fluid height with this utilization efficiency instead of the percentage of transduced cells reveals that microfluidics with the smallest fluid heights are actually the most efficient at utilizing the given amount of LV while the 96-wells all utilized less than 10% of the available LV (**Figure 4.8**). Utilization efficiencies greater than 100% observed in the microfluidic transductions indicate that titer may be underestimated, which have been shown to be a result of titration being conducted in diffusion-limited systems[15, 16]. As the titer was provided from the manufacturer, this underestimate of titer was unsurprising.

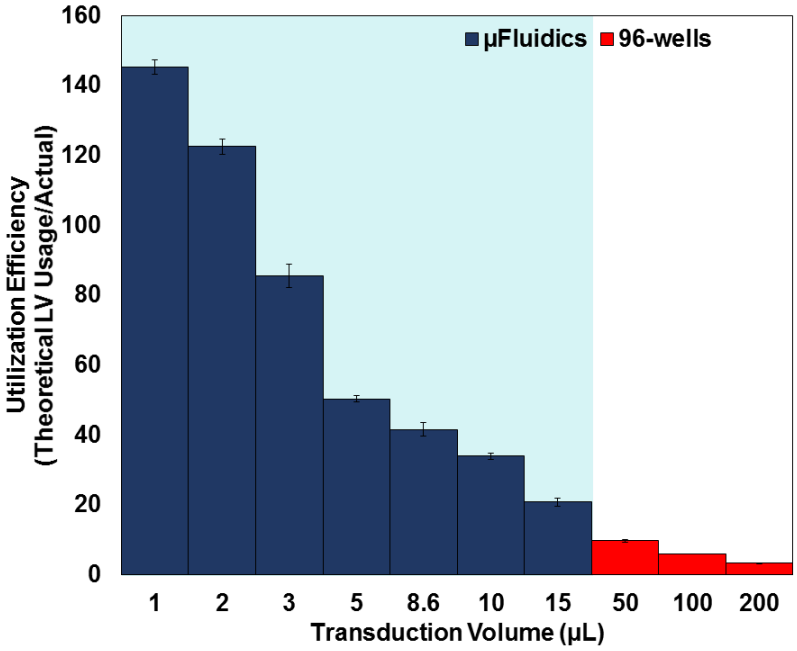

Figure 4.8: Comparison of utilization efficiencies for constant LV (v/v)% at various transduction volumes. Minimizing volumes more efficiently utilizes available LV. (*n = 2, 96-well conditions, n = 3, 2μL μFluidics, n = 4 All other microfluidics).* Data represent mean ± s.d. of technical replicates from one experiment. Transduction time = 4 hours.

4.3.3 The Effect of Cell Surface Density on Transduction Efficiency

We used the same amount of LV and changed the number of cells plated to determine if the cell surface density had an effect on transduction for 92μL microfluidics compared to 6-wells. As the number of cells loaded into the microfluidics and 6-wells increased, the MOI proportionally decreased. The range of MOI changed from 0.25 to 2 for 4 million to 500,000 cells, respectively. As expected, the percentage of transduced cells decreased as cell number increased due to the decreasing MOI (**Figure 4.9a**). However, calculating the utilization efficiencies shows that more cells were actually transduced in total as cell number increased (**Figure 4.9b**). This result supports basic analytical models of particle diffusion, which show that microfluidics should have a greater fraction of particles adsorbed to a surface for the given transduction time compared to 6-wells[95]. Moreover, the increased number of binding sites from greater cell densities allows more of

the available LV to transduce more cells. Thus, the highest utilization efficiency was observed for increasing cell numbers. Thus, transductions should utilize as high of a cell density as possible for maximum utilization efficiency.

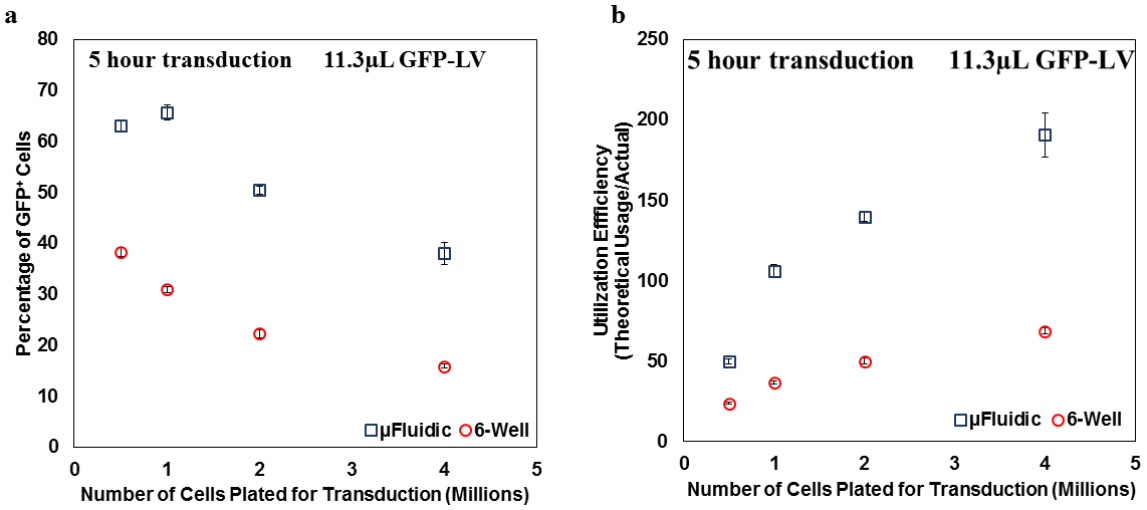

Figure 4.9: Effect of cell surface density on transduction. (**a**) For both systems, transduction decreased as the number of cells plated increased. (**b**) Analysis of utilization efficiency showed that for greater cell numbers, more LV was actually utilized.

4.3.4 Comparison of Microfluidics with Spinoculation

We sought to determine if our microfluidics outperformed other state of the art transduction methods. Of the other state of the art methods, spinoculation is more commonly used since the only requirement for use is to have a centrifuge. Although transduction was doubled compared to a static 6-well transduction, the microfluidics still produced the highest percentage of GFP^+ cells with a 30% increase over spinoculation and a 178% increase over the static 6-well (**Figure 4.10**). All following experiments are direct comparisons with the static 6-well because conditions can more accurately be matched,

bearing in mind that spinoculation would produce transduction levels somewhere in between the microfluidic and 6-well. With spinoculation, the extra steps proved to be cumbersome, and the extended time outside of a CO_2 environment were of concern since the media color was bright pink upon removal from the centrifuge.

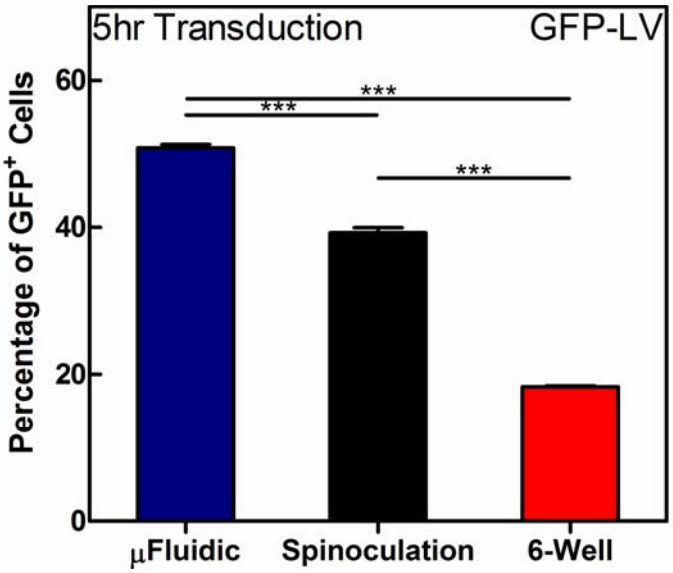

Figure 4.10: Microfluidic comparison to spinoculation. The microfluidic transductions were significantly higher than both achieved from spinoculation and the static 6-well.

4.3.5 Microfluidic Transduction Sensitivity to LV Half-life Fluctuations

Another factor that can affect transduction efficiency is the LV half-life, specifically the half-life sensitivity to temperature changes. We sought to determine if microfluidics would be less susceptible to LV temperature-based decay. All LV samples were used to transduce cells in either a microfluidic or 96-well for 5 hours using the same amount of LV (**Figure 4.11**). Compared to room temperature controls, negligible differences in LV samples that had been incubated at 37°C prior to transduction were observed for the first 5 hours of incubation. However, after 12 and 24 hours of pre-

incubation at 37°C, transduction was drastically reduced by as much as 70%. Furthermore, the reduction in microfluidic transductions between room temperature and 37°C pre-incubated LV at 12 and 24 hours were significantly lower than in 96-wells (*$p<0.05$, ***$p<0.001$). These results indicated that although temperature-dependent LV decay affected both systems, the microfluidics were still able to more efficiently utilize the remaining available LV as seen by the smaller decreases compared to room temperature controls for the longer pre-incubation times. This highlights the benefit of minimizing transduction times, as less of the vector suffers from temperature-dependent degradation.

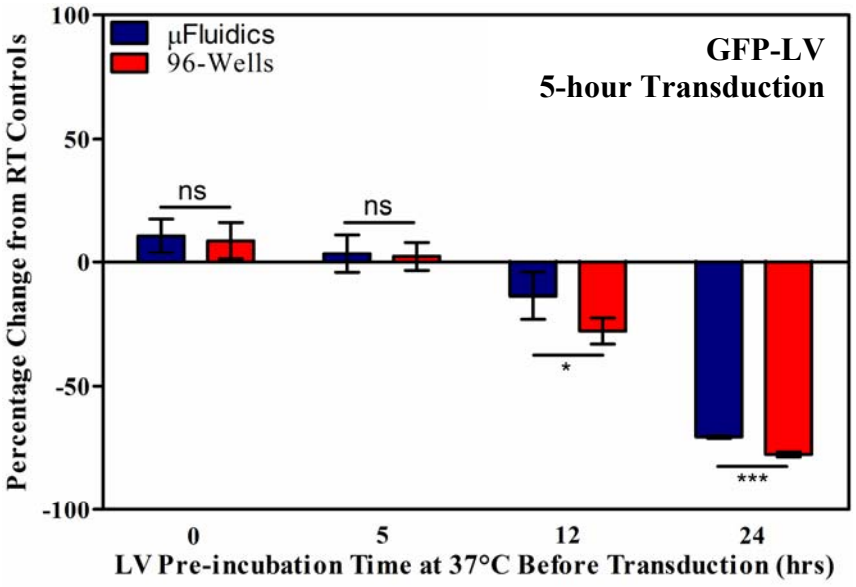

Figure 4.11: LV temperature-based decay in microfluidics vs. 6-wells. Comparison of LV pre-incubation at room temperature and 37°C prior to transduction demonstrates that negligible LV decay occurs within the first 5 hours. However, LV begins to significantly decay between 12-24 hours. Microfluidics demonstrate greater resistance to temperature-related vector degradation.

Microfluidic transductions were also consistently several fold higher than 96-well controls, though pre-incubation of LV for any amount of time resulted in decreased fold differences in transduction (**Figure 4.12**). For 12 and 24-hour LV pre-incubation times,

despite overall lower fold changes in transduction, LV that had been pre-incubated at 37°C produced significantly greater fold increases over 96-wells (*p<0.05, ***p<0.001).

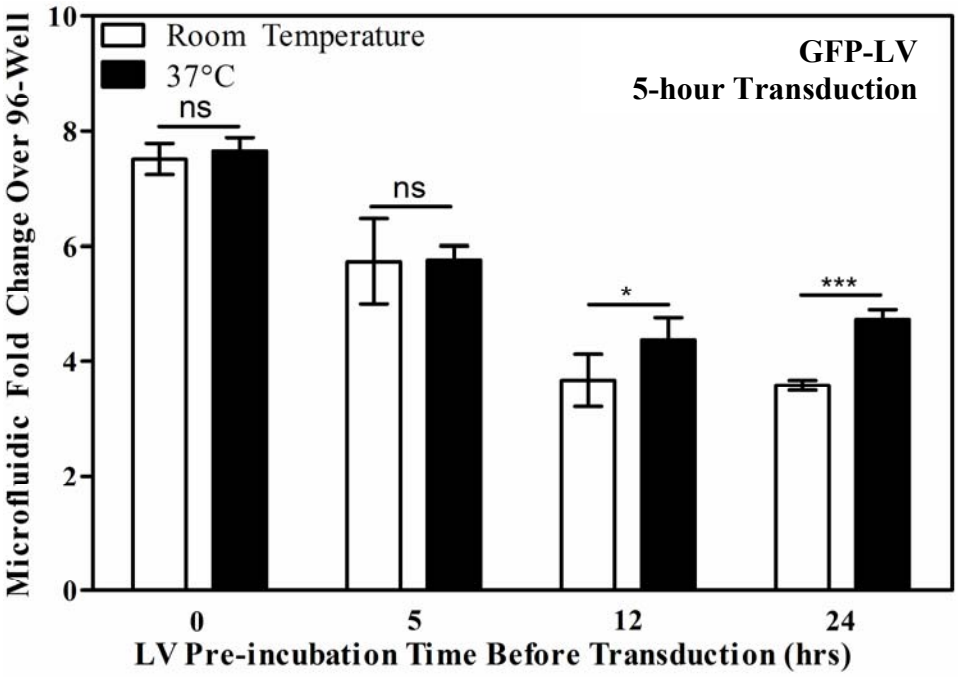

Figure 4.12: Comparison of the microfluidic fold change over 96-wells for various LV pre-incubation times. As pre-incubation time increases, the fold increases between microfluidics and 96-wells decreases, indicating that LV degradation has reduced the infectivity or amount of available LV for transduction.

4.3.6 Transduction Kinetics in Microfluidics

The amount of LV or LV v/v% concentration were previously shown to be important parameters for increasing transduction[17]. However, transduction time is also a significant factor when considering the time required for LV particles to diffuse to cells and the half-life of the vector[96]. As expected, increasing the amount of LV used, and therefore the LV v/v%, resulted in increased transduction. Gene transfer also increased proportionally with transduction time (**Figure 4.13a**). A basic COMSOL model of LV transport to cells in the microfluidic and 6-wells also demonstrated similar trends, though

LV had to be increased by threefold to match the experimental conditions, indicating that the titer may have been underestimated due to the diffusion-limited titration (**Figure 4.13b**), which is consistent with previous reports[16].

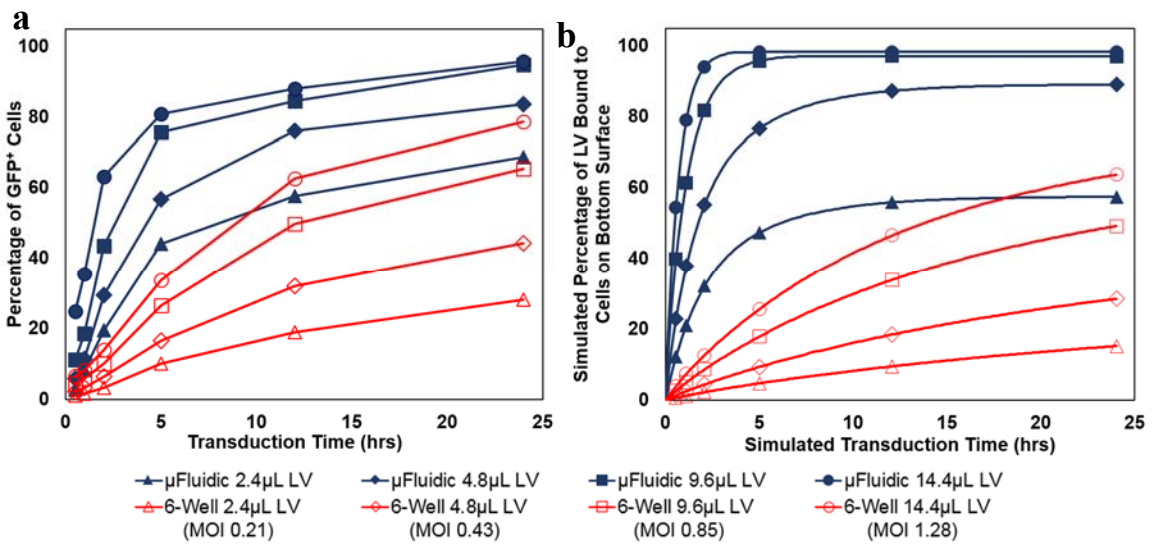

Figure 4.13: Assessment of transduction kinetics between a 6-well plate and our microfluidic system for various MOI. (**a**) Experimental data with MOI ranging from 0.21-1.28 (**b**) Basic COMSOL simulation of transductions in both systems demonstrating that the observed trends are due to physics-based differences facilitated by microfluidics. *In silico* concentration had to be increased to match experimental data, indicating that reported titers may be underestimates.

Furthermore, calculating the utilization efficiency for each condition demonstrated that the microfluidics were proportionally more efficient with time, though inversely proportionally with the amount of LV used (**Figure 4.14**). The high utilization efficiencies corroborate the underestimated titers, and indicate that the titer may be as much as 5-fold higher than originally measured. Interestingly, the utilization efficiency of transductions in the 6-wells did not change significantly in a concentration-dependent manner as the microfluidics.

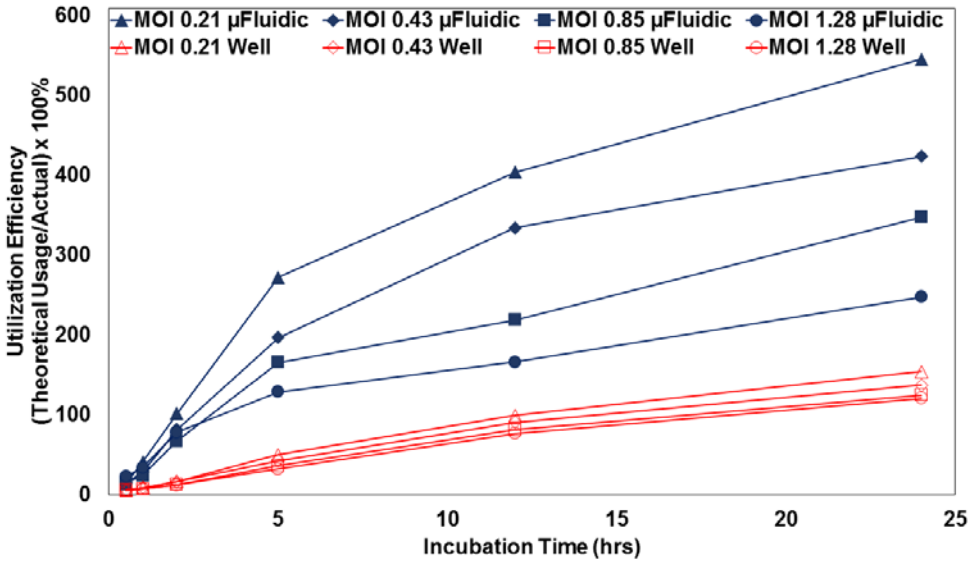

Figure 4.14: Utilization efficiency has much higher potential with microfluidics (µFluidics). The shorter diffusion lengths allow more of the available LV to reach the cells with increasing time. Lower MOI produces the greatest differences in utilization efficiency because the microfluidics are not diffusion-limited, and nearly all of the LV is used. The utilization efficiencies greater than 100% highlight the inaccurate titer, which may actually be 2-5 fold higher.

Finally, secondary transductions at MOI 0.43 between the microfluidics and 6-wells confirmed that the microfluidics were indeed more efficient in utilizing the available LV (**Figure 4.15**). An inverse relationship was observed between the primary transduction time and the percentage of GFP^+ cells from the secondary transduction using the residual LV. The secondary microfluidic transductions are consistently lower than the complementary secondary 6-well transductions, indicating that there was less LV left over from the microfluidic primary transductions. Thus, microfluidics utilized LV more efficiently compared to comparable well plates. In the current study, the secondary transductions served as a qualitative assessment of leftover vector. However, more accurate quantitation may potentially be obtained from performing concurrent titrations in which decreasing amounts of LV are used up to the maximum amount of LV originally used in

the primary transduction. In addition, the secondary transductions would need to be performed for longer periods of time so that the maximum amount of vector can reach the cells, though this would be an underestimate due to the short LV half-life and diffusion limitations of the 6-well. Alternatively, ultracentrifugation may potentially be used to re-concentrate the residual vector collected from the microfluidics and 6-wells to transduce new cells in microfluidics to eliminate the issues associated with diluting the LV out further, though further ultracentrifugation may result in reduced titer or infectivity from particle membrane disruption.

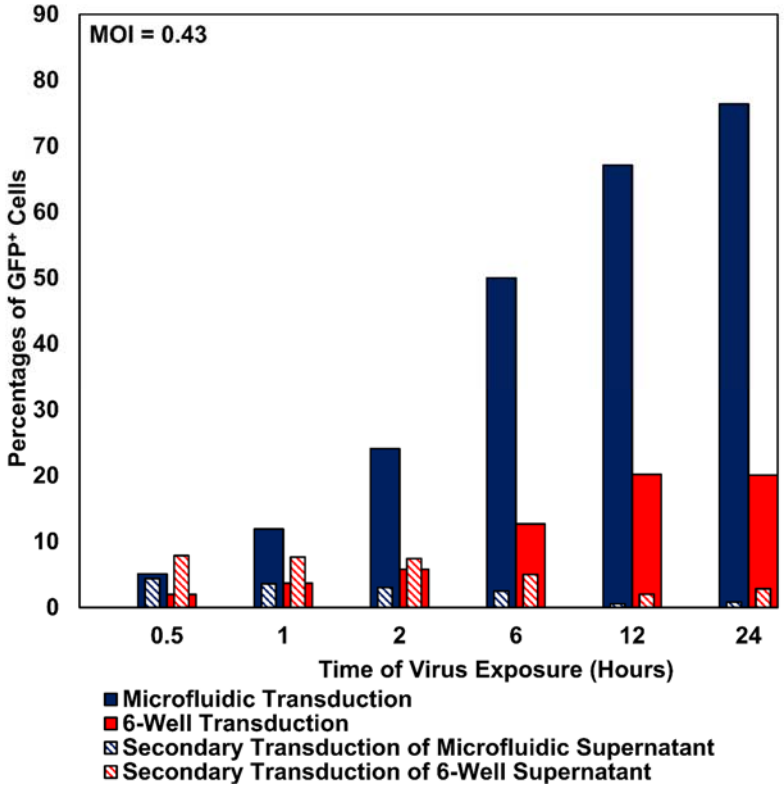

Figure 4.15: Microfluidics are able to more efficiently utilize available LV. Representative experiment of kinetic analysis of transduction and secondary transductions to assess leftover LV. Solid bars represent transductions carried out in either the µFluidic (blue) or 6-well (red). Striped bars represent transductions in which the leftover viral supernatant collected at each time point from the primary transductions were used to transduce fresh cells in 6-wells after re-suspending to 2 mL total volume for 6 hours.

4.3.7 MOI and Utilization Efficiency Are Inversely Proportional

For constant channel dimensions, increasing the MOI rapidly increased the LV v/v% concentration, which lead to nutrient deprivation and vector stock-mediated toxicity (**Figure 4.16**).

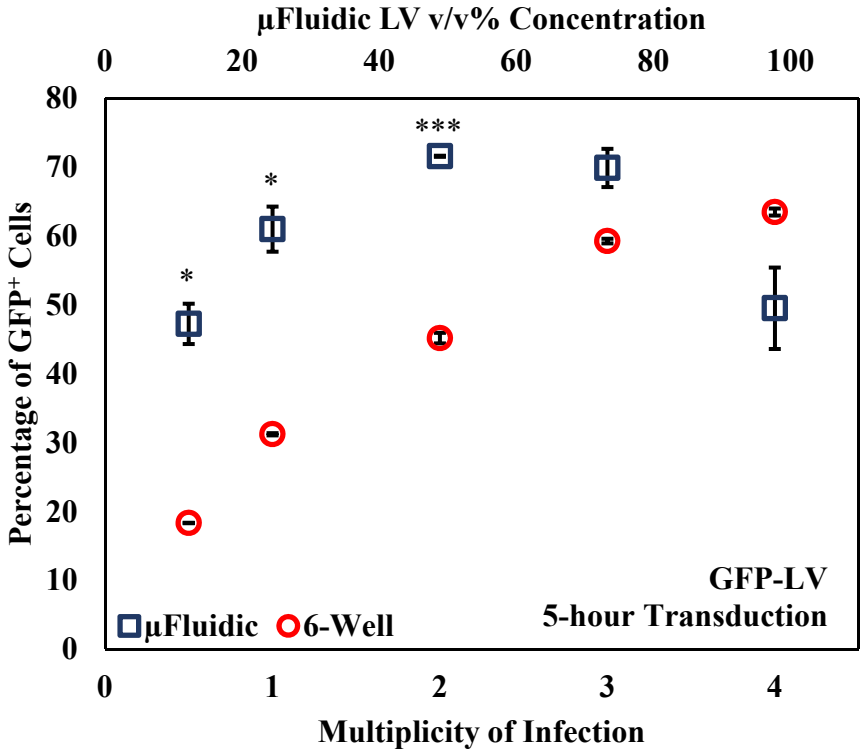

Figure 4.16: Comparison of microfluidic and 6-well transductions for increasing MOI. *p<0.05, ***p<0.001 two-tailed t-tests comparing microfluidics and 6-wells for each MOI.

As a result, microfluidic transductions initially increased proportionally with MOI, though transduction began to decrease past 50% LV v/v% concentration (**Figure 4.17**). This parabolic shape was not observed for 6-well transductions, in which transduction consistently increased proportionally with MOI. Even at MOI 4, the 6-well LV v/v% concentration was still only 9% versus 97.7% in the microfluidic. Thus, a consistent

decrease in fold change between the microfluidic and 6-well transductions were observed up to MOI 4, where the microfluidic transduction was lower than the 6-well.

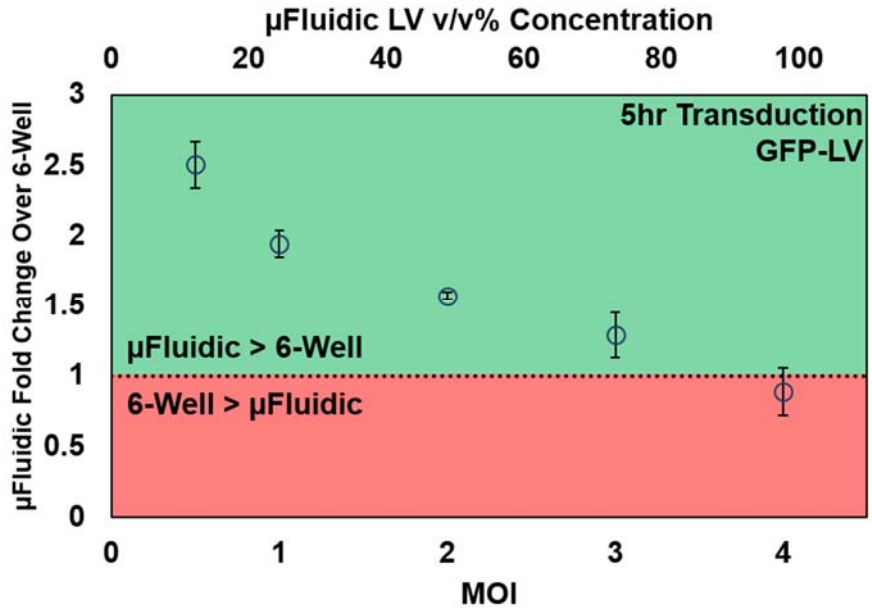

Figure 4.17: Fold change of microfluidic transductions over 6-wells *(n = 3)* at various MOI. Data represent mean ± s.d. of biological replicates from two experiments. Toxicity at high LV (v/v)% due to geometric constraints diminishes microfluidic transduction efficiency.

Assessing the utilization efficiency between the two systems showed that microfluidic transductions are several fold more efficient than 6-wells at low MOI (**Figure 4.18**). However, as the amount of vector was increased, the microfluidic utilization efficiency rapidly approached that of the 6-well, which steadily decreased at a much slower rate as MOI increased. These data highlight the diminishing returns of simply increasing the amount of LV used to achieve higher transduction. The microfluidics are able to make the most out of smaller amounts of LV, though toxicity from higher vector concentration quickly reduces the benefits.

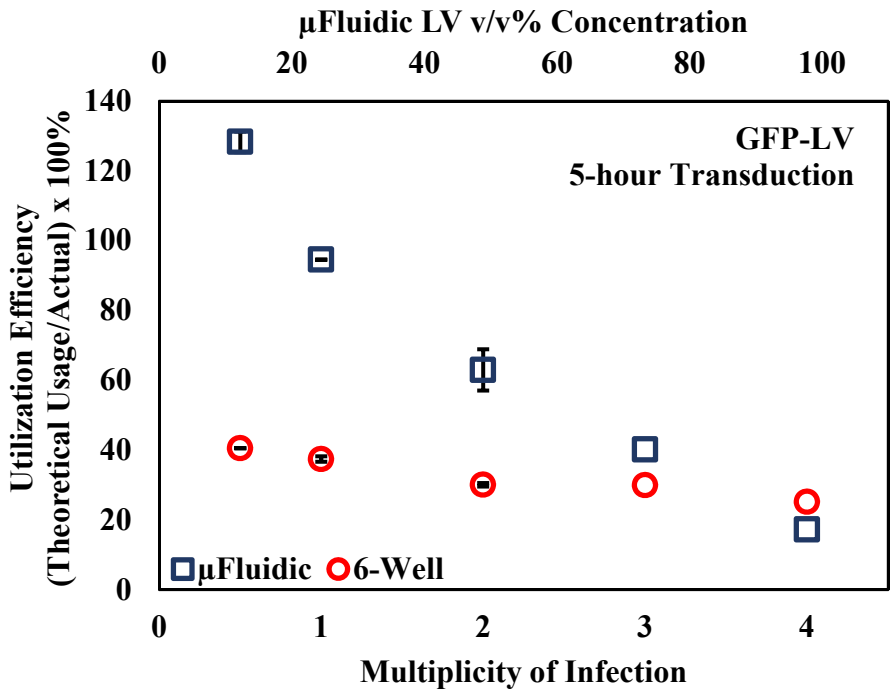

Figure 4.18: Utilization efficiency of microfluidic versus 6-well transductions at various MOI.

4.3.8 Consecutive Transductions Overcome Geometric Constraints of Microfluidics

To overcome the geometric constraints of microfluidic transduction that resulted in toxicity at high MOI as in **Figure 4.16**, we investigated the use of consecutive transductions to deliver multiple doses of vector at a lower LV v/v% concentration (**Figure 4.19**). (1x) transductions equated to MOI 4. Previous studies transducing adherent cells with adenovirus in a microfluidic showed that continuous perfusion resulted in heterogeneity in cell transduction that was biased toward the inlet where the initial concentration was higher[97]. This also assures that transduction is homogeneous along the width of the channel instead of being skewed along the velocity flow profile. Furthermore, with continuous perfusion, convection can provide a greater mass flux of vector, but viral particles will still have to diffuse between streamlines to reach the cells immobilized to the

bottom surface. Therefore, we decided to use consecutive transductions where virus would be allowed to diffuse under static conditions toward cells for short periods of time followed by re-filling steps to load more vector.

Under consecutive transduction conditions, cells in the microfluidic were exposed to two doses of vector at MOI 1.2, equating to a total (0.6x) MOI 2.4 transduction. Despite a 40% reduction in total vector usage, comparable levels of transduction were achieved, and the toxicity observed in the microfluidic with high concentration was rescued. Assessing the utilization efficiency of the three conditions also showed that the consecutive transductions were the most efficient method for higher MOI (**Figure 4.19b**). Consecutive transductions were conducted at (0.6x) instead of (1x) conditions due to the duration of transduction. From the kinetic experiments shown in **Figure 4.13**, it was determined that 5 hours was sufficient to achieve over 50% of the transduction obtained from a 24-hour transduction for each MOI in the microfluidics. Thus, we utilized two 4-hour transductions to achieve the same 8-hour transduction time as the static conditions to minimize wasted vector. Due to the constraints of a 30% LV (v/v)% concentration to maintain a low dose, the total amount of LV used was (0.6x) compared to (1x) in the static transductions.

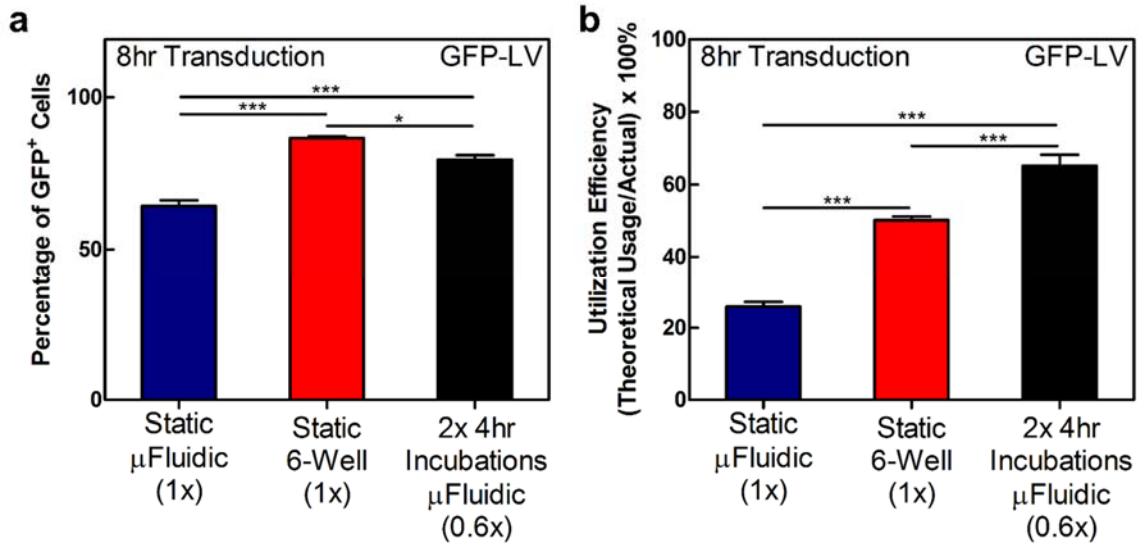

Figure 4.19: High LV (v/v)% leading to toxicity for high MOI can be rescued using low dose consecutive transductions. **(a)** (1x) MOI 4 microfluidic (µFluidic*)* transduction at 97.7% LV (v/v)% results in reduced transduction, but can be restored by using less LV at less toxic 30% LV (v/v)% for two 4-hour consecutive transductions, amounting to (0.6x) µFluidic transduction *(n = 6 (1x) static µFluidic and 6-Well, n = 5 (0.6x) µFluidic)*. *P<0.05, ***P<0.001, One-Way ANOVA. Data represent mean ± s.d. of biological replicates from four separate experiments ((1x) static conditions) and mean ± s.d. of technical replicates of one experiment ((0.6x) periodic filling microfluidic). **(b)** Virus savings and more efficient utilization can be achieved by consecutive transduction contrary to simply increasing MOI when high levels of transduction are desired.

4.4 Conclusions

We conducted an extensive sweep of various parameters that could contribute to transduction enhancement in the microfluidic to optimize conditions. Based on our results, we determined that minimizing the fluid height was a critical parameter. Previous vector titration protocols call for incubating cells in a total volume that is as small as possible. Due to surface tension and evaporation issues, there is a physical limit to the obtainable minimum height for conventional transduction systems (**Figure 4.20**). Thus, microfluidics may be perfect candidates for next generation transduction platforms.

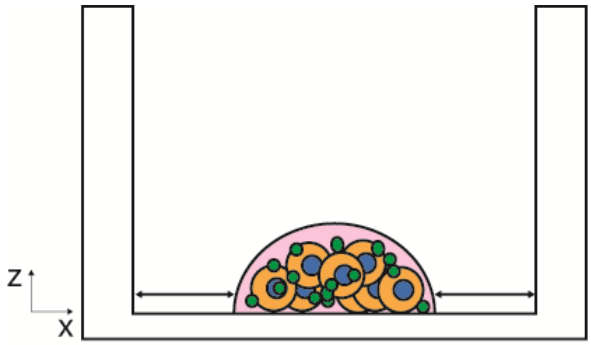

Figure 4.20: Schematic of surface-tension and evaporation limitations on minimum fluid height in standard systems.

Seeding cells at the highest density and using the minimum amounts of LV instead of pumping in more LV produced the most effective use of available vector. The saturating amounts of LV observed in some of the microfluidic transductions indicated that there was some sort of biological limitation rather than a diffusion limitation since increased concentration did not improve transduction proportionally. These factors are critical considerations for future device designs.

While the microliter-scale working volumes of microfluidic transductions confer benefit to transduction efficiency, it can also become a constraint depending on factors such as vector titer, nutrient requirements, and increased LV requirements depending on cell permissivity to infection. Static microfluidic transductions may physically be unable to accommodate the amount of LV particles required to infect all cells in the channel without toxicity resulting from high concentrations of viral stock formulation media. To address this limitation, we explored the possibility of periodically filling channels laden with RetroNectin-immobilized cells at safe LV v/v% concentrations. Previous studies have shown that transduction of adherent cell types using adenoviral and retroviral vectors can be enhanced with various perfusion regimes. LV can be diluted to safe levels and perfused to mitigate the toxicity of higher MOI in flow microfluidic transductions as well, though

this may require microfluidics that are specially designed for this specific mode of operation. One of the current strategies for large-scale transductions in cell culture bags uses RetroNectin coatings to adsorb vector onto the inner surfaces before loading cells and then simply flipping after some time to expose cells to fresh virus[55]. This method basically relies on multiple rounds of transduction in principle since cells are exposed to vector from one side of the bag and then flipped for exposure to more virus on the other side. Some mixing of unbound vector with cells may occur during the process of flipping, which may serve to enhance transduction. The microfluidic permits all of these mechanisms to be incorporated into a modified transduction protocol by enabling cells to be immobilized in the channel and then similarly performing multiple rounds of transduction. Furthermore, convective mixing can be more tightly controlled with perfusion and specific channel designs such as herringbone structures[98].

Constraints imposed by the target cell type and LV preparation or availability may make either time or virus savings more critical. Further considerations of the geometric constraints will then need to be considered to determine if a static or flow transduction is more appropriate (**Figure 4.21**). Microfluidics therefore serve as a flexible platform that can combine several transduction technologies to maximize efficiency.

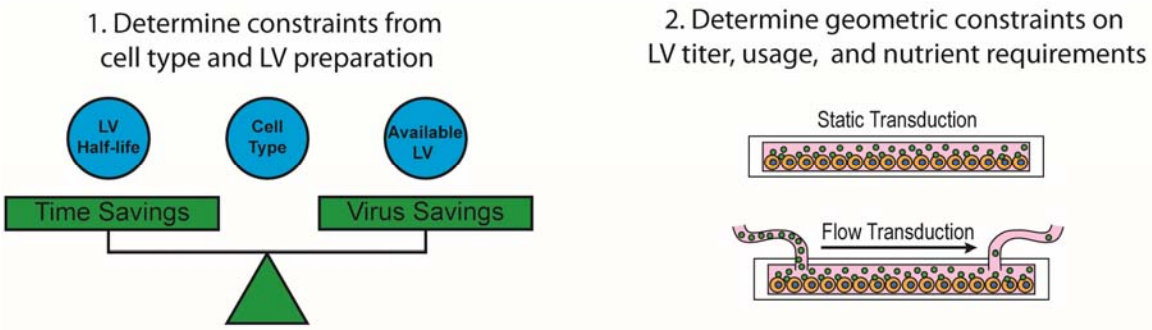

Figure 4.21: Illustration of the balance between time and virus savings afforded by the microfluidic and factors that determine the mode of usage.

CHAPTER 5: ASSESSING MICROFLUIDIC TRANSDUCTION EFFICACY IN PRIMARY HUMAN T CELLS

5.1 Introduction

Although cell lines provide essential insight necessary to characterize microfluidic lentiviral transductions, they present an ideal case for transduction efficiency due to their increased permissivity to infection[99]. Transduction of primary cells pose a much more challenging problem due to biological differences and heterogeneity of primary cell populations. For instance, LVs are commonly pseudotyped with the vesicular stomatitis virus glycoprotein (VSV-G) due to its broad tropism, allowing infection to a broad range of cell types[47]. Recent studies have identified the low-density lipoprotein receptor (LDL-R) as the receptor to VSV-G, which is expressed differentially in T cells depending on their activation state[71, 100]. Stimulation with interleukin-2 (IL-2) is therefore necessary to activate T cells and increase LDL-R expression levels, enabling detectable levels of transduction. T cells are becoming a major target for gene therapy due to increasing use of CAR T cells in cancer immunotherapy[22]. The issues of inefficient mass transport of existing systems combined with such biological barriers highlight the wastes generated in current clinical protocols.

5.2 Materials and Methods

5.2.1 Microfluidic Device Fabrication

CNC micro-milling as described in Section 3.2.2 was used to produce a mold for microfluidic devices to assess T cell lentiviral transduction kinetics. The channel height from these molds was 210µm, resulting in microfluidics with 200µL volumes. The height

was increased in the devices used for these experiments due to the lower titer of the GFP-LV. At 30% v/v% concentration, the MOI was still only 2.67. The 92µL microfluidics made from SU-8 molds were used for the fVIII-LV T cell transductions due to the much higher titers. All devices were coated with RetroNectin at a surface concentration of 2.1µg/cm^2.

5.2.2 T Cell Conditioning and Activation

Frozen human pan T cells were purchased from AllCells (AllCells, LLC., Alameda, CA, USA). Cells were thawed following the AllCells thawing protocol and allowed to recover in RPMI 1640 media supplemented with 10% FBS, L-Glutamine, 25 mM HEPES, and 1% Pen/Strep for 24 hours. CD3 and CD28-coated beads (Miltenyi Biotec Inc., San Diego, CA, USA) were then added to the cells at a 1:1 bead:cell ratio with 100 IU/mL human IL-2 (PeproTech, Rocky Hill, NJ, USA) for T cell activation. The cells and beads were then transferred to a 6-well plate at a density of 1-2x10^6 cells/mL/cm^2. Cells were ready for transduction after a 24-hour activation period.

5.2.3 T Cell Transduction

The same stock of GFP-LV from previous cell line transductions discussed in Chapter 4 were used for the T cell transduction kinetics experiments. The fVIII LV used to quantify T cell transduction efficiency was supplied by Expression Therapeutics, LLC (Tucker, GA, USA) and was prepared by commercial manufacturing organizations for clinical development of a CD34$^+$ fVIII-LV gene therapy product candidate. The fVIII-LV used a CD68 promoter, which is expressed in cells of the myeloid lineage such as granulocytes and monocytes. As such, T cells did not actually express fVIII, so VCN

analysis was used as the primary readout for transduction efficiency. A reduced dose of polybrene at 6μg/mL was used for all T cell transductions to avoid polybrene-associated toxicity.

5.2.4 T Cell Assessment of Transduction Efficiency

Cells that were transduced with the GFP-LV were stained with eFluor 780 viability dye (eBioscience, Inc., San Diego, CA, USA) at least 72 hours post-transduction. T cell purity was confirmed with a CD3-V450 (500A2) antibody (BD Biosciences, San Jose, CA, USA). Transduction efficiencies were determined as the percentage of GFP^+ live cells as obtained with a BD LSR II flow cytometer. Cell samples were blinded to the operator before processing for vector copy number. Genomic DNA was harvested from cells using the DNEasy blood and tissue kit (Qiagen, Valencia, CA, USA). Real-time quantitative PCR was used to determine vector copy number. fVIII-transduced cells received identical processing, without GFP assessment. An overview of the T cell conditioning from thawing to transduction assessment is summarized in **Figure 5.1**.

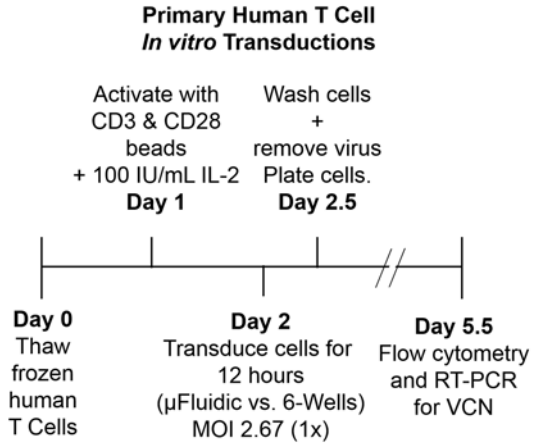

Figure 5.1: Conditioning of primary human T cells and LV transduction timeline.

5.3 Results and Discussion

5.3.1 Microfluidics Reduce LV Requirements in Primary Human T Cells

Transduction of primary human T cells has proven to be challenging due to biological barriers that are still not fully understood or characterized. We sought to determine if microfluidics could improve transduction by overcoming diffusion limitations, or if the notoriously low transduction was attributed mostly to biological barriers. We first assessed a variety of transduction times to determine the optimum time for T cells. As shown by eFluor 760 dead cell staining, cells were not negatively impacted for transduction times shorter than 12 hours, but cell death increased for 24-hour transductions (**Figure 5.2**). Specifically, cell death was significantly greater for the higher MOI (5x) 6-well condition, which indicates that cell death may be related to total amount of vector since the microfluidics were at the same vector concentration.

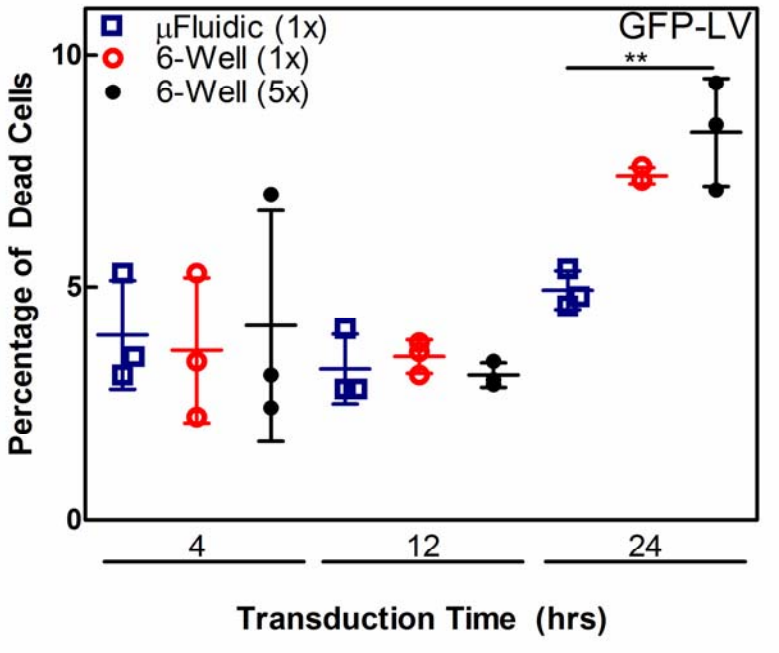

Figure 5.2: Percentages of dead T cells for each transduction time. Dead cells were quantified by flow cytometry using eFluor 780 staining.

GFP expression of cells transduced for 4 and 12 hours in either the microfluidic (1x), 6-well (1x), or concentrated 6-well (5x) demonstrated that the kinetics were increased between the microfluidic and 6-well using the same amount of LV (**Figure 5.3a**). Although the transduction was similar between the two conditions for 4-hour transductions, a nearly 20% increase in transduction was observed for 12-hour transductions. The concentrated 6-well (5x) initially yielded the greatest transduction for 4-hour transductions, but within 12 hours, the microfluidic was able to obtain the same level of transduction using 5-fold less LV. Vector copy number analysis confirmed that transgene integration correlated with GFP expression (**Figure 5.3b**).

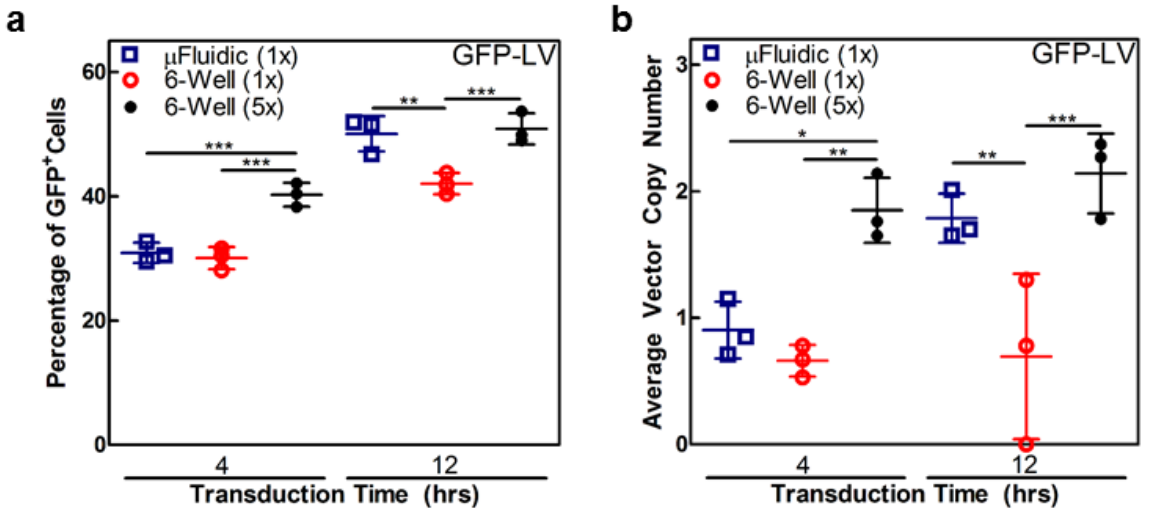

Figure 5.3: Transduction assessment of primary human T cells for 4 and 12 hour transductions. **(a)** Percentages of GFP^+ cells assessed by flow cytometry following transductions with a GFP-LV in microfluidics or 6-wells for either 4 or 12 hours. **(b)** Average vector copy number of transduced cells. (1x) transductions are MOI 2.67.

To better estimate the utilization efficiency of LV for our primary cell experiments, we defined a new utilization efficiency based on the VCN and the input MOI (Equation 8).

$$Utilizaion\ Efficiency_{VCN} = \frac{Estimated\ Total\ Vector\ Copies\ Integrated}{Viral\ Particles\ Used\ in\ Transduction} = \frac{VCN}{MOI}\ x\ 100\% \qquad (8)$$

Since the VCN represents the average number of vector copies per cell, the estimated total number of integrated vector copies can be calculated by multiplying the VCN by the number of cells initially transduced. Likewise, the number of viral particles used for transduction can be calculated by multiplying the MOI by the number of cells initially transduced. Therefore, the VCN utilization efficiency reduces to the ratio of the VCN and the MOI. Similar to the trends observed from the cell line transductions, the T cell utilization efficiency was highest for microfluidic transductions, and increased at a greater rate with increasing time (**Figure 5.4**).

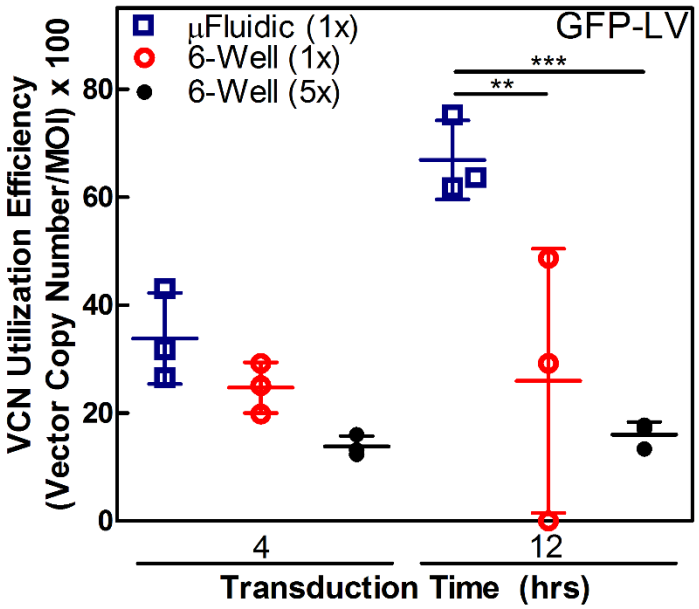

Figure 5.4: VCN utilization efficiency for various transduction conditions for 4 and 12-hour transductions (*n = 3)*. Data represent mean ± s.d. of technical replicates from one experiment. **P<0.01, ***P<0.001, Two-Way ANOVA.

5.3.2 Microfluidics Efficiently Transduce Primary T Cells Using FVIII-LV

With a slightly more optimized parameter space, we transduced primary human T cells with a preclinical $CD34^+$ fVIII-LV gene therapy product candidate that was developed by the Spencer/Doering laboratories. We tested our microfluidics with this LV for greater clinical relevance and its higher titer, which enabled greater MOI to be tested. Although fVIII was not produced due to the use of a CD68 myeloid-specific promoter, we obtained VCN as a readout for successful transduction. The (1x) microfluidics using MOI 20 resulted in the highest VCN compared to (1x) 6-wells that used the same amount of fVIII-LV (**Figure 5.5a**). Interestingly, the (0.25x) microfluidic conditions achieved the same amount of transduction compared to the (1x) 6-wells, indicating that a 4-fold reduction in LV usage may be possible using microfluidics. Calculation of the VCN utilization efficiency also shows that microfluidic transductions have the highest potential for efficient utilization of LV (**Figure 5.5b**).

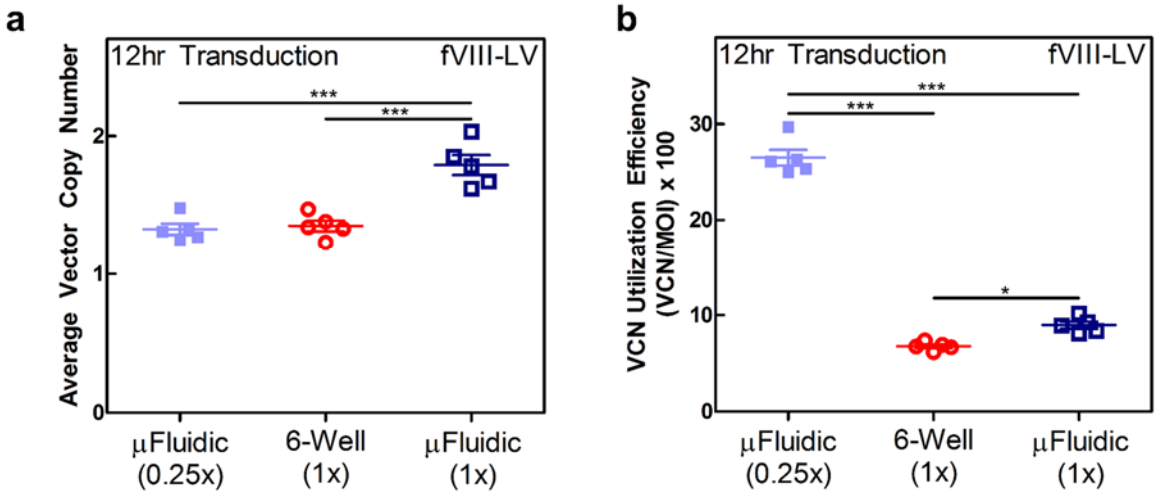

Figure 5.5: FVIII-LV transduction of primary human T cells *(n = 5)*. (1x) transduction is MOI 20. Data represent mean ± s.d. of technical replicates from one experiment. **(a)** Higher vector integration was achieved in the microfluidic (µFluidic) compared to a 6-well using the same amount of LV. However, using 75% less LV in a microfluidic resulted in comparable levels of gene transfer in the 6-well. **(b)** LV is more efficiently utilized for lower MOI transductions. **P<0.01, ***P<0.001, One-Way ANOVA.

5.4 Conclusions

Through these studies, we developed a better understanding of the capabilities and limitations of the microfluidic lentiviral transduction platform in regards to primary human cells. Although T cells are a notoriously difficult to transduce cell target, it was encouraging to see that improvements could still be realized compared to the current standard. Unlike the cell lines, transduction is limited by more than just diffusion limitations. Cellular barriers such as insufficient stimulation and restriction factors that resist infection significantly decrease the utilization efficiency of microfluidics. The methods in which activation and stimulation of cells played a large role in T cell susceptibility to transduction, and still requires much optimization. Although further evaluation is required, we demonstrated that T cells could successfully be transduced with relatively high efficiency using multiple LVs.

CHAPTER 6: ASSESSING MICROFLUIDIC TRANSDUCTION EFFICACY IN AN *EX VIVO* MURINE HEMOPHILIA A MODEL

6.1 Introduction

Hematopoietic stem cell-based gene therapy offers incredible potential to cure hematologic disorders such as hemophilia or sickle cell disease. Since these diseases have a genetic basis that results in altered or disrupted production of critical proteins, gene therapy can improve or even fully correct these disorders by targeting hematopoietic stem cells to re-populate the body with blood cells containing the corrected gene. In patients that cannot find a suitable bone marrow donor for allogenic bone marrow transplant, gene therapy offers an alternative method that utilizes a patient's own cells. For this type of therapy, it is not only important to achieve efficient genetic modification, but the stem cell properties must be preserved so that the cells can continue to self-renew[13]. We tested the microfluidic transduction device for safety and efficacy in a preclinical simulation of hemophilia A *ex vivo* hematopoietic stem cell gene therapy.

6.2 Materials and Methods

6.2.1 Animal Studies

All animal studies and procedures were performed at Emory University under the guidelines set by the Emory University Institutional Animal Care and Use Committee. C57BL/6 Exon-16 (E16)-disrupted hemophilia A mice were used in all animal experiments. Generation of this murine model for hemophilia A has been described previously. For transduction efficiency studies, both male and female mice between 8-10

weeks of age were used. No randomization was carried out to determine animal groups. Based on statistical power estimates (alpha = 0.05, power = 0.8, sigma = 0.3) assuming fVIII expression levels drawn from previous unpublished animal studies, a minimum of three mice per group would be needed to determine differences. Total animal numbers (*n*) for each group are given. An initial pilot experiment was conducted in which Sca-1^+ cells were transduced for 5 hours in microfluidics and compared to optimized 6-well transductions that had previously been investigated by the Spencer/Doering labs. The optimized protocol called for two doses of LV over a period of 28 hours. Due to the extremely high cell volumetric concentration used in the microfluidic, transduction times were reduced to 5 hours, which has been shown to be an effective length for microfluidic transduction without inducing detrimental effects from nutrient deprivation. Furthermore, extended *ex vivo* culture of stem cells has been shown to affect differentiation and self-renewal capacity of hematopoietic stem cells, and was therefore minimized for our studies[101]. The microfluidic transductions used either the same amount of LV or half as much. This experiment is outlined below in **Figure 6.1**, and informed the design of our second animal experiment, which aimed to compare and minimize vector dosage between systems for identical transduction times, outlined below in **Figure 6.2**.

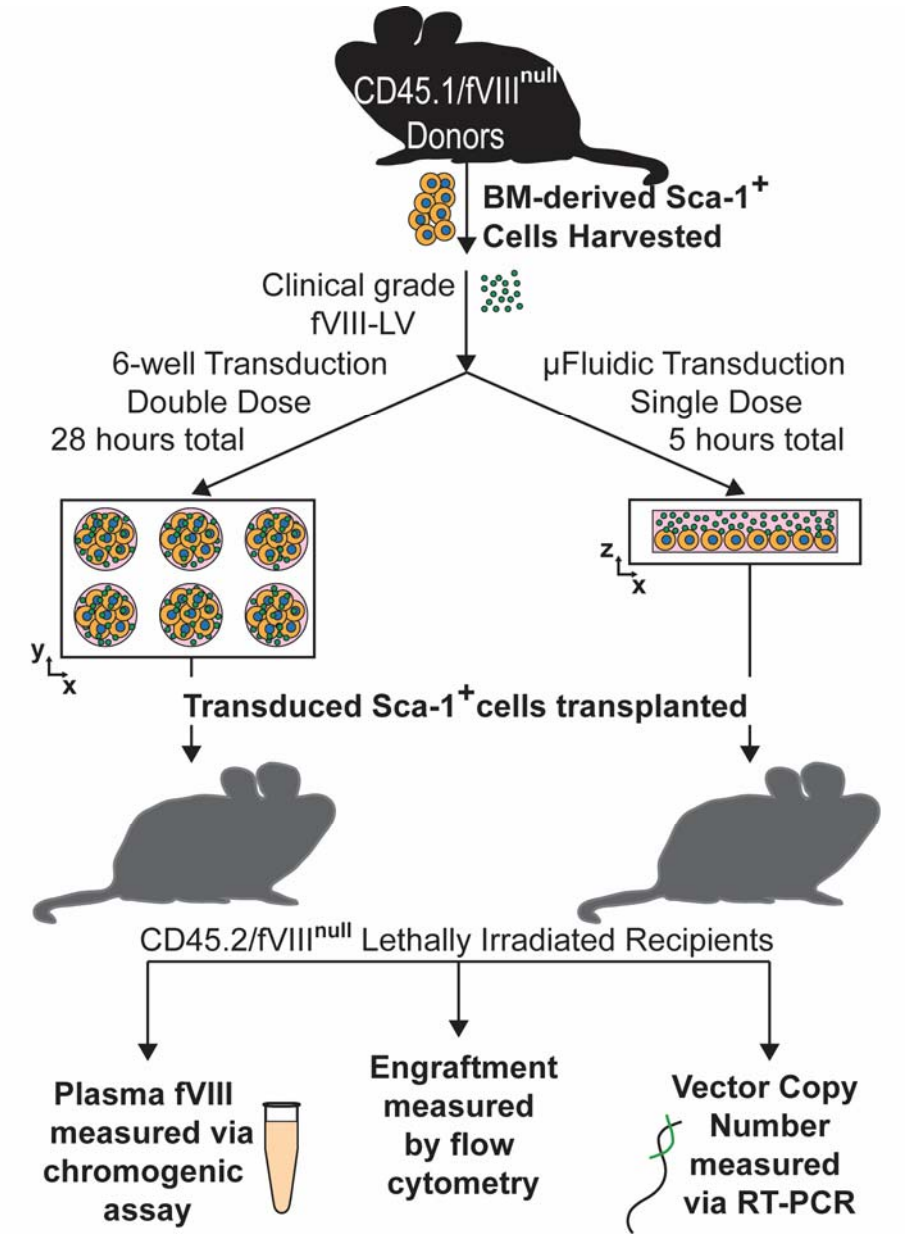

Figure 6.1: Schematic of pilot mouse experiments comparing microfluidic transductions to an optimized 6-well transduction protocol.

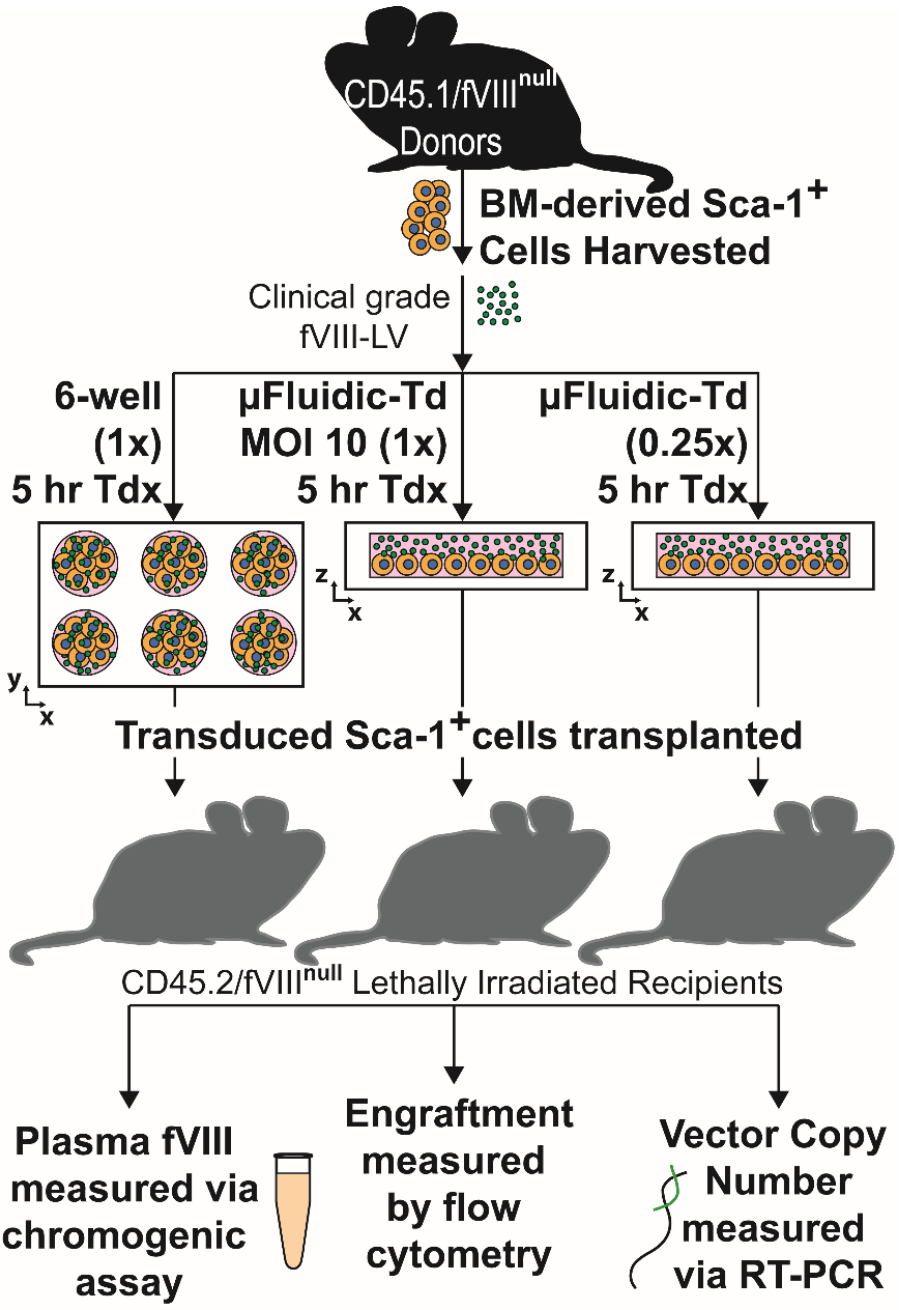

Figure 6.2: Schematic of mouse experiments comparing microfluidic transductions to an equivalent standard protocol using a 6-well plate.

6.2.2 Harvest and Culture of Mouse Sca-1$^+$ Cells

Bone marrow was isolated from cleaned hind leg femurs and tibias of C57BL/6 E16 hemophilia A mice with the CD45.1 allele. Sca-1$^+$ cells were incubated with biotin

anti-Sca-1 antibody followed by anti-biotin microbeads (Miltenyi Biotec, Inc., San Diego, CA, USA) and passed through a magnetic separation column for positive section. Isolated cells were then cultured overnight at a density of $2x10^6$ cells/mL in StemPro media supplemented with stem cell factor (100 ng/mL), murine interleukin-3 (20 ng/mL), human interleukin-11 (100 ng/mL), human Flt-3 ligand (100 ng/mL), StemPro nutrient supplement (40x), L-glutamine (100x), and penicillin/streptomycin (100x).

6.2.3 Transduction of Sca-1$^+$ Cells

On the day of transduction, 2 million cells were loaded into each bare microfluidic and 6-well with 8 μg/mL Polybrene as described above with a clinical grade fVIII-LV for 5 hours. Cells were then collected, washed, and re-suspended in fresh PBS for transplant.

6.2.4 Transplantation of Transduced Sca-1$^+$ Cells

At least four hours prior to transplantation, a separate cohort of 8- to 10-week-old C56BL/6 E16 hemophilia A mice with the CD45.2 allele were given two doses of lethal irradiation at 11 Gy Rad four hours apart. After transduction and washing of LV from the donor cells, 1,000,000 cells were transplanted into each host mouse via retro-orbital injection.

6.2.5 Bi-weekly Assessment of Sca-1$^+$ Cell Transduction and Engraftment

Mice were bled every two weeks for the first 8 weeks via tail vein microsampling. Flow cytometry was run on collected blood cells and stained for CD45.1 and CD45.2 to assess engraftment. The following antibody-fluorophore conjugates were used for flow cytometry: CD45.2-APC (558702), Gr1-APC-Cy7 (557661), Mac1-APC-Cy7 (557657),

CD45.1-PE (553776), CD3e-V450 (560801), and CD45R/B220-PE-Cy7 (552772) (BD Biosciences, San Jose, CA, USA). Complete blood counts were also conducted to monitor populations of various white blood cells including lymphocytes, monocytes, and granulocytes. Plasma was isolated and used to measure fVIII plasma levels via commercially available chromogenic substrate assay (Chromogenix Coatest SP FVIII, diaPharma, West Chester, OH, USA).

6.2.6 Quantification of Vector Copies in Blood, Spleen, and Bone Marrow

After 16 weeks, mice were euthanized, and cells from blood, spleen, and bone marrow were harvested for RT-PCR to quantify LV copy number. Vector copy number analysis were conducted as previously described in Section 5.2.4. The operator was blinded to the cell samples before processing for vector copy number.

6.3 Results and Discussions

6.3.1 Microfluidics Reduce Transduction Time in Primary Mouse Cells

Compared to mice transplanted with cells transduced following the standard 6-well protocol, mice that were transplanted with microfluidic-transduced cells utilizing the same or half the amount of fVIII-LV produced similar levels of plasma fVIII despite a nearly 5-fold reduction in LV exposure time. Utilizing this amount of vector, ranging from MOI 10-40 depending on the amount of cells transduced, all microfluidic-transduced cells restored the hemophilic mice to normal fVIII levels. Open shapes indicate transduction of 2 million cells versus 4 million cells, indicated with closed shapes. The 26.6μL 6-well transductions spanning 28 hours are historical data obtained by the Spencer/Doering lab. We compared

our modified shortened microfluidic transduction protocol to these data as a standard to demonstrate that the microfluidic could indeed reduce transduction times due to the greater LV availability and increased kinetics, which is beneficial for shortening *ex vivo* manipulation times to maintain stem cell properties.

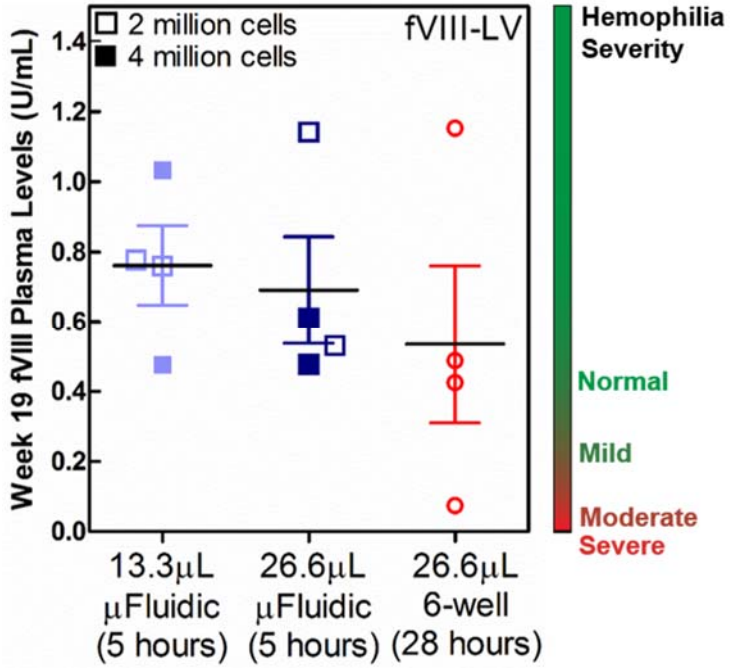

Figure 6.3: Plasma fVIII levels of mice transplanted with cells transduced in a microfluidic or 6-well. Amount of LV used and transduction times are indicated. Open shapes indicate 2 million cells were transduced while closed shapes indicate that 4 million cells were transduced.

The vector copy number of harvested blood cells showed that vector integration was highest in mice that were transduced with the least amount of LV (**Figure 6.4a**). Therefore, the VCN utilization efficiency was also highest (**Figure 6.4b**). These results indicate that biological barriers such as LV binding may have become rate limiting, leading to saturation since doubling the amount of LV did not further improve vector integration.

Combined with our previous data and basic analytical models of particle diffusion, we expected greater VCN due to the increased LV availability. As such, these data served as an upper limit of LV usage in our animal experiments since microfluidics using the same amounts of LV as the 6-wells did not demonstrate increased utilization efficiency, and only served to decrease transduction time. Overall, these data show that microfluidics can achieve sufficient gene transfer while reducing both LV usage and significantly reducing transduction times. Raw VCN and final fVIII data for all mice is shown in **Table 6.1**.

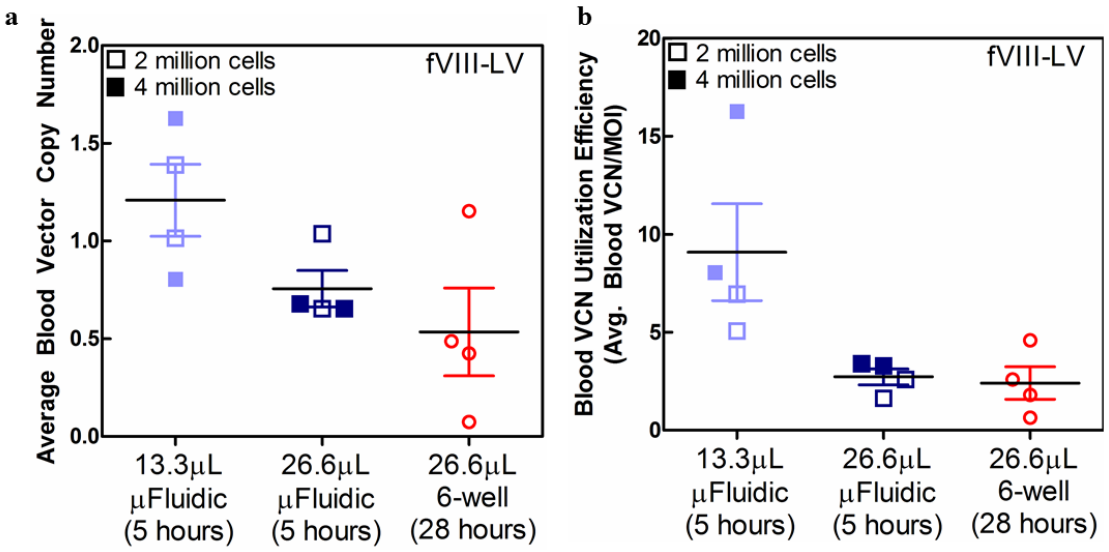

Figure 6.4: Assessment of vector integration in pilot mouse studies. **(a)** VCN analysis of blood cells harvested from mice in pilot experiment. **(b)** VCN utilization efficiency of harvested blood cells. Amount of LV used and transduction times are indicated. Open shapes indicate 2 million cells were transduced while closed shapes indicate that 4 million cells were transduced.

Table 6.1: VCN and final fVIII data for individual mice from pilot study.

Condition	VCN-Blood	VCN-SP	VCN-BM	fVIII (U/mL)
MOI 20, 2x10^6 cells	1.01	5.69	4.13	0.76
MOI 20, 2x10^6 cells	1.39	3.55	3.24	0.78
Average ± SEM	**1.20 ± 0.13**	**4.62 ± 0.75**	**3.68 ± 0.32**	**0.77 ± 0.01**
MOI 10, 4x10^6 cells	1.63	3.66	13.59	0.48
MOI 10, 4x10^6 cells	0.80	6.64	3.48	1.03
Average ± SEM	**1.22 ± 0.29**	**5.15 ± 1.05**	**8.54 ± 3.57**	**0.75 ± 0.2**
MOI 40, 2x10^6 cells	0.93	2.86	0.31	1.14
MOI 40, 2x10^6 cells	0.65	3.40	2.70	0.53
Average ± SEM	**0.79 ± 0.10**	**3.13 ± 0.19**	**1.50 ± 0.85**	**0.84 ± 0.22**
MOI 20, 4x10^6 cells	0.74	2.80	2.32	0.48
MOI 20, 4x10^6 cells	0.65	3.73	3.27	0.61
Average ± SEM	**0.70 ± 0.03**	**3.27 ± 0.33**	**2.80 ± 0.33**	**0.54 ± 0.05**
Mock TDX, 2x10^6 cells	**0.05**	**0.03**	**0.02**	**0.00**
Mock TDX, 4x10^6 cells	**0.01**	**0.01**	**0.03**	**0.00**
MOI 20x2, 6-Well Ctrl, 2x10^6 cells	0.72	-	-	0.074
MOI 20x2, 6-Well Ctrl, 2x10^6 cells	1.837	-	-	1.153
MOI 20x2, 6-Well Ctrl, 2x10^6 cells	1.037	-	-	0.425
MOI 20x2, 6-Well Ctrl, 2x10^6 cells	0.257	-	-	0.488
Average ± SEM	**0.96 ± 0.29**	**-**	**-**	**0.54 ± 0.20**

6.3.2 Microfluidics Best 6-wells in Direct Comparisons

Although our pilot experiment demonstrated potential advantages of microfluidic transduction in hematopoietic stem cell gene therapy, we sought to determine if direct comparisons showed similar trends as the cell line transductions. In this experiment, all cells were transduced for the same amount of time. Direct comparisons were made between 6-well and microfluidic transductions, indicated by (1x), which is MOI 10. A second set of microfluidic transductions were conducted at MOI 2.5 (0.25x) to determine if a reduced dose of LV in a microfluidic transduction could obtain similar levels of gene transfer as the 6-well. Overall, the amounts of LV used in this study were reduced by 2-8 fold to determine the minimum quantities of vector required to restore normal levels of fVIII in hemophiliac mice.

Over time, fVIII levels steadily increased across all conditions, and stabilized after 8 weeks (**Figure 6.5a**). The last three time points taken over a span of 8 weeks were averaged for each mouse to obtain an average plasma fVIII measurement (**Figure 6.5b**). Despite using half as much LV compared to the experiment described in Section 6.3.1, three of five mice produced normal levels of fVIII when transplanted with cells transduced in the microfluidics. Decreasing the LV dosage by four-fold still resulted in sufficient gene transfer, enabling all mice to produce moderate to mild levels of fVIII when transplanted with (0.25x) microfluidic cells.

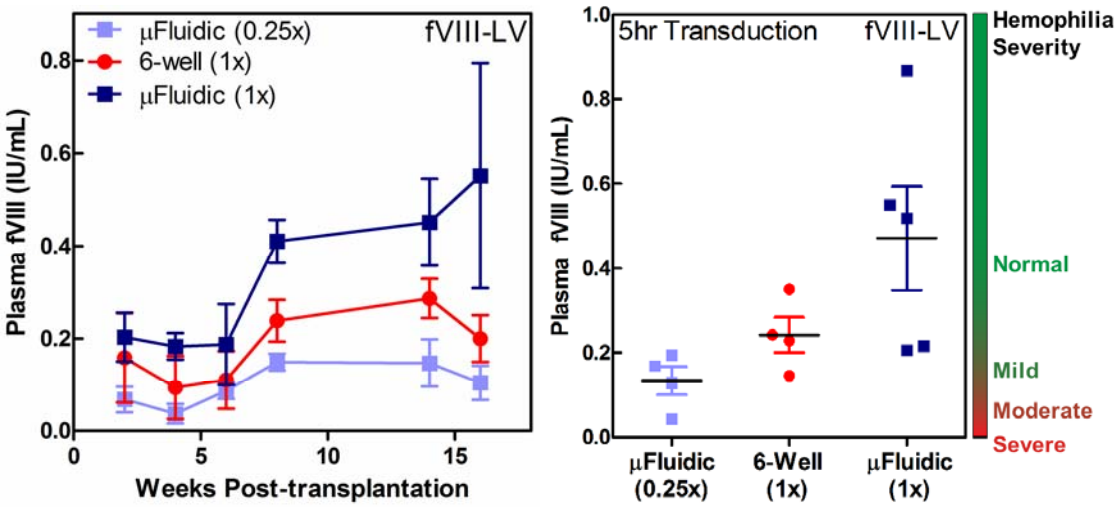

Figure 6.5: Assessment of fVIII production of mice transplanted with cells transduced in (0.25x) microfluidics, (1x) microfluidics, or (1x) 6-wells. (1x) transductions are MOI 10. **(a)** Progression of average fVIII production for each mouse group over 16 weeks. **(b)** Averaged plasma fVIII levels of individual mice between weeks 8 and 16. 3 mice from the (1x) microfluidic group were restored to normal fVIII levels.

6.3.3 Microfluidics Do Not Affect Mouse Survival or Engraftment

Cell viability can be difficult to assess following *in vitro* transductions since any cells that were negatively impacted by microfluidic transduction would quickly be selected against while viable cells continued to proliferate. Therefore, *in vivo* assessment of cell

engraftment was critical for determining if microfluidics negatively impacted the cells. Donor mice were selected for the CD45.1 allele while recipient mice had the CD45.2 allele. Due to lethal irradiation of recipient mice prior to transplantation, nearly all $CD45.2^+$ cells were eliminated. Therefore, all blood cells originating from the transplanted HSCs would be $CD45.1^+$ while poor engraftment would result in an increase in $CD45.2^+$ cells. Monitoring of white blood cell counts, particularly granulocyte, monocyte, and lymphocyte counts, were important to assess re-establishment of the immune system. Furthermore, due to the CD68-specific promoter used in the fVIII-LV, transgene expression would be directed toward cells of the myeloid lineage, which include granulocytes and monocytes. Flow cytometry showed that engraftment was high in all animals, and increased steadily over time, stabilizing after 8 weeks (**Figure 6.6a and b**). Other than a single outlier in each microfluidic group, all mice displayed >90% $CD45.1^+$ cells (**Figure 6.6c**) and <10% $CD45.2^+$ cells (**Figure 6.6d**).

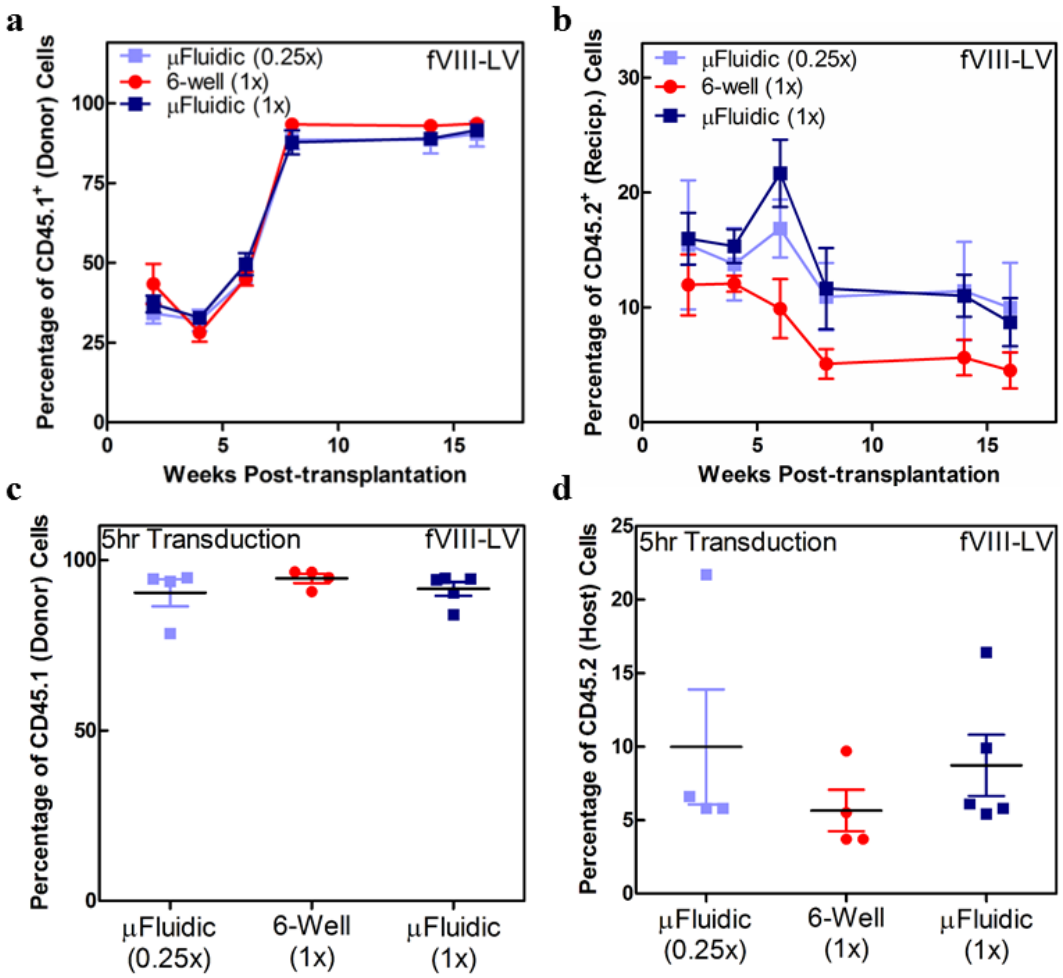

Figure 6.6: Engraftment of transplanted Sca-1$^+$ cells transduced in microfluidics compared to 6-wells. **(a)** Average percentage of CD45.1$^+$ cells over 16 weeks. **(b)** Average percentage of CD45.2$^+$ cells over 16 weeks. **(c)** Individual mouse CD45.1$^+$ cells at Week 16. **(d)** Individual mouse CD45.2$^+$ cells at Week 16.

All final white blood cell (**Figure 6.7a**), lymphocyte (**Figure 6.7b**), granulocyte (**Figure 6.7c**), and monocyte (**Figure 6.7d**) cell counts at Week 14 were within normal ranges as indicated by the two dashed lines. The lower limit for monocyte counts is at 0 cells/μL.

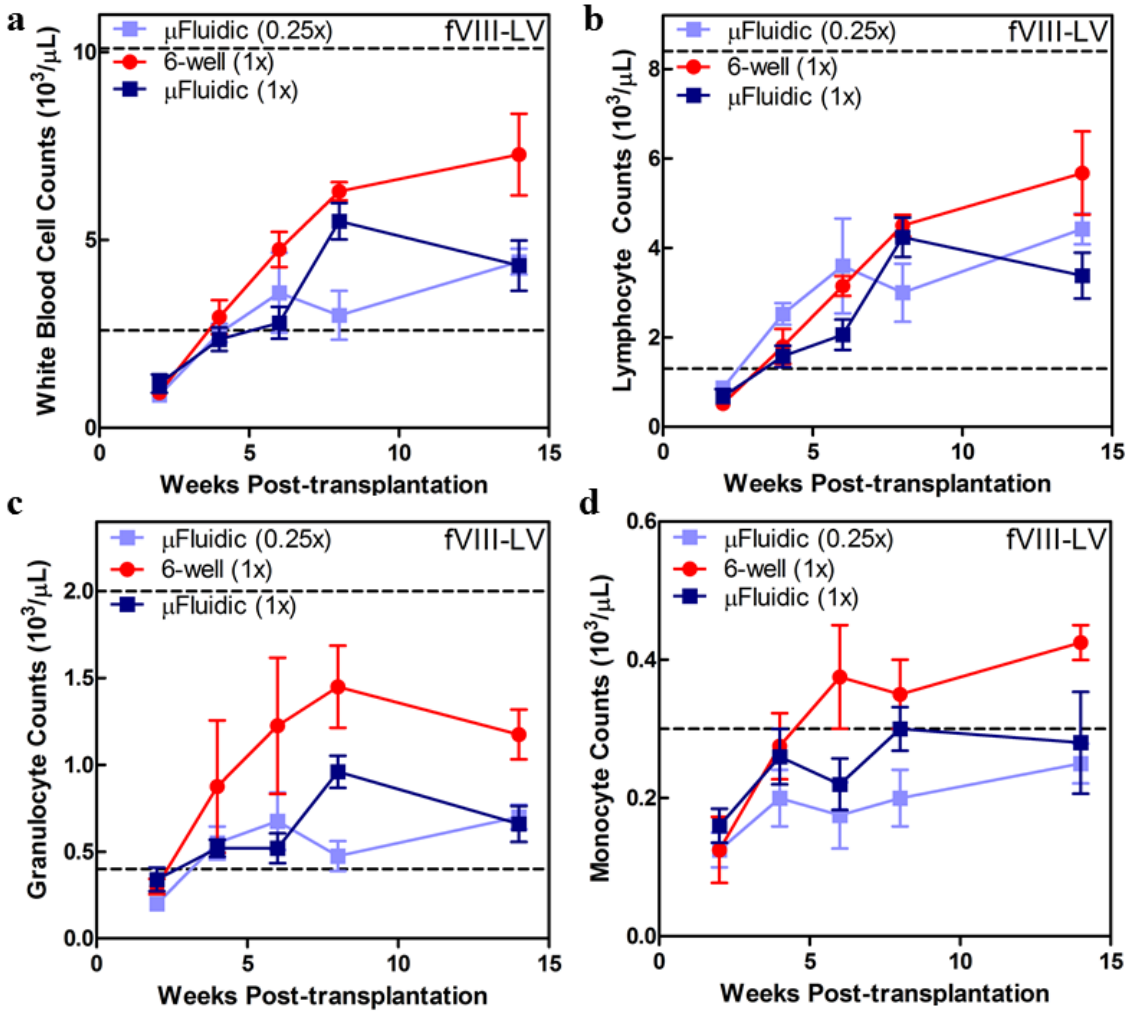

Figure 6.7: Mouse complete blood counts. **(a)** White blood cell, **(b)** lymphocytes, **(c)** granulocyte, and **(d)** monocyte counts over 14 weeks. Dashed lines indicate upper and lower bounds for normal levels. The lower bound for monocyte counts is 0.

6.3.4 Viral Vector Integration is Greater in Microfluidic Transductions

VCN utilization efficiency was calculated from the various tissues harvested and assessed for copy number (**Figure 6.8a**). Individual VCN for blood (**Figure 6.8b**), bone marrow (**Figure 6.8c**), and spleen (**Figure 6.8**). Comparable VCN utilization efficiency was achieved in both (1x) and (0.25x) microfluidics except for bone marrow cells. Though only blood VCN utilization efficiency was statistically significant compared to the 6-well

transductions ($p<0.05$), the majority of mice receiving cells transduced in microfluidics demonstrated greater utilization efficiency. Despite significantly lower vector dosages and transduction times, (1x) microfluidic transductions were significantly higher with the exception of bone marrow VCN. Individual VCN and average fVIII values for each mouse are given below in **Table 6.2**.

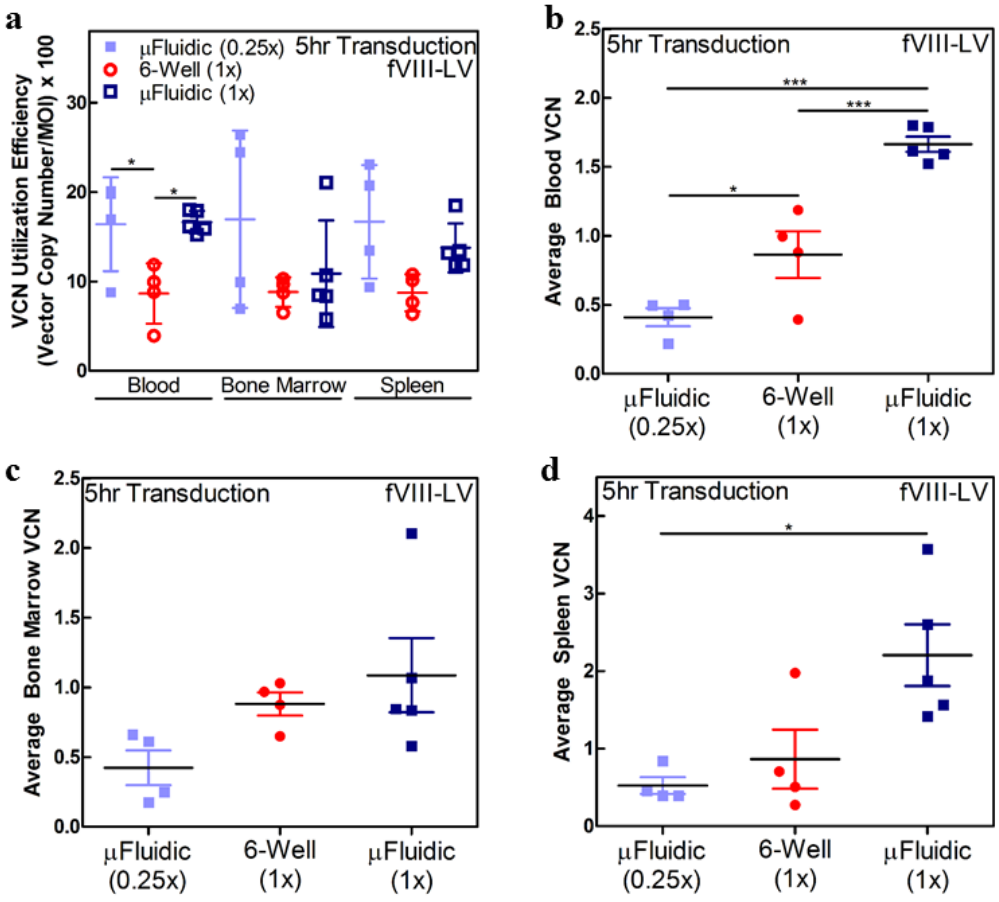

Figure 6.8: Analysis of vector integration in various mouse tissues. **(a)** VCN utilization efficiency of blood, bone marrow, and spleen. **(b)** Average VCN of harvested blood cells from individual mice per group. **(c)** Average VCN of harvested bone marrow cells from individual mice per group. **(d)** Average VCN of harvested spleen cells from individual mice per group.

Table 6.2: VCN and fVIII for individual mice in direct comparisons.

Sample	TDX Condition	Blood VCN	BM VCN	Sp VCN	8-week average fVIII
964N	**MOI 2.5 μfluidics**	0.501	0.174	0.338	0.044
964R	**MOI 2.5 μfluidics**	0.495	0.661	0.578	0.129
964LL	**MOI 2.5 μfluidics**	0.220	0.248	0.234	0.194
964LR	**MOI 2.5 μfluidics**	0.424	0.612	0.518	0.168
971R	**MOI 10 Well**	1.187	0.968	1.077	0.351
971L	**MOI 10 Well**	0.882	0.650	0.766	0.145
973N	**MOI 10 Well**	0.393	0.875	0.634	0.229
973L	**MOI 10 Well**	0.995	1.030	1.012	0.245
974N	**MOI 10 μfluidics**	1.593	2.106	1.849	0.206
974L	**MOI 10 μfluidics**	1.616	1.068	1.342	0.518
974R	**MOI 10 μfluidics**	1.522	0.845	1.183	0.215
974LL	**MOI 10 μfluidics**	1.801	0.836	1.319	0.549
974LR	**MOI 10 μfluidics**	1.789	0.580	1.185	0.868
HEMA	**N/A**	0.001	N/A	N/A	N/A

6.4 Conclusions

From these studies, we were able to definitively show that the microfluidic transduction platform did not have any negative impacts on cell viability, engraftment, or stem cell properties such as proliferation and differentiation. The long-term survival of these mice were not compromised as demonstrated by two separate cohorts which survived to 16 and 19 weeks post-transplant. All mice transplanted with microfluidic transduced cells from the pilot study using a minimized clinical vector dose produced normal levels of fVIII. Using even less vector in the direct 6-well comparisons, three of five mice were still restored to normal fVIII levels despite using half as much LV. Combined usage with RetroNectin or rapamycin may enable even greater levels of transduction to be achieved[102]. Although the transduction times were already significantly shortened compared to clinical protocols, assessment of transduction kinetics with these cells would be interesting to determine the minimum time required for effective transduction.

CHAPTER 7: CONCLUDING REMARKS AND FUTURE DIRECTIONS

In the current work, we translated state-of-the-art transduction protocols to a microfluidic platform enabling significant reduction in LV requirements by leveraging the micron-scale heights of microfluidics to overcome diffusion limitations of current systems. Moreover, the high surface area-to-volume ratio of microfluidics efficiently brings LV into cell contact before degradation occurs, reducing transduction times while minimizing LV waste and total amounts used by enabling large quantities of cells to be exposed to sufficient vector concentrations. Transduction efficiency can be further maximized by incorporating existing transduction-enhancing methods. Overall, the microfluidic platform outperforms current clinical transduction platforms in all aspects studied.

As shown from our primary cell data, diffusion limitations are not the only barriers to overcome in developing a novel microfluidic platform for gene therapy. While our system currently enables enhanced transduction simply from adapting existing protocols combined with leveraging the increased mass transport afforded by microfluidics, there are still many other areas where improvements can be targeted by changing the design or incorporating new microfluidic features that may also be used to actively enhance vector-cell interactions. Based on the insights gained from this work, it may be equally advantageous to leverage the microfluidic system to reduce the expensive cytokine requirements currently needed to effectively stimulate or activate primary cells for transduction. Future work can focus on using our microfluidics for short term cell culture or stimulation to build toward an all-in-one system that can be compatible with existing apheresis machines.

Among potential device improvements and implementations, additional efforts need to be put forth in further characterizing primary T cell and hematopoietic stem cell microfluidic transduction. One potential route is to assess CAR-LVs targeting CD19 for acute lymphoblastic leukemia. Our previous T cell work was only able to assess vector integration as a primary output due to limitations in LV availability. However, it should be a top priority to transduce T cells with a CAR-LV so that functional assays can be conducted for efficacy or safety profiling. With T cells, tumor cell-specific cytotoxicity could be measured to quantify the anti-cancer potential of microfluidic-generated CAR T cells. Future hematopoietic stem cell work should investigate the efficacy of microfluidics in transducing human $CD34^+$ cells, which are an even more difficult target for genetic modification. The cells could then be assessed with the human colony forming cell assay using methylcellulose-based media to determine if engraftment has been compromised. Alternatively, transduced human $CD34^+$ cells could be transplanted into humanized NOD SCID mice to assess engraftment potential.

Finally, continued efforts to scale up are necessary to make a true impact on gene therapy globalization and commercialization. While mock-ups of potential mold designs have been considered as discussed in Section 3.5, future designs do not have to be limited to PDMS-based devices. One potential idea is to take existing cell culture bags and use a hot embossing process to pattern channels within the bag so that the geometry can be constrained to have high surface area to volume ratio. Another thought would be to use gas permeable sheets of similar materials to cell culture bags and use a xurographic process to pattern channels and bond two layers together to form a channel in a bag again. This design

could eventually intersect with the previously discussed idea of having the device directly interface with apheresis machines.

Based on our current data as well as our experience with preclinical development of a $CD34^+$ fVIII-LV gene therapy product candidate, a clinical production run we estimate that an order of magnitude reduction in vector costs per patient may be attainable by using microfluidics. Since the LV manufacturing process currently induces high toxicity in the mammalian cell required for production, it is not possible to perform long-term continuous production. The more viable option is to develop methods to enhance efficiency. Any improvements in transduction efficiency will only be enhanced if better technologies arise for vector production, but improvements in vector production will not necessarily result in greater efficiency. As the current strategy in clinical gene therapy is to apply as much vector onto cells as possible without inducing detrimental toxicity, incorporating microfluidic transduction can significantly reduce the wastes inherent in current processes and overcome issues related to the various sources of variability in vector titration and inconsistent infectivity between various cell types. With clinical gene therapy rapidly advancing with definite evidence of success and licensed products, associated advances in vector manufacturing and utilization are going to be essential to routine clinical implementation and globalization.

REFERENCES

1. Aiuti, A. et al. Lentiviral hematopoietic stem cell gene therapy in patients with Wiskott-Aldrich syndrome. *Science* **341**, 1233151 (2013).
2. Cartier, N. et al. Hematopoietic stem cell gene therapy with a lentiviral vector in X-linked adrenoleukodystrophy. *science* **326**, 818-823 (2009).
3. Cavazzana-Calvo, M. et al. Transfusion independence and HMGA2 activation after gene therapy of human [bgr]-thalassaemia. *Nature* **467**, 318-322 (2010).
4. Maude, S.L. et al. Chimeric antigen receptor T cells for sustained remissions in leukemia. *New England Journal of Medicine* **371**, 1507-1517 (2014).
5. Zufferey, R. et al. Self-inactivating lentivirus vector for safe and efficient in vivo gene delivery. *Journal of virology* **72**, 9873-9880 (1998).
6. Naldini, L. Lentiviruses as gene transfer agents for delivery to non-dividing cells. *Current opinion in biotechnology* **9**, 457-463 (1998).
7. Ausubel, L.J. et al. Production of CGMP-grade lentiviral vectors. *BioProcess international* **10**, 32 (2012).
8. Millington, M., Arndt, A., Boyd, M., Applegate, T. & Shen, S. Towards a clinically relevant lentiviral transduction protocol for primary human CD34+ hematopoietic stem/progenitor cells. *PLoS One* **4**, e6461 (2009).
9. Scaramuzza, S. et al. Preclinical Safety and Efficacy of Human CD34+ Cells Transduced With Lentiviral Vector for the Treatment of Wiskott-Aldrich Syndrome. *Molecular Therapy* **21**, 175-184 (2013).
10. Davis, H.E., Morgan, J.R. & Yarmush, M.L. Polybrene increases retrovirus gene transfer efficiency by enhancing receptor-independent virus adsorption on target cell membranes. *Biophysical chemistry* **97**, 159-172 (2002).
11. O'Doherty, U., Swiggard, W.J. & Malim, M.H. Human immunodeficiency virus type 1 spinoculation enhances infection through virus binding. *Journal of virology* **74**, 10074-10080 (2000).
12. Lee, H.-J. et al. Retronectin enhances lentivirus-mediated gene delivery into hematopoietic progenitor cells. *Biologicals* **37**, 203-209 (2009).
13. Wang, C.X. et al. Rapamycin relieves lentiviral vector transduction resistance in human and mouse hematopoietic stem cells. *Blood* **124**, 913-923 (2014).
14. Johnston, J.M. et al. High-throughput screening identifies compounds that enhance lentiviral transduction. *Gene therapy* **21**, 1008-1020 (2014).
15. Zhang, B. et al. The significance of controlled conditions in lentiviral vector titration and in the use of multiplicity of infection (MOI) for predicting gene transfer events. *Genetic vaccines and therapy* **2**, 1 (2004).
16. Andreadis, S. et al. Toward a more accurate quantitation of the activity of recombinant retroviruses: alternatives to titer and multiplicity of infection. *Journal of virology* **74**, 1258-1266 (2000).
17. Haas, D.L., Case, S.S., Crooks, G.M. & Kohn, D.B. Critical factors influencing stable transduction of human CD34+ cells with HIV-1-derived lentiviral vectors. *Molecular Therapy* **2**, 71-80 (2000).
18. Bajaj, B., Lei, P. & Andreadis, S.T. High efficiencies of gene transfer with immobilized recombinant retrovirus: kinetics and optimization. *Biotechnology progress* **17**, 587-596 (2001).

19. Chuck, A.S., Clarke, M.F. & Palsson, B.O. Retroviral infection is limited by Brownian motion. *Human gene therapy* **7**, 1527-1534 (1996).
20. Blaese, R.M., Culver, K.W., Miller, A.D. & Carter, C.S. T lymphocyte-directed gene therapy for ADAnegative SCID: Initial trial results after 4 years. *Science* **270**, 475 (1995).
21. Biffi, A. et al. Lentiviral hematopoietic stem cell gene therapy benefits metachromatic leukodystrophy. *Science* **341**, 1233158 (2013).
22. Gill, S. & June, C.H. Going viral: chimeric antigen receptor T-cell therapy for hematological malignancies. *Immunological reviews* **263**, 68-89 (2015).
23. Beebe, D.J., Mensing, G.A. & Walker, G.M. Physics and applications of microfluidics in biology. *Annual review of biomedical engineering* **4**, 261-286 (2002).
24. Bilal, M.Y., Vacaflores, A. & Houtman, J.C.D. Optimization of methods for the genetic modification of human T cells. *Immunology and cell biology* **93**, 896-908 (2015).
25. Watson, J.D. & Crick, F.H.C. Molecular structure of nucleic acids. *Nature* **171**, 737-738 (1953).
26. Wolff, J.A. & Lederberg, J. An early history of gene transfer and therapy. *Human Gene Therapy* **5**, 469-480 (1994).
27. Wirth, T., Parker, N. & Ylä-Herttuala, S. History of gene therapy. *Gene* **525**, 162-169 (2013).
28. Friedmann, T. A brief history of gene therapy. *Nature genetics* **2**, 93-98 (1992).
29. Beutler, E. The cline affair. *Molecular Therapy* **4**, 396 (2001).
30. Cline, M.J. et al. Gene transfer in intact animals. *Nature* **284**, 422-425 (1980).
31. Mercola, K.E., Stang, H.D., Browne, J., Salser, W. & Cline, M.J. Insertion of a new gene of viral origin into bone marrow cells of mice. *Science* **208**, 1033-1035 (1980).
32. Graham, F.L. & van der Eb, A.J. A new technique for the assay of infectivity of human adenovirus 5 DNA. *Virology* **52**, 456-467 (1973).
33. Shimotohno, K., Mizutani, S. & Temin, H.M. Sequence of retrovirus provirus resembles that of bacterial transposable elements. *Nature* **285**, 550-554 (1980).
34. Wei, C.M., Gibson, M., Spear, P.G. & Scolnick, E.M. Construction and isolation of a transmissible retrovirus containing the src gene of Harvey murine sarcoma virus and the thymidine kinase gene of herpes simplex virus type 1. *Journal of virology* **39**, 935-944 (1981).
35. Tabin, C.J., Hoffmann, J.W., Goff, S.P. & Weinberg, R.A. Adaptation of a retrovirus as a eucaryotic vector transmitting the herpes simplex virus thymidine kinase gene. *Molecular and cellular biology* **2**, 426-436 (1982).
36. Miller, A.D., Jolly, D.J., Friedmann, T. & Verma, I.M. A transmissible retrovirus expressing human hypoxanthine phosphoribosyltransferase (HPRT): gene transfer into cells obtained from humans deficient in HPRT. *Proceedings of the National Academy of Sciences* **80**, 4709-4713 (1983).
37. Kantoff, P.W. et al. Correction of adenosine deaminase deficiency in cultured human T and B cells by retrovirus-mediated gene transfer. *Proceedings of the National Academy of Sciences* **83**, 6563-6567 (1986).

38. Rosenberg, S.A. et al. Gene Transfer into Humans — Immunotherapy of Patients with Advanced Melanoma, Using Tumor-Infiltrating Lymphocytes Modified by Retroviral Gene Transduction. *New England Journal of Medicine* **323**, 570-578 (1990).
39. Raper, S.E. et al. A pilot study of in vivo liver-directed gene transfer with an adenoviral vector in partial ornithine transcarbamylase deficiency. *Human gene therapy* **13**, 163-175 (2002).
40. Wilson, J.M. Lessons learned from the gene therapy trial for ornithine transcarbamylase deficiency. *Molecular genetics and metabolism* **96**, 151-157 (2009).
41. Hacein-Bey-Abina, S. et al. LMO2-associated clonal T cell proliferation in two patients after gene therapy for SCID-X1. *science* **302**, 415-419 (2003).
42. Debyser, Z. Biosafety of lentiviral vectors. *Current gene therapy* **3**, 517-525 (2003).
43. Dull, T. et al. A third-generation lentivirus vector with a conditional packaging system. *Journal of virology* **72**, 8463-8471 (1998).
44. Ylä-Herttuala, S. Endgame: glybera finally recommended for approval as the first gene therapy drug in the European union. *Molecular Therapy* **20**, 1831 (2012).
45. Morrison, C. [dollar] 1-million price tag set for Glybera gene therapy. *Nature biotechnology* **33**, 217-218 (2015).
46. Tiscornia, G., Singer, O. & Verma, I.M. Production and purification of lentiviral vectors. (2006).
47. Burns, J.C., Friedmann, T., Driever, W., Burrascano, M. & Yee, J.-K. Vesicular stomatitis virus G glycoprotein pseudotyped retroviral vectors: concentration to very high titer and efficient gene transfer into mammalian and nonmammalian cells. *Proceedings of the National Academy of Sciences* **90**, 8033-8037 (1993).
48. Verhoeyen, E. & Cosset, F.L. Surface-engineering of lentiviral vectors. *The journal of gene medicine* **6**, S83-S94 (2004).
49. Chen, S.-T., Iida, A., Guo, L., Friedmann, T. & Yee, J.-K. Generation of packaging cell lines for pseudotyped retroviral vectors of the G protein of vesicular stomatitis virus by using a modified tetracycline inducible system. *Proceedings of the National Academy of Sciences* **93**, 10057-10062 (1996).
50. Ory, D.S., Neugeboren, B.A. & Mulligan, R.C. A stable human-derived packaging cell line for production of high titer retrovirus/vesicular stomatitis virus G pseudotypes. *Proceedings of the National Academy of Sciences* **93**, 11400-11406 (1996).
51. Merten, O.-W., Hebben, M. & Bovolenta, C. Production of lentiviral vectors. *Molecular therapy. Methods & clinical development* **3**, 16017 (2016).
52. Abe, A., Miyanohara, A. & Friedmann, T. Polybrene increases the efficiency of gene transfer by lipofection. *Gene therapy* **5**, 708-711 (1998).
53. Seitz, B. et al. Retroviral vector-mediated gene transfer into keratocytes: in vitro effects of polybrene and protamine sulfate. *Graefe's archive for clinical and experimental ophthalmology* **236**, 602-612 (1998).
54. Lin, P., Correa, D., Lin, Y. & Caplan, A.I. Polybrene inhibits human mesenchymal stem cell proliferation during lentiviral transduction. *PloS one* **6**, e23891 (2011).

55. Dodo, K. et al. An efficient large-scale retroviral transduction method involving preloading the vector into a RetroNectin-coated bag with low-temperature shaking. *PloS one* **9**, e86275 (2014).
56. Brendel, C. & Williams, D.A. Unexpected help: mTOR meets lentiviral vectors. *Blood* **124**, 832-833 (2014).
57. Reiser, J. Production and concentration of pseudotyped HIV-1-based gene transfer vectors. *Gene therapy* **7**, 910-913 (2000).
58. Guo, J., Wang, W., Yu, D. & Wu, Y. Spinoculation triggers dynamic actin and cofilin activity that facilitates HIV-1 infection of transformed and resting CD4 T cells. *Journal of virology* **85**, 9824-9833 (2011).
59. Le Doux, J.M., Landazuri, N., Yarmush, M.L. & Morgan, J.R. Complexation of retrovirus with cationic and anionic polymers increases the efficiency of gene transfer. *Human gene therapy* **12**, 1611-1621 (2001).
60. Scherer, F. et al. Magnetofection: enhancing and targeting gene delivery by magnetic force in vitro and in vivo. *Gene therapy* **9**, 102-109 (2002).
61. Shamir, E.R. et al. Twist1-induced dissemination preserves epithelial identity and requires E-cadherin. *The Journal of cell biology* **204**, 839-856 (2014).
62. Chuck, A.S. & Palsson, B.O. Consistent and high rates of gene transfer can be obtained using flow-through transduction over a wide range of retroviral titers. *Human gene therapy* **7**, 743-750 (1996).
63. Chuck, A.S. & Palsson, B.Ø. Membrane adsorption characteristics determine the kinetics of flow-through transductions. *Biotechnology and bioengineering* **51**, 260-270 (1996).
64. Andreadis, S.T., Roth, C.M., Le Doux, J.M., Morgan, J.R. & Yarmush, M.L. Large-Scale Processing of Recombinant Retroviruses for Gene Therapy. *Biotechnology progress* **15**, 1-11 (1999).
65. Geraerts, M., Willems, S., Baekelandt, V., Debyser, Z. & Gijsbers, R. Comparison of lentiviral vector titration methods. *BMC biotechnology* **6**, 1 (2006).
66. Kutner, R.H., Zhang, X.-Y. & Reiser, J. Production, concentration and titration of pseudotyped HIV-1-based lentiviral vectors. *Nature protocols* **4**, 495-505 (2009).
67. Ricks, D.M., Kutner, R., Zhang, X.-Y., Welsh, D.A. & Reiser, J. Optimized lentiviral transduction of mouse bone marrow-derived mesenchymal stem cells. *Stem cells and development* **17**, 441-450 (2008).
68. Salmon, P. & Trono, D. Production and titration of lentiviral vectors. *Current protocols in human genetics*, 12-10 (2007).
69. Ellis, J. Silencing and variegation of gammaretrovirus and lentivirus vectors. *Human gene therapy* **16**, 1241-1246 (2005).
70. Andreadis, S.T., Brott, D., Fuller, A.O. & Palsson, B.O. Moloney murine leukemia virus-derived retroviral vectors decay intracellularly with a half-life in the range of 5.5 to 7.5 hours. *Journal of virology* **71**, 7541-7548 (1997).
71. Finkelshtein, D., Werman, A., Novick, D., Barak, S. & Rubinstein, M. LDL receptor and its family members serve as the cellular receptors for vesicular stomatitis virus. *Proceedings of the National Academy of Sciences* **110**, 7306-7311 (2013).

72. Shabram, P. & Aguilar-Cordova, E. Multiplicity of infection/multiplicity of confusion. *Molecular Therapy* **2**, 420 (2000).
73. Patterson, S., Gross, J., Bedford, P. & Knight, S.C. Morphology and phenotype of dendritic cells from peripheral blood and their productive and non-productive infection with human immunodeficiency virus type 1. *Immunology* **72**, 361 (1991).
74. Shin, Y. et al. Microfluidic assay for simultaneous culture of multiple cell types on surfaces or within hydrogels. *Nature protocols* **7**, 1247-1259 (2012).
75. Mecomber, J.S., Hurd, D. & Limbach, P.A. Enhanced machining of micron-scale features in microchip molding masters by CNC milling. *International Journal of Machine Tools and Manufacture* **45**, 1542-1550 (2005).
76. Islam, M., Natu, R. & Martinez-Duarte, R. A study on the limits and advantages of using a desktop cutter plotter to fabricate microfluidic networks. *Microfluidics and Nanofluidics* **19**, 973-985 (2015).
77. Bartholomeusz, D.A., Boutté, R.W. & Andrade, J.D. Xurography: rapid prototyping of microstructures using a cutting plotter. *Journal of Microelectromechanical Systems* **14**, 1364-1374 (2005).
78. Tran, R. et al. Simplified prototyping of perfusable polystyrene microfluidics. *Biomicrofluidics* **8**, 046501 (2014).
79. Wang, Y. et al. Benchtop micromolding of polystyrene by soft lithography. *Lab on a Chip* **11**, 3089-3097 (2011).
80. Young, E.W.K. et al. Rapid prototyping of arrayed microfluidic systems in polystyrene for cell-based assays. *Analytical chemistry* **83**, 1408-1417 (2011).
81. Iliescu, C., Taylor, H., Avram, M., Miao, J. & Franssila, S. A practical guide for the fabrication of microfluidic devices using glass and silicon. *Biomicrofluidics* **6**, 016505 (2012).
82. Xia, Y. & Whitesides, G.M. Soft lithography. *Annual review of materials science* **28**, 153-184 (1998).
83. Berthier, E., Young, E.W.K. & Beebe, D. Engineers are from PDMS-land, Biologists are from Polystyrenia. *Lab on a Chip* **12**, 1224-1237 (2012).
84. Zheng, Y. et al. In vitro microvessels for the study of angiogenesis and thrombosis. *Proceedings of the National Academy of Sciences* **109**, 9342-9347 (2012).
85. Golden, A.P. & Tien, J. Fabrication of microfluidic hydrogels using molded gelatin as a sacrificial element. *Lab on a Chip* **7**, 720-725 (2007).
86. Whitesides, G.M., Ostuni, E., Takayama, S., Jiang, X. & Ingber, D.E. Soft lithography in biology and biochemistry. *Annual review of biomedical engineering* **3**, 335-373 (2001).
87. Bélanger, M.C. & Marois, Y. Hemocompatibility, biocompatibility, inflammatory and in vivo studies of primary reference materials low-density polyethylene and polydimethylsiloxane: A review. *Journal of biomedical materials research* **58**, 467-477 (2001).
88. Myers, D.R. et al. Endothelialized microfluidics for studying microvascular interactions in hematologic diseases. *Journal of visualized experiments: JoVE* (2012).

89. Wang, L., Sun, B., Ziemer, K.S., Barabino, G.A. & Carrier, R.L. Chemical and physical modifications to poly (dimethylsiloxane) surfaces affect adhesion of Caco-2 cells. *Journal of biomedical materials research Part A* **93**, 1260-1271 (2010).
90. Toepke, M.W. & Beebe, D.J. PDMS absorption of small molecules and consequences in microfluidic applications. *Lab on a Chip* **6**, 1484-1486 (2006).
91. Sunkara, V. et al. Simple room temperature bonding of thermoplastics and poly (dimethylsiloxane). *Lab on a Chip* **11**, 962-965 (2011).
92. Sutton, K.S., Dasgupta, A., McCarty, D., Doering, C.B. & Spencer, H.T. Bioengineering and serum free expansion of blood-derived γδ T cells. *Cytotherapy* **18**, 881-892 (2016).
93. Le Doux, J.M., Davis, H.E., Morgan, J.R. & Yarmush, M.L. Kinetics of retrovirus production and decay. *Biotechnology and bioengineering* **63**, 654-662 (1999).
94. Tayi, V.S., Bowen, B.D. & Piret, J.M. Mathematical model of the rate-limiting steps for retrovirus-mediated gene transfer into mammalian cells. *Biotechnology and bioengineering* **105**, 195-209 (2010).
95. Valentine, R.C. & Allison, A.C. Virus particle adsorption I. Theory of adsorption and experiments on the attachment of particles to non-biological surfaces. *Biochimica et biophysica acta* **34**, 10-23 (1959).
96. Morgan, J.R., LeDoux, J.M., Snow, R.G., Tompkins, R.G. & Yarmush, M.L. Retrovirus infection: effect of time and target cell number. *Journal of virology* **69**, 6994-7000 (1995).
97. Luni, C., Michielin, F., Barzon, L., Calabrò, V. & Elvassore, N. Stochastic model-assisted development of efficient low-dose viral transduction in microfluidics. *Biophysical journal* **104**, 934-942 (2013).
98. Stroock, A.D. et al. Chaotic mixer for microchannels. *Science* **295**, 647-651 (2002).
99. Srivastava, K.K., Fernandez-Larsson, R., Zinkus, D.M. & Robinson, H.L. Human immunodeficiency virus type 1 NL4-3 replication in four T-cell lines: rate and efficiency of entry, a major determinant of permissiveness. *Journal of virology* **65**, 3900-3902 (1991).
100. Sakamoto, N. & Rosenberg, A.S. Apolipoprotein B binding domains: evidence that they are cell-penetrating peptides that efficiently deliver antigenic peptide for cross-presentation of cytotoxic T cells. *The Journal of Immunology* **186**, 5004-5011 (2011).
101. Bhatia, M. et al. Quantitative analysis reveals expansion of human hematopoietic repopulating cells after short-term ex vivo culture. *The Journal of experimental medicine* **186**, 619-624 (1997).
102. Petrillo, C. et al. Cyclosporin a and rapamycin relieve distinct lentiviral restriction blocks in hematopoietic stem and progenitor cells. *Molecular Therapy* **23**, 352-362 (2015).